STUDIES OF GASEOUS ALKYL NITRITE AND NITROUS ACID REACTIONS

A thesis
submitted in partial fulfilment
of the requirements for the Degree
of
Doctor of Philosophy in Chemistry
in the
University of Canterbury

by
D.R. Hastie

University of Canterbury
1977

ACKNOWLEDGEMENTS

I wish to thank my supervisor Dr C.G. Freeman for his advice and assistance during the course of this study. I would also like to thank: Dr M.J. M^{c}Ewan for acting in this capacity during Dr Freeman's absence overseas; Professor H.I. Schiff for providing a great deal of stimulus to this study; Dr A. Metcalfe for his assistance with the infrared measurements; and Professor L.F. Phillips, Dr R.G.A.R. MacLagan and Dr P.W. Harland for their helpful discussions. My thanks are also due to the technicians of the Chemistry Department glassblowing, electronic and mechanical workshops without whose assistance this project could not have been performed.

I gratefully acknowledge the receipt of postgraduate scholarships from the U.G.C. and B.P. (N.Z.) Limited which enabled me to pursue this course of study.

D.R. Hastie.

March 1977

CONTENTS

LIST OF FIGURES

LIST OF TABLES

ABSTRACT

Gaseous nitrous acid (HONO) was produced in a discharge flow-mass spectrometric system by the reaction of hydroxyl radicals with nitric oxide,

$$OH + NO + M \longrightarrow HONO + M.$$

A peak was observed at mass 47 (the parent peak of nitrous acid) showing that the acid could be detected mass spectrometrically. A totally satisfactory source of hydroxyl radicals could not be found and so studies of the reactions of nitrous acid could not be undertaken.

The reactions of ozone with methyl and ethyl nitrites were studied in a static reaction vessel using an infrared spectrometer for analyses. The reactions were found to be the simple oxidations yielding the nitrates

$$RONO + O_3 \longrightarrow RONO_2 + O_2$$

The rate expressions obtained for these reactions were

$$\log_{10}k(cm^3 molec^{-1} s^{-1}) = (-12.17 \pm 0.46) - \left(\frac{44.2 \pm 2.9 \text{ kJ.mol}^{-1}}{2.303RT} \right)$$

for R = methyl and

$$\log_{10}k(cm^3 molec^{-1} s^{-1}) = (-15.50 \pm 0.32) - \left(\frac{19.6 \pm 1.9 \text{ kJ.mol}^{-1}}{2.303RT} \right)$$

for R = ethyl.

The only unusual feature of these reactions was the unexplained extraordinarily low value of the Arrhenius parameter in the ethyl nitrite reaction.

The reactions of hydrogen atoms with methyl and ethyl nitrites were studied in a discharge flow-mass spectrometric system. The products observed in the methyl nitrite reaction were hydrogen, nitric oxide, methane,

water and formaldehyde. Methanol was detected at higher pressures with either methoxy radicals or nitroxyl molecules (or perhaps both) detected as intermediates. The products detected from the ethyl nitrite reaction were hydrogen, nitric oxide, ethane, water and possibly formaldehyde. Ethanol was detected at higher pressures, with acetaldehyde, the ethoxy radical and nitroxyl molecule detected as intermediates. Several products were verified by reacting the nitrite with deuterium atoms.

The primary reactions were shown to be :

$$H + RONO \longrightarrow RO + HNO$$
$$\longrightarrow RH + NO_2$$
$$\longrightarrow R_{-H}O + H_2 + NO$$

where in the methyl nitrite reaction the yield of methane was found to be $8.7 \pm 1.5\%$ of the consumed nitrite. The primary rate constant expressions obtained for the loss of nitrite were

$$\log_{10} k(cm^3 molec^{-1} s^{-1}) = (-10.61 \pm 0.20) - \left(\frac{16.2 \pm 1.0 \text{ kJ.mol}^{-1}}{2.303RT} \right)$$

for R = methyl and

$$\log_{10} k(cm^3 molec^{-1} s^{-1}) = (-11.06 \pm 0.20) - \left(\frac{13.84 \pm 1.04 \text{ kJ.mol}^{-1}}{2.303RT} \right)$$

for R = ethyl.

CHAPTER 1

INTRODUCTION

1. GENERAL INTRODUCTION

This study involves the analysis of the kinetics and mechanisms of the reactions of methyl and ethyl nitrites with ozone and hydrogen atoms.

The discharge flow-mass spectrometer system used in the hydrogen atom study was originally assembled with the intention of investigating the fast reactions of chlorine dioxide with hydrogen, oxygen and nitrogen atoms, the oxygen atom reaction having a rate constant of greater than 10^{-11} $cm^3 molec.^{-1} s^{-1}$. (1) However, before any reproducible results could be obtained the results of an examination of these reactions were published (2) and this project was therefore abandoned.

Nitrous acid has been postulated as an important atmospheric species (3,4) and it was planned to use the discharge flow system and mass spectrometer to make and detect gaseous nitrous acid. Following this, studies of the reactions of nitrous acid with important atmospheric species such as ozone and atomic hydrogen, nitrogen and oxygen were to be undertaken.

It proved impossible to unambiguously detect nitrous acid, so as an alternative methyl and ethyl nitrites were taken as model compounds for the acid. The heats of formation of these three compounds are

similar, as are their structures, with all exhibiting cis-trans isomerism. [5,6] The weakest bond in all three compounds is the O-NO bond, the bond dissociation energies being 206.3 kJ mol^{-1} in nitrous acid and 175.0 and 175.7 kJ mol^{-1} in methyl and ethyl nitrite respectively. The alkyl nitrites are of interest in their own right as they have been postulated as intermediates in photochemical smog [7] and little gasphase kinetics has been carried out on carbon, nitrogen, oxygen compounds. If the nitrite was reacted with an energetic species such as an atom it appeared likely that the alkoxy radical would be a primary product. Alkoxy radicals have been postulated as being important in photochemical smog [7] but all kinetic information involving them is either estimated or obtained indirectly. The main reason for this lack of information is that the alkoxy radical has no distinctive optical spectra and the e.s.r spectrum [8] is very poorly resolved making the radical very difficult to detect. It was hoped to be able to study some kinetics of the alkoxy radical by finding a fast alkyl nitrite reaction to produce the radical and use the mass spectrometer for its detection.

There was no detectable reaction between nitrogen atoms and the nitrites. In addition the reaction with oxygen atoms appeared to be too slow to conveniently obtain kinetic data with the discharge flow system available. A study of this reaction which confirmed the slow rate, was published during the course of this work.[9]

The reaction of hydrogen atoms was found to be faster than that with oxygen atoms. Since it was also easier to produce concentrations of hydrogen atoms above 0.10 Torr than it was with oxygen atoms, the reaction could be conveniently studied in the discharge flow system.

The reactions of the nitrites with ozone proved to be too slow to measure in the flowing system, but since both species are stable it was possible to introduce the reagents into a static system where the reaction proceeded at a measurable rate. Continuous monitoring of concentration of a given species and product analyses were performed using an infrared spectrophotometer.

2. SUMMARY OF THE THESIS

Chapter II is a review and examines the importance of gas phase hydrogen atom, ozone, nitrite and nitrous acid reactions with special emphasis being placed on their atmospheric significance. Laboratory methods of studying the fast reactions of hydrogen atoms are covered as are previous studies of nitrite reactions.

Chapter III gives the details of the equipment and procedures used to obtain the kinetic and mechanistic data.

Chapter IV describes the attempts to detect gaseous nitrous acid in the discharge flow-mass spectrometric system, suggests reasons for the failure to unambiguously do so and suggests potentially more productive approaches.

Chapters V and VI examine the data obtained from the nitrite reactions with ozone and hydrogen atoms respectively. The rate constants, stoichiometry and products are quoted and mechanisms postulated.

Chapter VII summarises all the results obtained, draws conclusions and indicates possible directions for future research.

The Appendices contain the thermochemical data and some notes on the safe handling of ozone. The mathematics involved in describing heat transfer into the flow tube along with full details of the data analysis are included. Finally the computer programmes used in this study are described and sample outputs reproduced.

CHAPTER II

REVIEW

1. HYDROGEN ATOM REACTIONS

(1) History and Importance of Hydrogen Atom Reactions

Langmuir [10-12] found that low pressure hydrogen gas in contact with a heated metal filament at between 1300 and 2500 K became "active", suggesting that the hydrogen was being dissociated into atoms. His evidence for the production of atoms included a reduction in pressure when pure hydrogen was activated, which he attributed to atom absorption, either chemical or physical, on the vessel walls. Mixtures of hydrogen and oxygen gave pressure changes credited to the production and subsequent reaction of hydrogen atoms. Also, the reduction of tungstic oxide, WO_3, and platinum oxide, PtO_2, on the vessel walls by "active hydrogen" gave evidence for H-H bond rupture and the long life of the atoms at low pressure. Tollefson and LeRoy used this heated filament method to produce hydrogen atoms at low pressure and attempted to study their reactions with acetylene. [13] The production of atoms by this method has not been widely used as discharge methods have been found to give better yields of atoms.

Wood [14] showed that hydrogen atoms produced in a low pressure electrical discharge could be pumped from the discharge region and showed that they persisted for

over 0.2 seconds. Bonhoeffer [15-17] developed what is generally known as a Wood-Bonhoeffer tube, in which hydrogen atoms are pumped from an electrical discharge into a reaction tube containing an inlet which allows addition of a reagent to react with the atoms. Full experimental details of this technique can be found in the book of Gowenlock and Melville. [18] Other early workers to use the Wood-Bonhoeffer tube were Gieb, Rodebush and Harteck and the work up to 1934 covering the reactions of hydrogen atoms with O_2, CO, NO, HCN, NH_3, CH_3NH_2, SO_2 and C_6H_6 has been summarised.[19,20] Despite the large number of reactions studied the limited experimental techniques available (generally only wet chemical analysis of trapped products) prevented the full investigation of the kinetics and mechanisms. Very little progress was made in overcoming these deficiencies until the late 1950's. A review of the experimental methods used, and the reactions studied up to the early 1950's is given by Steacie. [21]

The first major increase of interest in atomic gas phase reactions came in the 1950's. Combustion was known to propagate via atomic and radical intermediates but the complexity of a flame or explosion made direct measurements of the reactions involved impossible. Therefore it was desirable that methods of studying the elementary reactions in isolation be devised. Also, the airglow and observation of hydroxyl radical emission in the sky [22] led to an upsurge of interest in the chemistry of the atmosphere. As with the combustion problem, studies

of the elementary reactions were required especially those involved in hydrogen-oxygen and hydrogen-nitrogen-oxygen systems. This interest in atmospheric chemistry has been greatly accelerated in the last ten years by the problems of smog and possible disturbance of the atmospheric ozone layer. The latter problem led to the C.I.A.P.* programme involving several hundred workers in studies related to the stratosphere (See Section II.2. (1)).

Hydrogen atoms are important in combustion processes because in the reaction zone of a hydrogen or hydrocarbon flame the hydrogen atom has one of the highest concentrations of any active species, atom or radical, sometimes reaching above 10% of the total gas flow. (23) This high concentration coupled with the high reactivity makes it one of the most important species in the flame. Hydrogen atoms are also important in the upper regions of the atmosphere. At 80km the hydrogen atom concentration has been calculated at 3×10^{-8} Torr in a total pressure of 6×10^{-3} Torr. This makes atomic hydrogen the fourth most abundant species after the unreactive molecular forms of oxygen and nitrogen, although it is probably 1 to 2 orders of magnitude lower in concentration than atomic oxygen. (24)

---

* Climatic Impact Assessment Programme Sponsored by U.S. Department of Transportation (1971-1975).

The upsurge of interest in atomic reactions was coupled with advances in technology which enabled an expansion in the capability of experimental techniques and provided new methods of studying reactions. The main improvements came in atom production and methods for the in situ identification and estimation of gaseous species.

As a result of all these factors the number of reactions under study increased greatly and has continued to do so to the point where reviewers have difficulty in keeping up with the output of papers. Regular reviews appear approximately biennially in various annual reports [25,26] and data on high temperature reactions are now being collated and evaluated. [27] The C.I.A.P. programme led to a critical evaluation of the rate data relevant to atmospheric studies [28] and a copy of the suggested kinetic data report has been published in the book of McEwan and Phillips. [29] Finally, the large number of conferences on gas kinetics yield publications which contain the currently accepted values for kinetic data, [30] the most regular conferences being those of the Combustion Institute. [31]

(2) Experimental Methods for the Study of Hydrogen Atom Reactions

(a) Flames. In the primary reaction zone of hydrogen and hydrocarbon flames high concentrations of hydrogen atoms, up to 10% of the total gas flow, [23] are produced and although recombination is rapid

concentrations of 1% further up the flame are common.[32] As the bulk of the gas moves up the flame these atoms react with other species as in a conventional flow reactor. Hydrogen atoms along with many other atoms and radicals have been detected mass spectrometrically[33] but generally flame studies use optical spectroscopic techniques because of the high temperatures involved - between 1000 and 3000K.[34]

The emission from added sodium, lithium or copper atoms in the flame is dependent on hydrogen atom concentration, and a knowledge of the mechanisms involved has led to methods of obtaining hydrogen atom concentrations.[35-38] Since flames are generally burnt at a total pressure of one atmosphere most of the hydrogen atom reaction rates obtained have been for third order recombination processes, although much kinetic data has been inferred from the effect of trace additives on hydrogen atom concentration.

A regular review of flame chemistry is afforded by the biennial conferences of the Combustion Institute the papers and discussions from which are published.[31]

(b) Shock Tubes. This technique provides an alternative method of determining rate constants at high temperatures but at a wider range of pressures and temperatures than is possible with flames.

The sudden release of a high pressure of a buffer gas, e.g. helium, into a low pressure reactant gas in a reaction tube, produces a supersonic shock wave which

travels down the tube generating temperatures from 1000 to 20,000K within nanoseconds. This temperature rise lasts for several hundred microseconds and all measurements must be taken within this time. The sudden temperature rise dissociates a major proportion of the reactant gas producing atoms and/or radicals whose subsequent reactions can be followed, generally by absorption or product emission, to yield kinetic data. Several reviews on experimental techniques and applications to simple systems are available [39-41] and the Combustion Institute Symposia devote a session to shock tube studies. [31]

(c) Flash Photolysis. There are two basic flash photolysis techniques. The first being the "one off" experiment devised by Norrish and Porter [42] which uses a single high energy flash, the second uses a lower energy repetitive flash and requires signal averaging techniques to give the required data.

In the first method the gas sample is subjected to an extremely high powered light pulse of up to 25kJ delivered within 10 microseconds, which photolyses the sample producing atoms or radicals under either adiabatic or isothermal conditions. In the standard experiment a second, lower energy, spectroscopic flash is fired a known time after the initial flash and the absorption spectrum of the gas sample over the entire wavelength range is recorded on a photographic plate. In this way many reactive intermediates have been identified and the rates of their decay through reaction

determined by varying the time between the initial and spectroscopic flashes. It is also possible to use a continous light source and a spectrometer to monitor the absorbance of a particular species as a function of time after the initial flash. A recent advance has been the use of atomic resonance fluorescence to specifically detect hydrogen atom concentrations after the flash, the advantage of this method over absorption being its higher sensitivity. (43)

In the second method a lower powered flash lamp is pulsed to produce the required atoms and decay in atom concentration can be measured by atomic resonance fluorescence in the period the lamp is off. Since only small concentrations of atoms are produced these fluorescence signals are very weak and single photon counting and signal averaging techniques are required to give a sufficiently large signal. The reactions of hydrogen atoms with formaldehyde and phosphine have been studied this way, the atoms being produced by the photolysis of the formaldehyde (44) and phosphine (45) respectively.

A review by Willets covers the evolution of flash photolysis and serves as a good introduction to the technique and its applications. (46)

(d) Continuous Photolysis. This method differs from flash photolysis in that rather than using a single high powered flash to photolyse the sample, the light source is lower powered and operates continuously.

This gives a steady production of atoms and generally takes many minutes to achieve the same extent of photolysis as the flash.

In a typical experiment the reagents are photolysed to produce hydrogen atoms either directly from molecules such as formaldehyde or hydrogen sulphide, or by mercury photosensitised decomposition of hydrogen or a suitable hydrogen containing compound. The atoms produced can then react with the reagents present in the system and once the photolysis has ceased analysis for products is usually carried out by gas chromatography or mass spectrometry. This method is usually used to obtain relative rate constants by having more than one reagent in the system, but has not been widely used. The most important uses of the technique have been reviewed by Thrush [47] and Cvetanovic. [48]

(e) Crossed Molecular Beams. The usefulness of crossed molecular beams has been realised by kineticists for some time, their advantage being that the effects of individual collisions can be studied. Examination of the angular distribution of reactants and products after collision gives an understanding of the molecular dynamics of a collision whether it is reactive or unreactive. Initially the difficulty of producing high concentration beams meant that only alkali metal atom reactions could be studied. [49] Recently methods have been developed for increasing beam density and more sensitive detection using mass spectrometers [50,51] and

laser induced fluorescence [52] has allowed a wider range of reactions to be studied.

It is now possible to analyse the emission spectra of products and recent papers report the use of laser induced fluorescence to obtain internal energy distribution in product molecules [53] such as hydroxyl radicals in the reaction of hydrogen atoms with nitrogen dioxide. [57]

(f) Discharge Flow Systems. This has been the most widely used method for studying the reactions of hydrogen atoms because the atoms can readily be generated and reaction times in the millisecond range are easily obtained. A standard discharge flow system is a modified version of the Wood-Bonhoeffer tube. The electrical discharge has been replaced by an electrodeless microwave or r.f. discharge which gives a more stable atom output over a much wider pressure range and obviates the need for the electrodes to be in contact with the gas thereby reducing the possibility of contamination. A mixture of a buffer gas, usually helium or argon, and hydrogen is passed through the discharge to produce the atoms. The gas mixture is then passed down the flow tube with velocities from 1-20 ms^{-1} and pressures from 10^{-1} to 10 Torr are maintained by high capacity vacuum pumps. A second reactant is added to the flowing gases and as they flow down the tube the reaction can proceed, the distance down the tube being a measure of the reaction time.

The major impetus to the method came in the late

1950's with the development of simple specific and reliable methods of atom, radical and neutral detection. The most important methods for atom detection include a number of titration methods along with e.s.r., optical and mass spectrometry.

Since most hydrogen atom reactions have been studied using discharge flow systems and such a system was used in this work a more detailed discussion of the uses of discharge flow systems will be reviewed in the next section.

(3) The Use of Discharge Flow Systems in Studies of Hydrogen Atom Reactions

The usefulness of a discharge flow system in studying hydrogen atom reactions depends on the availability of methods for measuring concentrations and a knowledge of the limitations of the method. This section will examine both of these problems.

(a) Methods of Measuring Concentration

(i) Gas Chromatography: This technique is only of use in determining concentrations of stable products but is capable of doing this quantitatively and with a very high degree of sensitivity. Products are either trapped out from the flow system or bled into a sample bulb for later analysis. The method has been used in studies of the reactions of hydrogen atoms with ethylene [54] and deuterium atoms with hydrogen. [55] It cannot detect atoms or radical intermediates and since the sample is stored and analysed later there is no reaction time resolution possible.

(ii) Calorimetric Methods : These methods were devised to measure atom concentrations and involve inserting an active surface into the flow tube. The heat given out when atoms recombine on the surface can be measured and related to concentration. These methods are non-specific and have been superseded by more specific methods.

(iii) Electron Spin Resonance (e.s.r.) : An e.s.r. cavity can be incorporated into a discharge flow system and can specifically detect any species containing an unpaired electron. For example it can detect $H(^2S)$ $N(^4S)$ $O(^3P)$ $O_2(^3\Sigma_g^+)$ but not $Ar(^1S)$ or $He(^1S)$. Hydrogen atoms have an absorption doublet and relative or absolute concentrations can be determined. [56] Examples of reactions studied using e.s.r. detection of hydrogen atoms include reactions with hydrogen chloride, [57,58] ethylene [59] and nitrogen dioxide. [60]

(iv) Atomic Absorption : This method is specific to the chosen atom and for hydrogen atoms Lyman α radiation is passed into the flow tube the amount absorbed being proportional to the atom concentration. This technique has been used for studies of hydrogen atom reactions with acetylene and ethylene, [61] silane and germane. [62] This method of detection has not been widely used for two reasons, firstly, the error is high as it requires measuring the small difference between high light intensities, and secondly, the low sensitivity in the case of hydrogen atoms. An

absorbance of 0.029 corresponded in one system to an atom concentration of 5×10^{-4} Torr. (61)

(v) Atomic Resonance Fluorescence : This method of atom detection was originally developed to measure hydrogen atom concentrations in a flash photolysis system (43) but has found applications in other experimental methods including discharge flow systems. In the case of hydrogen atoms Lyman α radiation is shone into the flow tube where some will be absorbed by the hydrogen atoms in the tube. These will then fluoresce and the fluorescence is measured at right angles to both the flow tube and the incident radiation. The advantages of this method are that the fluorescence intensity is linearly related to atom concentration at low pressures, and the high sensitivity being able to detect 3×10^{-7} Torr of atoms in the flow tube. (63)

(vi) Chemical Methods : The most widely used method of determining hydrogen atom concentration is by use of the "titration" reaction with nitrogen dioxide. (64) Provided reaction time is sufficiently long the overall reaction is

$$2H + 3NO_2 \longrightarrow 3NO + O_2 + H_2O$$

The end point of this reaction can be detected mass spectrometrically by measuring NO_2 consumption, or by directly monitoring the atom concentration using e.s.r. An e.s.r. study has confirmed the 2:3 stoichiometry of the titration reaction provided the walls of the flow

tube are poisoned against atom recombination. If wall reactions become important the stoichiometry can change to $10OH : 11NO_2$. (60)

Atom concentrations can also be determined by admitting nitric oxide to the flow tube downstream of the reactant inlet. (65,66) The reaction of hydrogen atoms with nitric oxide produces the excited nitroxyl molecule which gives infrared chemiluminescence.

$$H + NO + M \longrightarrow HNO^* + M$$

$$HNO^* \longrightarrow HNO + h\nu$$

The intensity of this luminescence is given by

$$I \propto [H][NO]$$

The proportionality constant contains a geometrical factor, an instrumental factor and the total pressure. To determine concentration using this method it is normal to use a titration reaction to determine [H] and hence the proportionality constant. Once this is done absolute concentrations of atoms can be determined. This reaction can also be used to detect the end point of the titration reaction with nitrogen dioxide because $I = 0$ when $[H] = 0$.

(vii) Mass Spectrometers : These instruments have been the most popular method of measuring concentration and the history of their use with discharge flow systems is well documented. (67,68) The main advantage of mass spectrometers over the other methods mentioned is their versatility. Provided the sampling system is well designed atoms and radicals such as H, N, O, OH, HO_2, NH_2 and CN can be detected (69) as can all stable molecules. It is a relatively simple procedure

to calibrate the spectrometer towards a stable species (see Section III.4.(3)) and to obtain absolute concentrations at the point of sampling. Calibration of the spectrometer towards NO_2 enables absolute hydrogen atom concentrations to be obtained using the titration reaction. Direct measurements of hydrogen atoms at M1 (mass peak 1) are complicated by contributions from molecular hydrogen and are generally not undertaken. With a specially designed electron gun it is possible to control the electron energy so that distinction between possible species of the same mass can be made on the basis of appearance potentials. Similarly it is possible to separate a parent ion from a fragment ion originating from a more complex molecule the latter generally having a higher appearance potential. The mass spectrometer is also highly sensitive being able to detect partial pressures of less than 10^{-8} Torr in the ion source.

The sampling and pumping systems must hold the mass spectrometer ion source at less than 10^{-4} Torr whilst the flow tube is at pressures from 10^{-1} to 10 Torr. With this criterion established the reacting gases experience a pressure drop of at least three orders of magnitude on sampling. This quenches the reaction and no allowance need be made for additional reaction after sampling. This pressure drop means the limit of sensitivity of a mass spectrometer towards samples in the flow tube is from 10^{-3} to 10^{-5} Torr.

The major disadvantage of the conventional mass

spectrometer is that for large molecules a large number of fragments are formed under electron bombardment, thus complicating the search for reaction products. A well designed electron gun can help overcome this problem by running at low electron energies but the sensitivity is greatly reduced and the higher filament temperatures required to run at these energies lowers filament life. Photoionisation, where the molecule is ionised by high energy radiation corresponding to 11 - 14 eV, produces less fragmentation and although it has been used in some studies [70,71] it too suffers from the disadvantage of low sensitivity.

(b) Limitations of Discharge Flow Systems.

The exact mathematical description of the fast flow of a discharged gas through a cylindrical tube becomes extremely complex, even for a simple parabolic velocity profile, when volume and surface recombination, radial and axial diffusion and the viscous pressure drop are taken into account.

It is normally assumed that in a discharge flow system that the concentration gradients are too small to give axial or radial diffusion, that surface recombination of atoms is small, and that the flow is "plug" - meaning that all sections of the gas move at the same velocity.

The walls of a flow tube provide a surface on which atoms can recombine and to prevent this it is necessary to poison the walls. This is usually done by

coating them either with orthophosphoric acid, [72] boric acid, [58] teflon [73] or a mixture of silanes [74] which greatly reduces the rate of recombination, often by up to 4 orders of magnitude. [47] It has been found that in the absence of wall coating, chlorine atoms cannot be detected but that they are readily detected on poisoning the flow tube walls. [58] The same effect is to be expected with hydrogen atoms thus wall coatings are essential. The gas phase recombination of atoms is a three body reaction and providing the total pressure is kept low this reaction is too slow to proceed significantly. Hence, at pressures below 1 Torr with walls poisoned, the conditions prevailing in this work, atom recombination is negligible.

Mulcahy and Pethard [75] have examined mathematically the error in the calculated rate constant arising from the assumptions of a linear velocity profile and no diffusion. They found the error to depend on the extent of reaction and the parameter μ given by

$$\mu = \frac{2\,tc}{L^2} \cdot \left(D + \frac{r^2u^2}{48D} \right)$$

where tc and L are the reagent contact time and distance, r is the tube radius, u the average velocity and D the diffusion coefficient. Using the most extreme values prevailing in this study of tc = 20 ms, L = 20 cm, r = 1 cm, u = 1000 cm s^{-1} and D = 100 cm^2s^{-1} the value obtained for μ is 0.031. This value indicates that even

at 70% reaction the error in the calculated rate constant is only about 2%. As a rule of thumb Mulcahy [76] suggests that if the error in k is to be less than 10% in experiments involving up to 25% reaction the experimental conditions should be such that tc/L^2P is less than about 5×10^{-3} $s.cm^{-2}Torr^{-1}$. (Where P is the total pressure). Using the above values and the total pressure of 0.1 Torr, $tc/L^2P = 5 \times 10^{-4}$ an order of magnitude below the limit set. Hence the velocity profile and diffusion effects are not important in this study.

The main source of error in this work is the viscous pressure drop down the tube and for the simple Poiseuille flow the pressure difference between two points a distance x apart is given by

$$P_2^2 - P_1^2 = \frac{16 F \eta RTx}{\pi r^4}$$

Here F is the gas flow rate, η the gas viscosity, T the temperature and R the gas constant. It was calculated that in some experiments the pressure drop was as high as 25% so the data analyses have had to include this effect. The full description of the effect of the pressure drop can be found in Appendix IV.

2. THE IMPORTANCE OF GASEOUS NITRITES, NITROUS ACID AND OZONE

The major interest in nitrites, ozone and nitrous acid at present lies in their relevance to atmospheric chemistry and a brief introduction to the structure

of the atmosphere is necessary before the chemistry can be considered. A full description of the atmosphere can be found in the book of M^{c}Ewan and Phillips. (77)

The atmosphere is divided into several regions dependent on altitude. The lowest of these is the troposphere which stretches from ground level to the tropopause, the height of which can vary from 8 to 15 km depending on season, latitude and time of day. The troposphere is characterised by a decrease in temperature with increasing altitude from 300 to 200K and it contains all the air movement responsible for the weather. Between the tropopause and the stratopause at about 80 km lies the stratosphere which has a temperature inversion, the temperature increasing from 200 to 300K in this region. This makes the stratosphere extremely stable to vertical mixing and although horizontal wind currents are strong there is very little vertical movement. These two regions are of most interest to chemists but above the stratopause are the mesosphere and the thermosphere which encompass the ionosphere where ion chemistry becomes important but this will not be discussed here.

(1) Ozone and Oxides of Hydrogen and Nitrogen in the Stratosphere

There is a great deal of ultraviolet (U.V.) radiation produced by the sun which if it was not largely absorbed by the atmosphere would be injurious to life on earth. The dangerous wavelengths are those less than

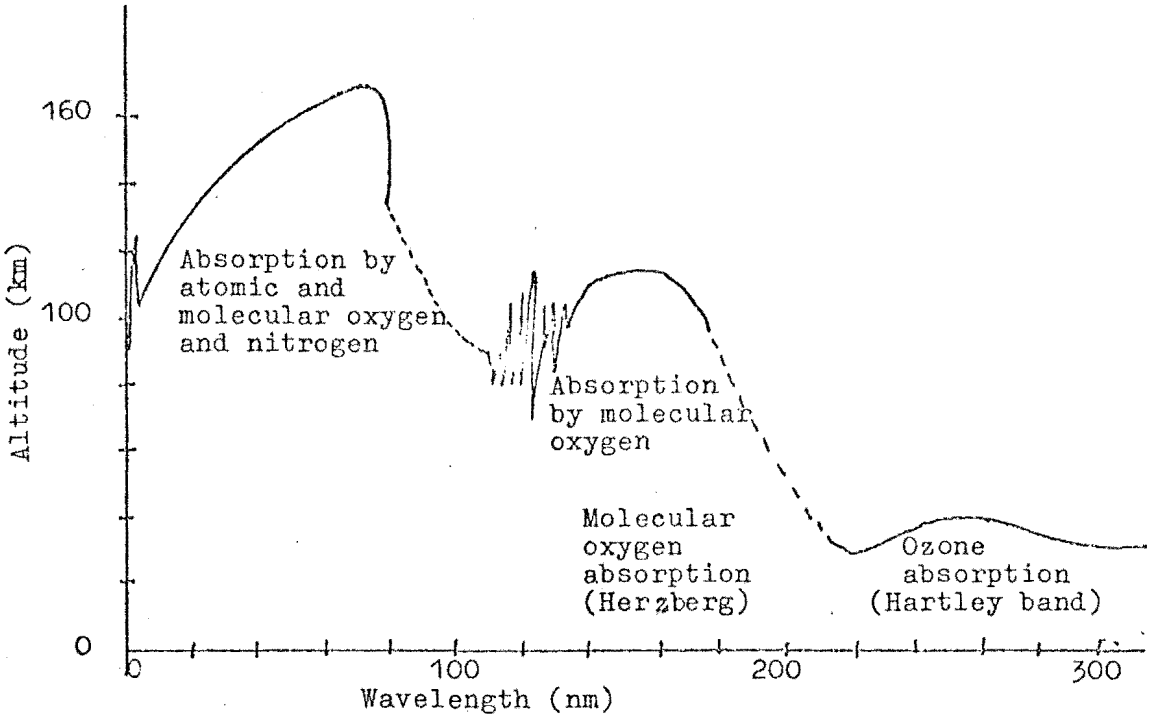

Figure II.1 Altitude of maximum light absorption as a function of wavelength

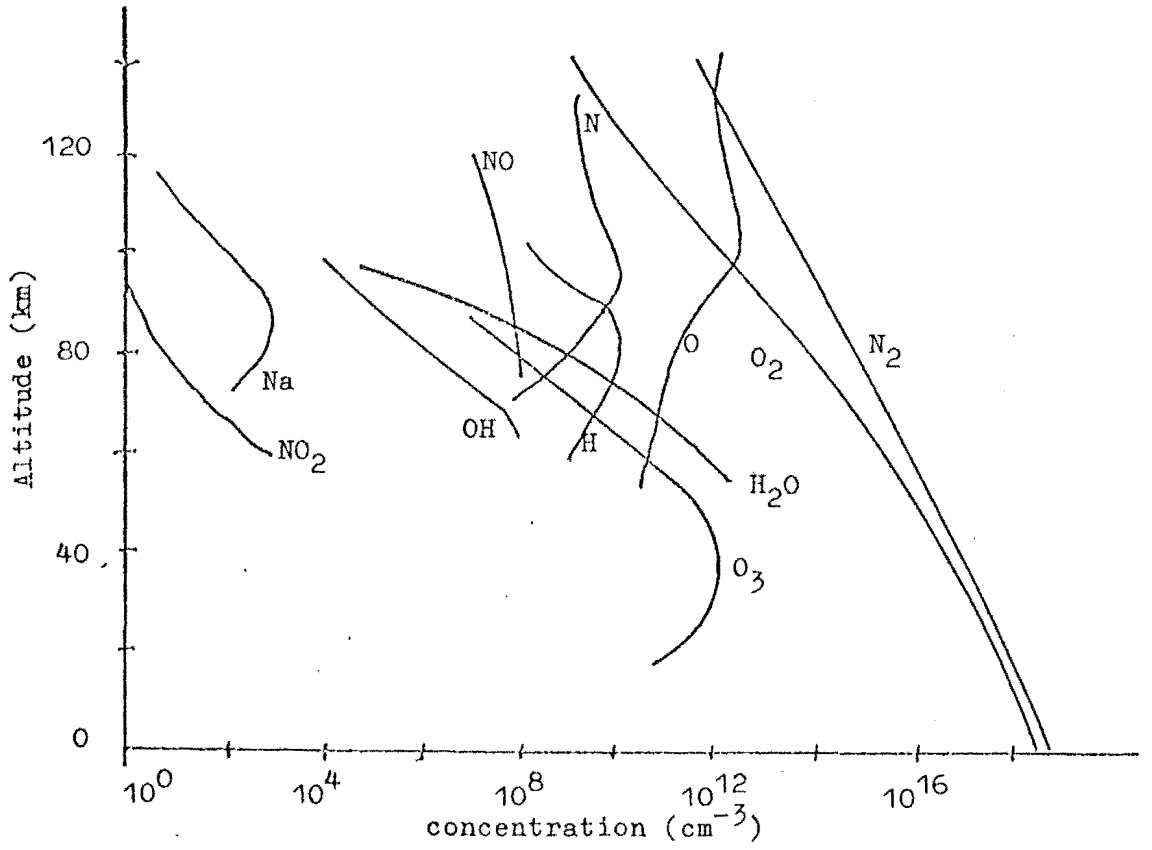

Figure II.2 Representative concentration profiles of neutral species in the atmosphere

300nm and Figure II.1 [78] shows the absorption of this radiation as a function of altitude and absorbing species. The radiation below 180nm is absorbed in the outermost regions of the atmosphere by the strong atomic and molecular absorptions of oxygen and nitrogen. For wavelengths below 242nm the weaker forbidden Herzberg continuum of molecular oxygen absorbs in the lower, denser regions of the stratosphere around 40km. This absorption produces atomic oxygen which reacts with molecular oxygen to give ozone which in turn absorbs strongly in the Hartley band and continuum system between 200 and 300nm. Hence, above 20km most of the harmful radiation has been filtered.

Nitrogen and oxygen are chemically stable and exist in high concentrations at all altitudes (see Figure II.2) [79] so their filtering action will be unaffected by any additional compounds in the atmosphere. However ozone is highly reactive, has a maximum concentration some four orders of magnitude less than nitrogen and oxygen at the same altitude, and is confined to a relatively narrow band in the stratosphere. It would appear as though ozone is in a delicate balance in the stratosphere and that its concentration could be perturbed by additional atmospheric constituents. The possible effect on life of a small change in ozone has been studied recently and it has been predicted that significant biological and climatic changes would result.

The most noticeable effect on humans would be an

increase in the incidence of skin cancer. It has been estimated that the additional U.V. radiation reaching earth due to a 5% decrease in ozone concentration would cause, on average, an increase of 10% in skin cancer cases in the United States. (80) Preliminary experiments show that crops such as peas and beans subjected to additional ultraviolet radiation show signs of growth suppression, (81) suggesting that ozone depletion could cause reductions in the yields of such crops. The effects of increasing U.V. radiation penetrating into the troposphere on world climate are unclear. It appears as if a reduction in ozone would cause an increase in surface temperature although the causes of the ozone depletion would themselves cause uncertain climatic changes. (82) All that can be said with certainty is that the climate would be affected but the present understanding of world climate is insufficient to predict the effects of perturbations.

The first explanation of ozone production in the atmosphere was published in 1930 by Chapman. (83) The production mechanism consisted of oxygen photolysis to give oxygen atoms and their reaction with molecular oxygen to produce ozone.

$$O_2 + h\nu \quad (\lambda < 242nm) \longrightarrow 2O \quad \ldots\ldots (1)$$

$$O + O_2 + M \longrightarrow O_3 + M \quad \ldots\ldots\ldots (2)$$

net production $3O_2 + h\nu + M \longrightarrow 2O_3 + M$

The destruction mechanism consisted of ozone photolysis and reaction with oxygen atoms to give oxygen.

$$O_3 + h\nu\ (\lambda < 1100nm) \longrightarrow O + O_2 \quad \ldots\ldots\ldots\ldots (3)$$

$$O + O_3 \longrightarrow 2O_2 \quad \ldots\ldots\ldots\ldots (4)$$

net destruction $2O_3 + h\nu \longrightarrow 3O_2$

This mechanism is known as the Chapman mechanism and reactions 1-4 as the Chapman reactions. It is the absorption of radiation in this mechanism which is responsible for the heating of the stratosphere and the production of the temperature inversion. Using reactions 1-4 it is possible to determine the concentration equation for ozone, (84)

$$\frac{d[O_3]}{dt} + \frac{2k_4 J_3 [O_3]^2}{k_2 [O_2][M]} = 2 J_1 [O_2]$$

where k_2 and k_4 are the rate constants for reactions 2 and 4 and J_1 and J_3 are the rate constants for the absorption processes. J takes account of the wavelength variation of the incident radiation, the absorption cross section, and the quantum efficiency of the primary process. For short times in which the incident radiation is constant the ozone concentration will be time independent. In this case the equation reduces to :

$$[O_3]^2 = \frac{k_2 J_1 [O_2]^2 [M]}{k_4 J_3}$$

As altitude decreases $[O_2]$ and $[M]$ increase so that $[O_3]$ should also increase. However J_1 depends on radiation less than 242nm which is largely filtered at altitudes above 30 km, so below this height J_1 decreases rapidly and so the ozone concentration passes through a maximum at about 30 km. This simple mechanism along with the temperature inversion is able to explain the presence of

the ozone layer in the stratosphere.

This mechanism remained virtually unchallenged until the 1950's when reactive species such as OH began to be identified in the atmosphere. (22) Measurements of ozone concentrations and experimental values of the rate constants became available and calculations showed that this mechanism could not account for some 80% of the ozone produced, even with the inclusion of air motion and ground level destruction. (85) It has since been found that the net destruction mechanism is that given by Chapman, but the reactions are catalysed by many of the naturally occuring reactive species in the stratosphere such as H, OH, HO_2, NO and NO_2.

The products of water photolysis H, O, OH, HO_2 which are referred to as the odd hydrogen compounds have for several years been thought to influence the ozone balance. (86-90) Three catalytic destruction cycles are now known to be important because of the concentrations present and the known rates of reaction. Above 45km the hydrogen and oxygen atom densities are high and so reaction 4 can be replaced by the catalytic cycle (91)

$$H + O_3 \longrightarrow OH + O_2$$

$$O + OH \longrightarrow H + O_2$$

net reaction $O + O_3 \longrightarrow 2O_2$ . . . . . (4)

Between 30 and 45km where OH and HO_2 are more abundant a second cycle becomes more important. (91)

$$OH + O_3 \longrightarrow HO_2 + O_2$$

$$O + HO_2 \longrightarrow OH + O_2$$

net reaction $O + O_3 \longrightarrow 2O_2$ . . . . . (4)

These two schemes occur only in regions of low ozone concentration and so will not have a marked effect on total ozone concentration. However there is a further catalytic cycle involving hydrogen oxides which takes place below 30km and this replaces the complete ozone destruction mechanism of Chapman. (91)

$$OH + O_3 \longrightarrow HO_2 + O_2$$

$$HO_2 + O_3 \longrightarrow OH + 2O_2$$

net reaction $2O_3 \longrightarrow 3O_2$

Recent calculations have shown that these three schemes would account for an additional 10% of ozone consumed. (92)

The major catalytic cycle destroying ozone involves the odd nitrogen oxides (NO_x) viz. NO, NO_2, N_2O_5, HNO_2 and HNO_3. The most abundant of these are NO, NO_2 and chemically unreactive HNO_3. Nitrous oxide N_2O is produced at the earth's surface by bacterial action and since it is inert below the tropopause it ultimately reaches the stratosphere. Once in the stratosphere it is photolysed by the shorter wavelength radiation and is largely converted to molecular nitrogen and oxygen, However the photolysis produces some nitric oxide and furthermore the (O^1D) atoms produced from the photolysis can react with nitrous oxide to produce nitric oxide (93-95)

$$N_2O + h\nu \longrightarrow N_2 + O(^1D)$$

$$\longrightarrow N + NO$$

$$O(^1D) + N_2O \longrightarrow NO + NO$$

$$\longrightarrow N_2 + O_2$$

It has also been suggested that the oxidation of naturally occurring ammonia may be a significant source of nitric

oxide. (94) The interconversion of odd nitrogen oxides, with the exception of nitric acid, is rapid and once the source of nitric oxide is established so is the source of all other odd nitrogen oxides,

The catalytic cycle based on the nitrogen oxides is (93-95)

$$NO + O_3 \longrightarrow NO_2 + O_2$$

$$O + NO_2 \longrightarrow NO + O_2$$

net reaction $O + O_3 \longrightarrow 2O_2$ . . . . . (4)

Estimates of nitrogen oxide concentrations in the stratosphere are difficult to establish accurately because of their low concentrations and the large natural variations. Present indications suggest that the concentrations are sufficiently high for the above catalytic cycle to account for the destruction of 70% of the produced ozone.

Hence the Chapman reactions and the catalytic cycles involving odd hydrogen and nitrogen compounds quantitatively account for the ozone balance in the stratosphere.

The atmosphere contains many constituents at low concentrations and so direct studies of its chemistry are impracticable. Many groups have attempted to study the chemistry of the atmosphere by modeling its behaviour using computers. (94,91,95,96) This they have done by using known solar fluxes, known chemical reactions and their rates, a model for air movements and a set of initial concentrations to calculate the concentration profiles of reactive stratospheric

species such as NO, NO_2, HNO_3 and O. The test of these models is whether the calculated profile agrees with that measured. At present the major features of a profile, the order of magnitude of concentration and its approximate altitude dependence, can be simulated. However, the low precision of model calculations and measured profiles mean that deficiencies in the models do not become obvious.

One of the major reasons for the present detailed knowledge of the chemistry of the stratosphere and particularly ozone chemistry, is that there has been concern that the ozone layer could be depleted artificially and that more U.V. radiation could reach the earth. The main suggested cause of this depletion appeared to be the exhaust fumes from supersonic transport aircraft (SSTs) which fly in the stratosphere at altitudes of about 20km. These fumes which contain both hydrogen and nitrogen oxides would be deposited directly into the stratosphere and could upset the delicately balanced ozone concentration. In 1971 the U.S. Department of Transportation set up the Climatic Impact Assessment Programme (C.I.A.P.) to study the effects of exhaust gases from SSTs on ozone concentration, on climate and on biology . This programme involved several hundred workers and much of the present knowledge of the stratosphere has been gained as a result.

Other than waiting to observe the ultimate effect on ozone concentration of a fleet of SSTs the only way

to study the problem is to use the atmospheric models to predict the change in ozone concentration of say, 500 SSTs flying 5 hours per day at 20km. The major effect would be an ozone depletion due to the depositing of nitrogen oxides from the engine exhausts. The lack of measurements of natural levels and the fact that many of the proposed SST engines are not yet operational meant that estimates of the increase in nitrogen oxides in the atmosphere as a result of SSTs have ranged from one third to more than double [85] the natural level. Many groups applied their models to the problem and most of these are summarised by Johnstone. [85] The calculated ozone depletion for the above conditions ranged from 8 to 23% with an average of 15% which represents a real problem since, for example, this would increase the incidence of skin cancer by some 30%. [80] However conservationists and the economic climate have ensured that the large numbers of SSTs envisaged a decade ago will not be built in the near future. If large numbers of these aircraft are ever built it is clear that either the nitrogen oxide exhaust levels will need to be strictly controlled or the aircraft must fly at lower altitudes if the ozone layer is not to be significantly depleted.

The variation in the calculated ozone depletion was not a function of the SST inputs but was due to differences in the chemical models of the unpolluted atmosphere. It must therefore be concluded that the chemistry is not sufficiently well understood for

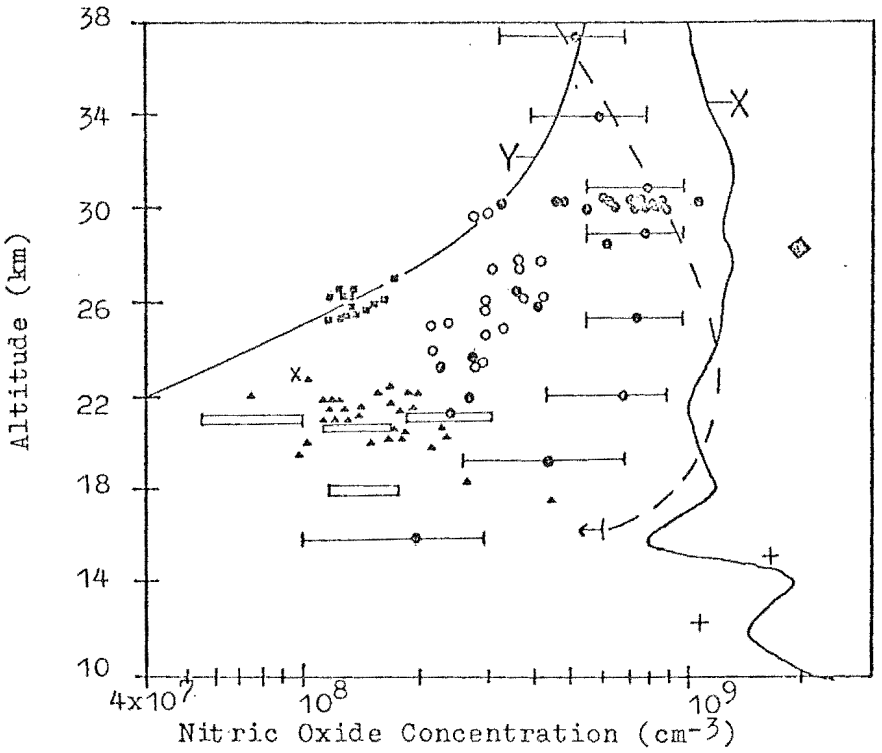

FIGURE II.3 MEASURED NITRIC OXIDE PROFILES

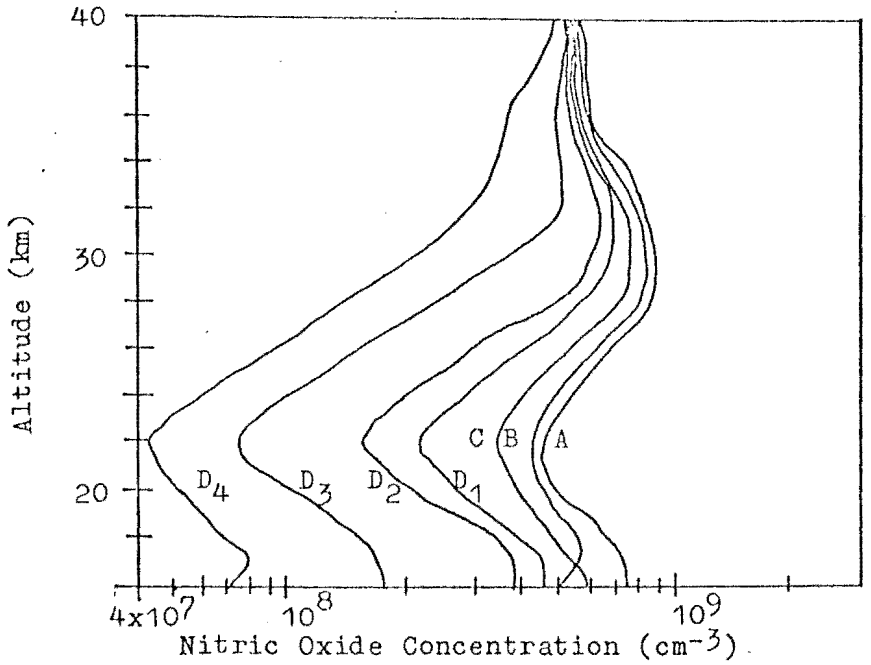

FIGURE II.4 CALCULATED NITRIC OXIDE PROFILES

modelling groups to take identical initial conditions and obtain the same results.

The calculated nitric oxide profiles X and Y of M^{c}Elroy and M^{c}Connell [94] in Figure II.3 show the wide variation which can still be achieved within a given model and that experimental measurements cannot be used to fully test the model. The figure shows a number of measurements of nitric oxide concentration made at different times and using a number of different techniques. It should be noted that there is a large natural variation in concentration and workers have noted a variation of up to a factor of three at the same altitude over a four hour balloon flight, [97] and also in measurements at the same point exactly one year apart. [98] These fluctuations are due to localised effects and air movements which are not well described in current models. The large differences in measured concentration are somewhat exaggerated by the timing of experiments. Those performed at noon would be expected to yield higher concentrations than those at twilight because of the increased rate of nitrogen dioxide photolysis. The curves X and Y on the figure represent the maximum and minimum nitric oxide profiles attainable with the model by adjusting unknown parameters within their boundary limits. This shows that any measured profile can be accommodated by the model as it stands. Both the precision of the model and the measured profiles need to be improved before a more accurate picture of the chemistry can develop.

To improve the model it is necessary to better define some of the more important experimentally obtained inputs to the model such as quantum yields and rate constants. The most important of these have been listed by Garvin et al.. [99] The modellers can only improve their models by including additional reactions or excluding them if they have no effect on the calculated profiles.

Schiff[4] has provided a good example of the type of problem a modeller faces in improving his model. Nitrous acid is formed by the reaction

$$H O_2 + NO_2 \longrightarrow HNO_2 + O_2 \quad \ldots\ldots\ldots (5)$$

with a rate constant of greater than $3 \times 10^{-13} cm^3 molec.^{-1} s^{-1}$. The acid is lost by photolysis but could be oxidised to nitric acid by ozone at an as yet unknown rate.

$$HNO_2 + O_3 \longrightarrow HNO_3 + O_2 \quad \ldots\ldots\ldots (6)$$

These last two reactions are not included in models of the stratosphere. Figure II.4 shows a family of nitric oxide profiles calculated using the model of M^{c}Elroy and M^{c}Connell [94] and including the two nitrous acid reactions. Curve A is the reference profile which omits both reactions. If either reaction is included singly the effect is not large. For curve B k_5 has been set an order of magnitude higher than the limit at $2 \times 10^{-12} cm^3 molec.^{-1} s^{-1}$ and k_6 at zero. Similarly curve C is obtained with k_5 at zero and k_6 $1 \times 10^{-13} cm^3 molec.^{-1} s^{-1}$. When both reactions are included there is a large synergic effect where curves D_1, D_2, D_3 and D_4 were obtained with k_5 at 2×10^{-12} and k_6 at 1×10^{-17},

2×10^{-17}, 1×10^{-16} and 1×10^{-14} $cm^3 molec.^{-1} s^{-1}$ respectively. These profiles all lie within the range of experimental values and it must be concluded that if k_6 is greater than $1 \times 10^{-17} cm^3 molec.^{-1} s^{-1}$ then both these reactions are important and should be included in the model. Only if the rate of k_6 is shown to be less than $1 \times 10^{-17} cm^3 molec.^{-1} s^{-1}$ can the two reactions be discounted.

In summary the major features of the chemistry of the atmosphere can be explained by current models although uncertainties in some experimental quantities lead to widely variable results. The present need is to improve experimental inputs to these models for only then can the models be more rigorously tested.

(2) Photochemical Smog

The word smog was originally derived to describe the mixture of smoke and fog responsible for the loss in visibility and increase in bronchial irritation in what was known as the London "pea-souper". Lately it has been used to describe any atmospheric condition which, as a result of pollution, produces a loss in visibility and some physical discomfort in humans. Photochemical smog results from the action of sunlight on the exhaust fumes of internal combustion engines and occurs in most large cities which have large numbers of vehicles, sunlight and a stable air mass. The last of these conditions may be brought about by a temperature inversion over a valley or basin, the Los Angeles basin

being the prime example. Photochemical smog (hereafter referred to simply as smog) is formed on sunny days with low humidity and typical symptoms are high oxidant levels, some loss in visibility due to a whitish haze, eye irritation in humans and crop damage. (101)

A full discussion of the mechanism and effect of smog is outside the scope of this review but there are several comprehensive reviews available. (3,101-109) In this section I will give a simplified version of the currently accepted models showing the importance of nitric oxide, nitrogen dioxide, ozone, alkenes, nitrous and nitric acids, their esters, hydroxyl, hydroperoxy, alkoxy and alkylperoxy radicals.

The number of published measurements on the time dependence of pollutant concentrations is small because variations in weather conditions, the very low concentrations being measured and the variable nature of pollutant inputs mean that results are usually irreproducible. A typical concentration time profile is shown in Figure II.5. (101) To reduce the overall pollutant problem to simply a chemical one, most measurements are made in artificial "smog chambers". In these studies typical concentrations of pollutants such as nitric oxide, nitrogen dioxide, alkene (to represent all reactive hydrocarbon), carbon monoxide and water are put into the chamber together with purified air and subjected to radiation from a light source which simulates the sun. The photo-chemically induced reactions then take place and concentrations are measured as a function of time by

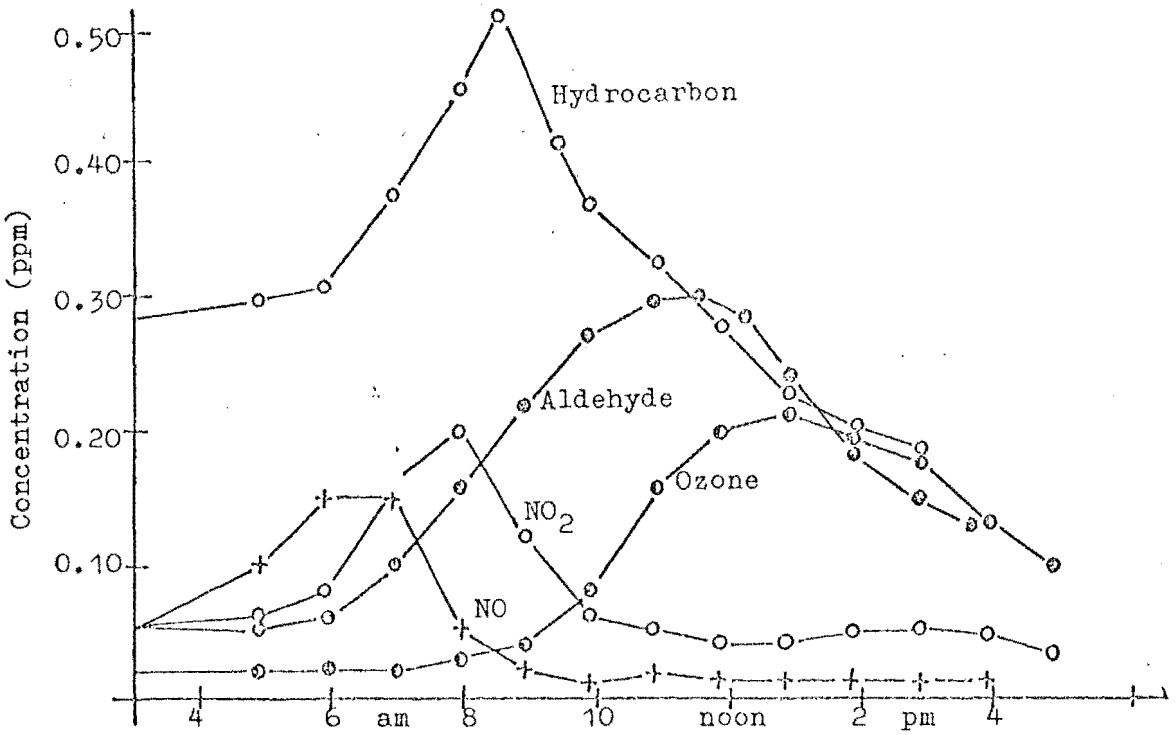

FIGURE II.5 AVERAGE CONCENTRATIONS OF POLLUTANTS ON A SMOGGY DAY IN LOS ANGELES

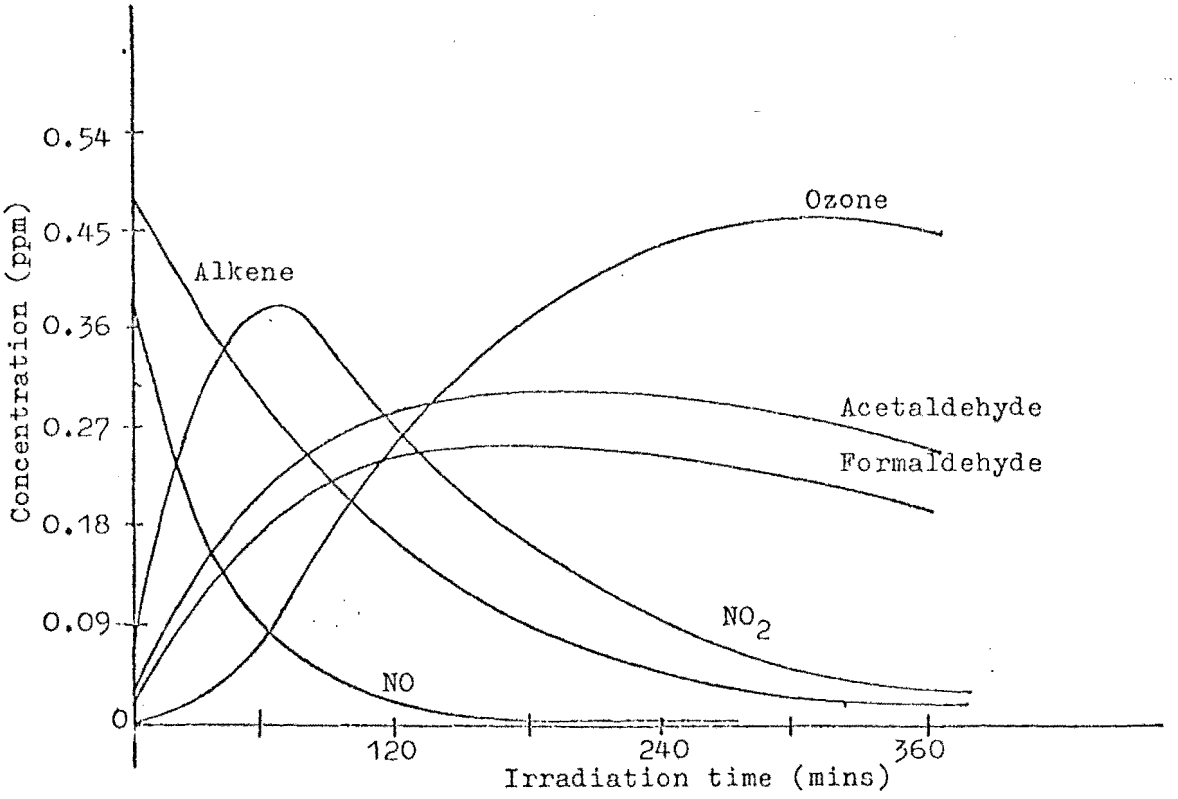

FIGURE II.6 CONCENTRATION PROFILES OF POLLUTANTS OBTAINED FROM A SMOG CHAMBER

gas chromatography, long path length I.R. or sometimes Fourier Transform Spectrometers. The advantages of using a smog chamber to obtain data are:the number of initial reagents is less; all non chemical variables are eliminated; product analysis is easier; and the effect of a single pollutant can be determined by varying its initial concentration. The results are concentration time profiles such as are shown in Figure II.6.[104] The smog chamber results show the same general features as the measured atmospheric results, viz., a rapid decrease in nitric oxide concentration in the presence of sunlight, a maximum in the concentration of nitrogen dioxide and an increase in ozone concentration only when most of the nitrogen dioxide has been consumed.

There are two approaches to the problem of understanding smog production. The first is to vary the initial concentrations of trace pollutants in the smog chamber to find which of these species has the most effect on the resultant concentration profiles. For example, carbon monoxide was found to be an important species in smog when it was observed that the addition of a trace of CO to a smog chamber mixture greatly increased the rate of removal of nitric oxide.[106] The second, which benefits from the first, is to devise a mechanism for smog production, use this to calculate concentration-time profiles for all species and to compare these with experimental values from smog chambers. The closer the agreement between the profiles the better

the model. The ultimate aim of these studies is to fully understand the causes of smog and suggest methods to control it.

The main features to be explained in Figure II.6 are: the slow oxidation of the alkene; the relatively rapid oxidation of nitric oxide; the maximum in the concentration profiles of nitrogen oxides; the ultimate disappearance of the nitrogen oxides; and the appearance of ozone only when the total nitrogen oxide concentration falls.

The major source of the input pollutants is the internal combustion engine. Nitric oxide is formed from molecular oxygen and nitrogen by the extreme heat and in the exhaust system some of this will be oxidised to nitrogen dioxide by the termolecular reaction,

$$2NO + O_2 \longrightarrow 2NO_2 \quad \ldots\ldots\ldots\ldots (1)^*$$

but once these products escape into the atmosphere, dilution ensures that this reaction is too slow to be significant. Nitrogen dioxide, since it is the principal light absorbing species, is the initiator of the smog through the decomposition

$$NO_2 + h\nu \longrightarrow NO + O \quad \ldots\ldots\ldots\ldots (2)$$

which has a quantum yield of unity in the wavelength range 295-430nm. The majority of oxygen atoms produced react with molecular oxygen to produce ozone

$$O + O_2 + M \longrightarrow O_3 + M \quad \ldots\ldots\ldots\ldots (3)$$

---

* The numbering of equations recommences with each new section.

Where the nitric oxide concentration is high it will be oxidised to nitrogen dioxide by the ozone

$$NO + O_3 \longrightarrow NO_2 + O_2 \quad \ldots\ldots\ldots (4)$$

This three-step mechanism explains the late appearance of ozone because while either nitrogen oxide is present ozone will react rapidly with nitric oxide and its concentration will be kept low. Once both of the nitrogen oxides disappear then the ozone concentration will increase.

The sum of reactions 2, 3 and 4 is nil yet the nitrogen dioxide which is readily photolysed is, in the early stages of reaction, produced at a faster rate than it is destroyed. This implies that one or more species in addition to ozone are responsible for the oxidation of nitric oxide to nitrogen dioxide. It is now generally accepted that the oxidation is performed by ozone or a peroxy, radical the general reaction being

$$\left.\begin{matrix} O_3 \\ RO_2 \\ HO_2 \\ RCO_3 \end{matrix}\right\} + NO \longrightarrow NO_2 + \left\{\begin{matrix} O_2 \\ RO \\ OH \\ RCO_2 \end{matrix}\right. \quad \ldots (5)$$

Smog chamber studies have shown that the addition of a small amount of carbon monoxide greatly increases the rate of nitric oxide loss [106] and the above reactions 2 to 5 are not sufficient to explain this increase. A chain mechanism in which one hydroxyl radical can oxidise several nitric oxide molecules in the presence of carbon monoxide has been used to explain the increase.

$$OH + CO \longrightarrow H + CO_2$$

$$H + O_2 + M \longrightarrow HO_2 + M$$

$$HO_2 + NO \longrightarrow OH + NO_2$$

net reaction $CO + NO + O_2 \longrightarrow CO_2 + NO_2$

The observed rate of alkene removal is faster than would be expected from oxidation by ozone and oxygen atoms alone and again radical intermediates are needed to explain the rate of alkene disappearance. Calvert et al. (105) have used a mechanism consisting of over 200 reactions to computer simulate smog chamber conditions and by fitting this mechanism to smog chamber data have determined the major creation and loss processes of the active species in smog eg. OH, HO_2, RO, RO_2, NO_3 and O_2 ($^1\Delta$). Using this method they showed that OH radicals are responsible for over 80% of the alkene consumption in the early stages of a smog chamber experiment. The other species which become important at longer times are ozone, hydroperoxy (HO_2), oxygen atoms, and alkoxy radicals (RO). The reactions of nitrogen trioxide (NO_3) and singlet molecular oxygen ($O_2(^1\Delta)$ with the alkene are insignificant. (109) The importance of hydroxyl radicals in the oxidation of the alkene has been supported by the work of Lloyd et al.. (110) They have measured the initial rates of disappearance of a series of alkanes, alkenes and aromatic hydrocarbons in a smog chamber experiment. Assuming that the observed hydrocarbon loss is solely due to reaction with hydroxyl radicals they obtained a series of relative rate constants for hydroxyl radical, hydrocarbon reactions. These rates appear to agree well with values obtained for hydroxyl radical reactions in

conventional kinetic systems supporting the assumption of hydroxyl only attack on the hydrocarbon in the smog chamber.

The conclusions of Calvert et al. based on this mechanism must be treated carefully as the results are highly sensitive to mechanistic changes. In an earlier paper [111] they showed that alkoxy radical attack on the alkene was important but the subsequent inclusion of the additional reaction

$$CH_3O + O_2 \longrightarrow CH_2O + HO_2$$

greatly lowered the concentration of the radical so the effect of its attack on the alkene was substantially reduced.

A large number of radicals are required to explain the chemistry of the smoggy atmosphere but at present only the hydroxyl radical has been directly detected. [112, 113] The production and rates of reactions of these radicals are of primary importance to the complete understanding of smog. Several radicals are assumed to come from the ozone, oxygen atom oxidations of the alkene. Particularly important are the hydroperoxy (HO_2) and alkylperoxy (RO_2) radicals. These are important in the nitric oxide oxidation and upon reduction produce the equally important hydroxyl and alkoxy radicals.

The sources of radicals are numerous and as an example consider the sources of the hydroxyl radical OH. According to the model of Calvert et al. [105] the most important source of OH is from hydroperoxy oxidation of nitric oxide

$$HO_2 + NO \longrightarrow OH + NO_2 \quad \ldots\ldots\ldots (5c)$$

the other major source is from the photolysis of nitrous acid

$$HONO + h\nu \longrightarrow OH + NO \quad \ldots\ldots\ldots (9)$$

Although it has been identified in a smog chamber [114] the source of nitrous acid is still not fully understood. It can be formed by reaction of hydroperoxy radicals with nitrogen dioxide [100]

$$HO_2 + NO_2 \longrightarrow HONO + O_2 \quad \ldots\ldots\ldots (10)$$

by the reverse of reaction 9 or by the termolecular reaction

$$H_2O + NO + NO_2 \rightleftharpoons 2HNO_2 \quad \ldots\ldots\ldots (11)$$

The homogeneous gas phase rate of reaction 11 is slow and it is ignored in the model of Calvert et al., however it appears as if the reaction is heterogeneous. It may be possible for the reaction to take place on the surface of suspended soot or dust particles or in water droplets. If this is the case the reaction may well be a significant source of nitrous acid in a polluted atmosphere. Similar reactions are responsible for the production of other radicals in the smog.

The ultimate decrease in nitrogen dioxide concentration represents the effect of the irreversible reactions removing nitrogen from the NO/NO_2 cycle. Examples of these reactions in decreasing order of importance are:

$$OH + NO_2 + M \longrightarrow HONO_2 + M \quad \ldots\ldots\ldots (12)$$

$$CH_3CO_3 + NO_2 + M \longrightarrow CH_3CO_2ONO_2 + M \quad \ldots\ldots\ldots (13)$$

$$CH_3O + NO_2 + M \longrightarrow CH_3ONO_2 + M \quad \ldots\ldots\ldots (14)$$

The product of reaction 13 is peroxyacetyl nitrate (P.A.N.) which has been identified as one of the major eye irritants in smog. (101)

The major features of Figure II.6 can be explained by current models although there is a danger that with the number of unknown rate constants what should be a test of a mechanism could become an exercise in curve fitting. (103) The simulations are still sensitive to small changes in mechanism and rate constant values. Dodge and Hecht (109) have endeavoured to find the reactions which introduce the most uncertainty into a simulation. They have taken a restricted model of 31 reactions and for each reaction calculated its S*U index. The S is the sensitivity of the concentration profiles to the value taken for the rate constant. The reaction of hydroxyl radical with the alkene has an S value of 28 showing the profiles are strongly dependent on the value taken for this rate constant whereas the reaction of oxygen atoms with alkene has far less effect with an S value of 2. The U is the known or estimated uncertainty in the rate constant. The S*U index is the product of these quantities so that reactions with high sensitivity and high uncertainty have high S*U values and more accurate data on the reactions is desired in order to better define the model. Reactions with high S*U values were those for the production and destruction of nitrous acid, and reactions of the OH, HO_2, RCO_3, RO and RO_2 radicals. These reactions have high uncertainties in the production, detection and estimation

of the reactive species.

The major challenge for experimentalists is to attempt to reduce the uncertainties in these sensitive reactions to impose more stringent restrictions on the models and so increase their accuracy and reliability. The ultimate aim of devising measures for smog control can only be considered once a full understanding of the mechanism of smog production is realised.

3. PREVIOUS STUDIES OF ALKYL NITRITE REACTIONS

Until the last year or two the interest in the gas phase chemistry of alkyl nitrites has been restricted to photolysis and pyrolysis studies. However recently, three direct studies of alkyl nitrite reactions have been carried out.

(1) Photolysis of Alkyl Nitrites

There have been many studies of the photolysis of the alkyl nitrites, [8,115-122] but most of the earlier studies yielded little information as techniques were not available to detect photolysis products.

A number of pieces of significant experimental work have lead to a better understanding of the mechanism of the photolysis. These are now summarised. Nitroxyl (HNO) was detected by infrared spectroscopy in the photolysis of methyl nitrite in an argon matrix. [117] Photolysis in an esr cavity at 77K showed no evidence for methyl radical production and a poorly resolved quartet absorption was assigned to the methoxy radical. [8]

Examination of the flash photolysis of methyl nitrite in the presence of added nitric oxide showed that nitroxyl was not formed in the primary photolytic step but in the reaction of methoxy radicals with nitric oxide. (120)

The most extensive study of the photolysis of pure nitrite has been undertaken by Wiebe et al.. (121-122) They examined the photolysis of methyl nitrite at 366nm alone, and in the presence of nitric oxide, nitrogen dioxide, oxygen or carbon monoxide using mass spectrometric and gas chromatographic analysis. The quantum yield for the photolysis was found to be 0.76 and products detected in the absence of added compounds were formaldehyde, methanol, water, nitrogen, carbon monoxide, nitric and nitrous oxides. The mechanism postulated was:

$CH_3ONO + h\nu \longrightarrow CH_3O^* + NO$

$CH_3O^* + M \longrightarrow CH_3O + M$ . . . . . (1)

$CH_3O + NO \longrightarrow CH_2O + HNO$ . . . . . (2a)

$\longrightarrow CH_3ONO^*$ . . . . . (2b)

$CH_3ONO^* + M \longrightarrow CH_3ONO + M$ . . . . . (3)

$2HNO \longrightarrow N_2O + H_2O$ . . . . . (4a)

$\longrightarrow H_2O_2 + N_2$ . . . . . (4b)

$HNO + 2NO \longrightarrow N_2 + HNO_3$ . . . . . (5)

$CH_3O^* \longrightarrow CH_2O + H$ . . . . . (6)

$H + NO + M \longrightarrow HNO + M$ . . . . . (7)

(the asterisks indicate excited species).

They were able to determine the branching ratios for reactions 2 and 4 as

$$\frac{k2a}{k2a+k2b} = 0.145 \quad \text{and} \quad \frac{k4a}{k4b} = 51$$

The quantum yield of nitrous oxide was determined and was high at low pressures, up to 0.25, but at high pressures decreased to 0.055 as all the excited methoxy was collisionally quenched. In the high pressure limit the yield of nitrous oxide was used as a measure of the extent of reaction 2. Alone and in the presence of added nitric oxide reaction 2 is the major loss process for methoxy radicals but with added carbon monoxide the nitrous oxide yield falls indicating that the radicals are reacting with the carbon monoxide. Some carbon dioxide was detected but not sufficient for this to be the major product from carbon monoxide.

In the absence of additional compounds and at small extents of photolysis the minor products can be produced by the radical reactions

$$2CH_3O \longrightarrow CH_2O + CH_3OH \quad (9a)$$

$$\longrightarrow CH_3OOCH_3 \quad (9b)$$

$$CH_3O + HNO \longrightarrow CH_3OH + NO \quad (10)$$

however once the nitric oxide concentration builds up these reactions become of little importance. Carbon monoxide appears to come from methoxy removal probably via reaction with formaldehyde

$$CH_3O + CH_2O \longrightarrow CH_3OH + CHO \quad (11)$$

with the CHO giving CO upon further reaction.

In the presence of oxygen or nitrogen dioxide the additional product formed is methyl nitrate coming from reaction of methoxy with nitrogen dioxide

$$CH_3O + NO_2 \longrightarrow CH_3ONO_2 \quad (12a)$$

$$\longrightarrow CH_2O + HONO \quad (12b)$$

where it was found that $k_{12a} \sim k_{12a} + k_{12b}$. This agrees with Baker and Shaw [123] who found $\frac{k_{12a}}{k_{12a} + k_{12b}} = 0.91$.

Wiebe et al. postulated the oxidation of nitric oxide to be performed by the HO_2 radical via the reactions

$$CH_3O + O_2 \longrightarrow CH_2O + HO_2 \quad \ldots\ldots\ldots (13)$$

$$HO_2 + NO \longrightarrow OH + NO_2 \quad \ldots\ldots\ldots (14)$$

with the OH being scavenged by either nitric oxide or nitrogen dioxide.

Gay et al. [124] have photolysed a range of nitrites in both air and pure oxygen in a 460 litre vessel equipped with a multipass cell of path length 172 or 344 metres and a Fourier Transform IR Spectrometer operating in the range of 700-3400 cm^{-1}. This equipment is capable of detecting concentrations of species in the parts per million (ppm) range. Between 2 and 10 ppm. of the nitrite were photolysed in an atmosphere of purified air and in the case of methyl nitrite the products were formaldehyde, carbon monoxide, nitric acid, ozone, formic acid, nitrogen dioxide and dinitrogen tetroxide (N_2O_5). The mechanism invoked was virtually the same as that of Wiebe in the presence of oxygen but additional reactions were required to account for the lesser additional products.

$$CH_3ONO + h\nu \longrightarrow CH_3O + NO$$

$$CH_3O + \begin{cases} NO \longrightarrow CH_2O + HNO & \ldots\ldots\ldots (2a) \\ NO_2 \longrightarrow \quad\; HNO_2 & \ldots\ldots\ldots (12b) \\ O_2 \longrightarrow \quad\; HO_2 & \ldots\ldots\ldots (13) \end{cases}$$

$$HCO + O_2 \longrightarrow HO_2 + CO \quad \ldots\ldots\ldots (15a)$$

$$\longrightarrow HCO_3 \quad \ldots\ldots\ldots (15b)$$

$$2HCO_3 \longrightarrow 2HCO_2 + O_2 \quad (16)$$

$$HCO_2 + CH_2O \longrightarrow HCOOH + HCO \quad (17)$$

$$OH + NO_2 + M \longrightarrow HONO_2 + M \quad (18)$$

$$N_2O_5 + H_2O \longrightarrow 2HONO_2 \quad (19)$$

$$NO + O_3 \longrightarrow NO_2 + O_2 \quad (20)$$

$$NO_2 + O_3 \longrightarrow NO_3 + O_2 \quad (21)$$

$$NO_2 + NO_3 \longrightarrow N_2O_5 \quad (22)$$

$$NO_2 + h\nu \longrightarrow NO + O \quad (23)$$

$$O + O_2 + M \longrightarrow O_3 + M \quad (24)$$

Reactions 15 and 18 were implied by Wiebe but not specifically included in his mechanism and reactions 20 to 25 and/or reactions 13 and 14 could be used to explain the oxidation of nitric oxide in both experiments. Gay computer modelled this system extending the above mechanism to 55 reactions and 26 species and achieved a good fit to the experimental data.

Photolysis of ethyl nitrite under similar conditions gave essentially the same products as methyl nitrite except that peroxyacetyl nitrate (P.A.N.) was a major product. The mechanism for P.A.N. production is:

$$CH_3CH_2ONO + h\nu \longrightarrow CH_3CH_2O + NO$$

$$CH_3CH_2O + NO \longrightarrow CH_3CHO + HNO$$

$$CH_3CHO + OH \longrightarrow CH_3CO + H_2O$$

$$CH_3CO + O_2 + M \longrightarrow CH_3\text{-}CO_3 + M$$

$$CH_3\text{-}\underset{\underset{O}{\|}}{C}\text{-}O_2 + NO_2 + M \longrightarrow CH_3\text{-}\underset{\underset{O}{\|}}{C}\text{-}O\text{-}O\text{-}NO_2 + M$$

P.A.N.

The observation of P.A.N. in this system supported the mechanism postulated for its production in smog.

(2) Pyrolysis of Alkyl Nitrites

The study of the pyrolysis of alkyl nitrites is similar to that of the photolysis in that the initial bond rupture is the same and the secondary reactions following this bond rupture are likely to be the same. The difference is in the temperature at which the experiment is performed.

As with the photolysis there have been many studies of the pyrolysis of nitrites but the early studies [125-130] produced little detailed information.

The first detailed quantitative study of the pyrolysis of nitrites was carried out on ethyl nitrite by Levy. [131] He used a mass spectrometer and an infrared spectrometer to detect products of the pyrolysis at concentration levels which were impossible for earlier workers. He pyrolysed between 10 and 50 Torr of nitrite at temperatures of 434 to 474K and detected nitrous oxide, acetaldehyde, ethanol and nitric oxide but neither methane nor formaldehyde. The addition of large amounts of nitric oxide increased the yields of acetaldehyde and nitrous oxide while addition of acetaldehyde suppressed the production of nitrous oxide. He postulated the mechanism:

$$C_2H_5ONO \longrightarrow C_2H_5O + NO \quad \ldots\ldots\ldots (1)$$

$$C_2H_5O + NO \longrightarrow CH_3CHO + HNO \quad \ldots\ldots\ldots (2)$$

$$2HNO \longrightarrow H_2O + N_2O \quad \ldots\ldots\ldots (3)$$

$$C_2H_5O + HNO \longrightarrow C_2H_5OH + NO \quad \ldots\ldots\ldots (4)$$

with the following additional reactions becoming important in the presence of added acetaldehyde

$$C_2H_5O + CH_3CHO \longrightarrow C_2H_5OH + CH_3CO \quad . . . . . (5)$$

$$CH_3CO \longrightarrow CH_3 + CO \quad . . . . . (6)$$

If reaction 4 is slow compared to reaction 2 then any removal of ethoxy radicals by other nitric oxide will lower the nitrous oxide yield as is found when acetaldehyde is added.

Adler et al. (132) examined the products of alkyl nitrite pyrolyses by trapping out the products and found carbonyl compounds consistent with the above mechanism but they also detected lower carboxyl compounds. These are consistent with the unimolecular decomposition of the alkoxyl radical. The observations of Rice and Rodowskas (130) suggested the decomposition

$$CH_3 - CH_2O \longrightarrow CH_3 + CH_2O$$

and Adler et al. found products consistent with the decomposition.

$$R_1R_2R_3CO \longrightarrow R_1 + R_2R_3CO$$

Adler et al. also found that the bond fission took place at the carbon to which the oxygen is attached and that an alkyl radical formed in preference to an hydrogen atom.

The most extensive study of methyl nitrite pyrolysis was undertaken by Phillips (133) who pyrolysed samples between 147 and 244°C and using an IR spectrometer detected formaldehyde, methanol, nitrous and nitric oxides, carbon monoxide, nitrogen, hydrogen cyanide, water and CH_2NOH. He varied surface to volume ratios in his reaction vessels and obtained the same yields and on this basis he discounted heterogeneous reactions

in all but very dirty systems. The mechanism he postulated was similar to that of Levy.

$$CH_3ONO \longrightarrow CH_3O + NO \quad (1')$$

$$CH_3O + NO \longrightarrow CH_2O + HNO \quad (2')$$

$$2HNO \longrightarrow N_2O + H_2O \quad (3')$$

$$2CH_3O \longrightarrow CH_2O + CH_3OH \quad (7)$$

$$CH_3O + CH_2O \longrightarrow CH_3OH + HCO \quad (8)$$

$$HCO + NO \longrightarrow HNO + CO \quad (9)$$

$$CH_3O + CH_3ONO \longrightarrow CH_3OH + CH_2O + NO \quad (10)$$

Addition of cyclohexene as a hydrogen donor increased methanol and nitric oxide yield but reduced nitrous oxide consistent with reaction 2' being replaced by

$$CH_3O + H - C_6H_9 \longrightarrow CH_3OH + C_6H_9$$

Addition of formaldehyde slightly decreased nitrous oxide yield, but markedly increased methanol and carbon monoxide yield. On the other hand addition of acetaldehyde completely prevented nitrous oxide production but yields of methanol, nitric oxide and hydrogen cyanide increased. The attack of methoxy on formaldehyde will increase methanol and carbon monoxide yields via reactions 8 and 9 and still produce nitroxyl so keeping the nitrous oxide yield the same. Attack on acetaldehyde does not produce nitroxyl and the source of nitrous oxide is lost.

$$CH_3O + CH_3CHO \longrightarrow CH_3CO + CH_3OH \quad (11)$$

$$CH_3CO \longrightarrow CH_3 + CO \quad (12)$$

$$CH_3 + NO + M \longrightarrow CH_3NO \longrightarrow CH_2NOH + M \quad (13)$$

$$CH_2NOH \longrightarrow HCN + H_2O \quad (14)$$

To check that reaction 10 was important he produced

ethoxy radicals from diethyl peroxide under conditions where no methyl nitrite decomposition occurs. He found both ethanol and ethyl nitrite as reaction products. These were formed by the reactions

$$C_2H_5O + CH_3ONO \longrightarrow C_2H_5OH + CH_2O + NO \quad . \; . \; . \quad (10')$$

$$C_2H_5O + NO + M \longrightarrow C_2H_5ONO + M$$

showing reaction 10 to be important.

A recent study of the pyrolysis of a series of nitrites, from methyl nitrite to tertiary butyl nitrite, suggests that the initial bond rupture to produce alkoxy radical and nitric oxide may not be the only course for pyrolysis. Batt et al. (134) have pyrolysed 10^{-4} to 10^{-5}M of the nitrite in 0.9 atm of carbon tetrafluoride restricting pyrolysis to 1% decomposition and analysing the products by gas chromatography. Under these conditions the alkoxy radicals are lost by unimolecular decomposition to give a carbonyl compound and an alkyl radical. By following the appearance of the carbonyl compound the rate of decomposition was determined. Since methoxy radicals contain only one carbon there is no decomposition path open, so a large excess of isobutane was used as a hydrogen donor and the rate of appearance of methanol followed. In all cases addition of large amounts of nitric oxide suppressed the carbonyl or methanol production, by making the reaction with nitric oxide more favourable than the unimolecular decomposition.

$$RO + NO \longrightarrow RONO$$

$$RO + NO \longrightarrow RO_{-H} + HNO$$

The carbonyls produced in this reaction can be easily distinguished from those of the unimolecular decomposition since they contain the same number of carbons as the initial nitrite. However in cases where the nitric oxide concentration was too low for the last reaction to proceed there was still a small amount of the heavier carbonyl compound formed e.g. methyl nitrite produced formaldehyde and, ethyl nitrite acetaldehyde as well as formaldehyde. These products are consistent with the single step elimination of nitroxyl (HNO).

$$RONO \longrightarrow RO_{-H} + HNO$$

Pyrolysis of tertiary butyl nitrite produces a little isobutene apparently from the elimination of nitrous acid

$$(CH_3)_3 - CONO \longrightarrow (CH_3)_2 - C{=}CH_2 + HONO$$

The reactions which give nitroxyl show an increasing carbonyl yield with surface to volume ratio and for methyl and isopropyl nitrites the low Arrhenius factors also indicate heterogenous reactions. However for ethyl nitrite the Arrhenius parameter suggest a homogeneous reaction and the reason for this difference is not yet clear.

Mendenhall et al. [135] have used the technique of very low pressure pyrolysis (VLPP) to attempt to detect directly the products of the pyrolysis of methyl nitrite. Nitrite pressures of between 0.1 and 1.0 mTorr were pyrolysed at 650K in a chamber which was coupled to a mass spectrometer. They detected nitroxyl, nitric oxide and methanol using deuterated methyl nitrite to confirm the assignments. They were however unable to

detect methoxy radicals and the kinetic analysis showed anomalies so they concluded that the reactions occurring were largely heterogeneous.

(3) Elementary Reactions of Alkyl Nitrites

The only results of gas phase reactions of alkyl nitrites to be published prior to the completion of this work were the reactions with hydroxyl radicals [136] and oxygen atoms. [9] In addition there was an unpublished study of the hydrogen atom reaction with methyl nitrite. [137]

The reaction of methyl nitrite with hydroxyl radicals was studied by adding the nitrite to an $H_2O_2/NO_2/CO$ reaction mixture which reacts by the mechanism

$$H_2O_2 + NO_2 \longrightarrow OH + HNO_3 \quad \ldots\ldots\ldots (1)$$

$$OH + CO \longrightarrow H + CO_2 \quad \ldots\ldots\ldots (2)$$

$$H + NO_2 \longrightarrow OH + NO \quad \ldots\ldots\ldots (3)$$

$$OH + CH_3ONO \longrightarrow \text{products} \quad \ldots\ldots\ldots (4)$$

$$OH + NO_2 + M \longrightarrow HNO_3 + M \quad \ldots\ldots\ldots (5)$$

It has been shown that a plot of $[H_2O_2]_0/[CO_2]$ against $[CH_3ONO] / [CO]$ is linear with slope k_4/k_2 and since k_2 is known k_4 can be determined by measuring the yield of carbon dioxide using a gas chromatograph. The rate constant k_4 was found to be $1.3 \times 10^{-12} cm^3 molec.^{-1} s^{-1}$ at 298K. No attempt was made to detect the products of reaction (4).

The reaction of methyl and ethyl nitrites with oxygen atoms has been studied in a discharge flow system

with emission from the oxygen atom - nitric oxide reaction being used to measure the atom concentration. (9) Examination of the stoichiometry led to the mechanism

$$O + CH_3ONO \longrightarrow OH + CH_2O + NO$$

and $$O + OH \longrightarrow H + O_2$$

The reaction of oxygen atoms with formaldehyde is fast and under the conditions used goes to completion.

$$O + CH_2O \longrightarrow OH + CHO$$

$$O + CHO \longrightarrow OH + CO$$

$$\longrightarrow H + CO_2$$

$$OH + O \longrightarrow O_2 + H$$

$$H + HCO \longrightarrow H_2 + CO$$

Using this mechanism the rate constant expression for the primary reaction was found to be

$$k = 2.3 \times 10^{-11} \exp\left(\frac{-21.8\ kJ.mol^{-1}}{RT}\right)$$

The analogous mechanism applies for the ethyl nitrite reaction and

$$k = 4.3 \times 10^{-11} \exp\left(\frac{-20.3\ kJ.mol^{-1}}{RT}\right)$$

The units of k are $cm^3 molec.^{-1} s^{-1}$

Moortgat et al. (137) have studied the reaction of methyl nitrite with hydrogen atoms in a discharge flow system coupled to a photoionisation mass spectrometer. They used total pressures of 1.5-4 Torr, atom concentrations of 30-120 mTorr and nitrite concentrations of 3-21 mTorr and obtained the rate constant of the primary reaction in $cm^3 molec.^{-1} s^{-1}$ as

$$k = (4.3 \pm 0.9) \times 10^{-13} \exp\left(\frac{-7.95 \pm 0.21\ kJ\ mol^{-1}}{RT}\right)$$

They identified NO, CH_3OH, CH_4, C_2H_6, CH_2O and H_2O as the major products and detected methyl and hydroxyl radicals as intermediates. They identified the primary step as :

$$H + CH_3ONO \longrightarrow CH_3OH + NO \quad \ldots\ldots\ldots (1)$$

$$\longrightarrow CH_2ONO + H_2 \quad \ldots\ldots\ldots (2)$$

$$\longrightarrow CH_3O + HNO \quad \ldots\ldots\ldots (3)$$

where pathway 1 represented $47\pm5\%$ of the total pathway. They identified and/or postulated the following secondary reactions

$$CH_2ONO \longrightarrow CH_2O + NO \quad \ldots\ldots\ldots (4)$$

$$H + CH_3O \longrightarrow CH_2O + H_2 \quad \ldots\ldots\ldots (5a)$$

$$\longrightarrow CH_3 + OH \quad \ldots\ldots\ldots (5b)$$

$$H + CH_2O \longrightarrow H_2 + CHO \quad \ldots\ldots\ldots (6)$$

$$OH + CH_2O \longrightarrow H_2O + HCO \quad \ldots\ldots\ldots (7)$$

$$H + CHO \longrightarrow H_2 + CO \quad \ldots\ldots\ldots (8)$$

$$H + HNO \longrightarrow H_2 + NO \quad \ldots\ldots\ldots (9)$$

where 5a represent between 0 and 61% of the total path. They confirmed the production of methanol by reacting methyl nitrite with deuterium atoms and formaldehyde by using d_3 methyl nitrite.

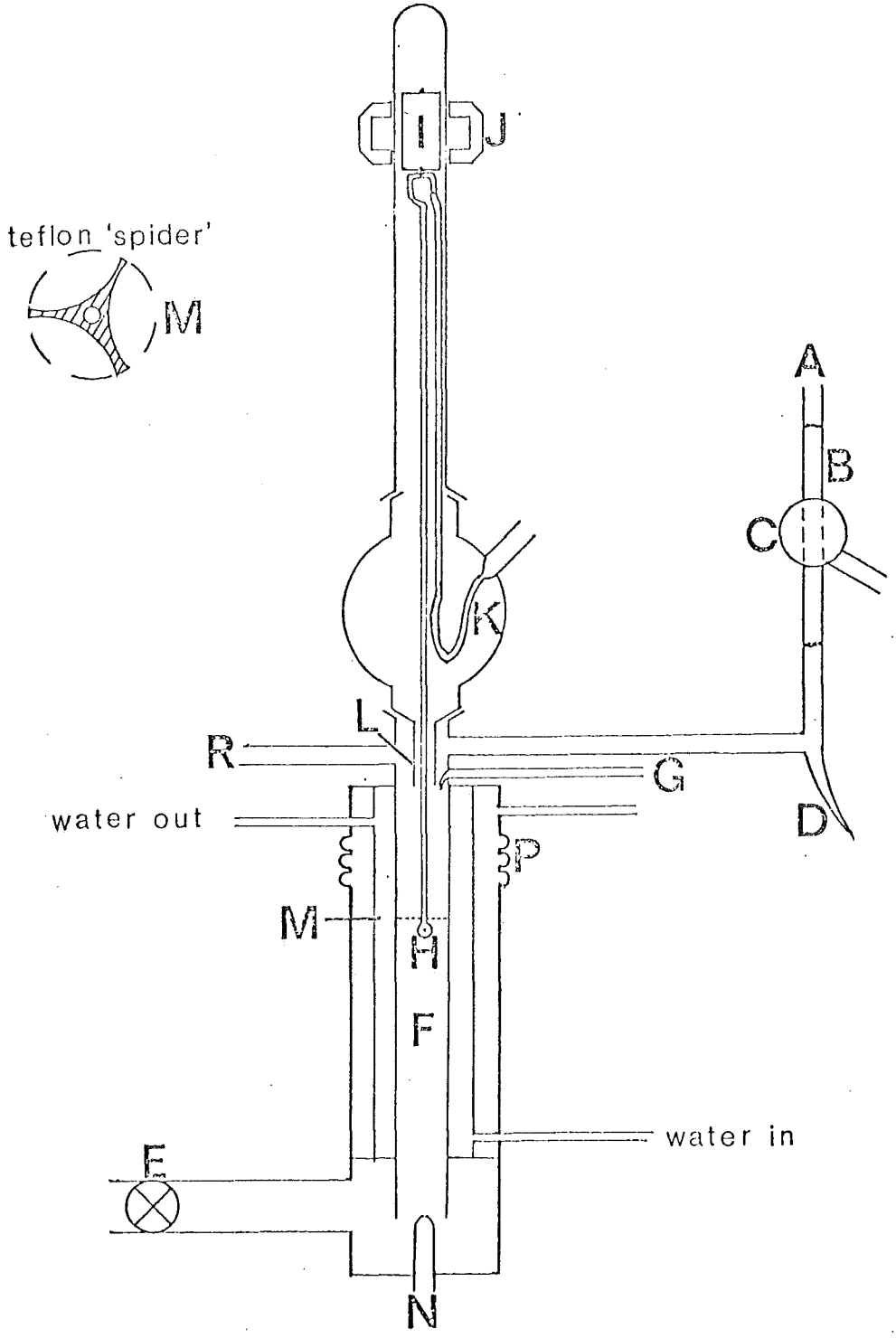

Figure III.1 Schematic Diagram of Discharge Flow System

CHAPTER III

EXPERIMENTAL

1. APPARATUS

(1) Discharge Flow System

Measurements on the reaction of the alkyl nitrites with hydrogen atoms were carried out in a conventional discharge flow system coupled to a mass spectrometer as shown in Figure III.1. A mixture of argon and hydrogen was admitted to the flow system at A and passed through a section of 12mm O.D. quartz tubing (B). Hydrogen atoms could be produced in this region by applying microwave power from a Microtron 200 generator unit, operated in the range 25-100 watts, via a type 213L air-cooled cavity (C). The light trap (D) and the two right-angle bends between the quartz section and the main flow tube were incorporated to prevent the Lyman α radiation produced within the discharge entering the flow tube and photolysing the nitrite. The gases then passed down the flow tube (F), a section of 20mm O.D. pyrex tubing, past the sampling leak to the ion source of the mass spectrometer (N) and out of the system through a large-bore greaseless stopcock (E). The flow was maintained by a Heraeus R150 Roots pump capable of 1500 $l.min^{-1}$ over the range 0.6 to 0.01 Torr backed by a Welch model 1397 2 stage rotary pump with a pumping speed of 400 $l.min^{-1}$ above 0.1 Torr. Typical flow velocities and total pressures were $2m.s^{-1}$ at 0.2 to 0.4 Torr with

only the rotary pump operating and 14 $m.s^{-1}$ at 0.10 to 0.15 Torr with the roots pump also operating.

Nitrogen dioxide used in determining the atom concentration was admitted through the inlet G some 35cm from the mass spectrometer sampling leak. The nitrite was admitted via a length of flexible P.V.C. tubing (K) and a length of axially placed 3mm O.D. tubing terminating in a glass sphere (H) with 6 small jets on its circumference. This jet assembly was attached to a soft iron slug (I) within the tube and the time available for reaction before the nitrite reached the sampling inlet to the mass spectrometer was varied by using a pair of external magnets (J) to move this slug and hence the nitrite inlet jet (H). The inlet jet (H) was maintained in the centre of the flow tube by the guide sleeve (L) and a small three legged teflon "spider" (M).

For reaction temperatures other than room temperature most of the flow tube section was encased in a water jacket through which water from a thermostatically controlled water bath was pumped. Calculations (see Appendix III) showed that in this work the temperature difference between gas and heated wall became negligible within 8mm of entering the heated section so this arrangement was sufficient to heat the gas. It was impossible to construct the heating jacket to enclose all of the flow tube and the 3cm closest to the sampling jet could not be directly heated. It will be shown that any variation in temperature within this region has no effect on the calculated rate constant

(section III.4(4) and Appendix IV). The water jacket was surrounded by an evacuable jacket to minimise heat exchange with the surroundings and a set of glass bellows (P) were incorporated to prevent strain when the jacket was evacuated.

The pressure in the flow tube was measured using a Consolidated Electrodynamic Corporation "micromanometer" Type 4155 which was connected to the tube at R. This differential pressure device was supplied with a reference vacuum of better than 10^{-5} Torr by a 2 stage mercury diffusion pump backed by either an Edwards Speedivac ES150 or an Hitachi 4VP-C3 2 stage 100 $l.min^{-1}$ rotary pump and was capable of measuring pressures from 0 to 0.5 Torr with an accuracy of 1×10^{-4} Torr.

The argon flow was measured by a calibrated capillary flow meter and the flows of all gases were controlled by Edwards Speedivac LB1B needle valves.

For the majority of experiments the walls of the flow tube were coated with orthophosphoric acid to minimise wall recombination of atoms, [72] although with new, acid-cleaned flow tubes there was also found to be no appreciable wall recombination. The phosphoric acid coating was deposited by filling the flow tube with a 10% solution of orthophosphoric acid, draining the solution out and pumping the water off the coated walls. To prevent the acid entering the ion source of the mass spectrometer through the leak, the mass spectrometer was slightly pressurised throughout the entire procedure.

A small portion of the central part of the gas

stream was continuously sampled into the ion source of the mass spectrometer via the sampling leak (N). Sampling leaks were prepared in the manner described by Dunn. [68] The instrument used in most of this work was an EAI QUAD 1210 Residual Gas Analyser. The mass spectrometer was used as supplied by the manufacturers except that when the tungsten filaments burnt out they were replaced by thoriated iridium. [138] These filaments were prepared by coating 0.005 in. diameter iridium wire with finely powdered thoria deposited using a cataphoretic process in an alcohol bath. [139] Also, the electrometer supplied was replaced by a Cary 401 Vibrating Reed Electrometer the output of which was displayed on a Yokogawa model 3046 chart recorder. This device measures the voltage drop when the ion current is passed through an input resistor of either 10^{10}, 10^{11} or $10^{12}\Omega$. It is possible to detect currents as low as 10^{-16} amps in this way but in this work currents measured were greater than 3×10^{-14} amps.

The mass spectrometer was evacuated by two Edwards Speedivac Model 2M3B mercury diffusion pumps operated with liquid air cooled traps and backed by a Welch model 1402B single-stage rotary pump. The pressure inside the mass spectrometer with the flow tube pumped out was 5×10^{-7} Torr and this was raised to 8×10^{-6} and 1×10^{-5} Torr for typical fast and slow flow reaction conditions respectively. These pressures are as measured on an uncorrected Veeco RG75 ionisation gauge head with an RG-2A controller.

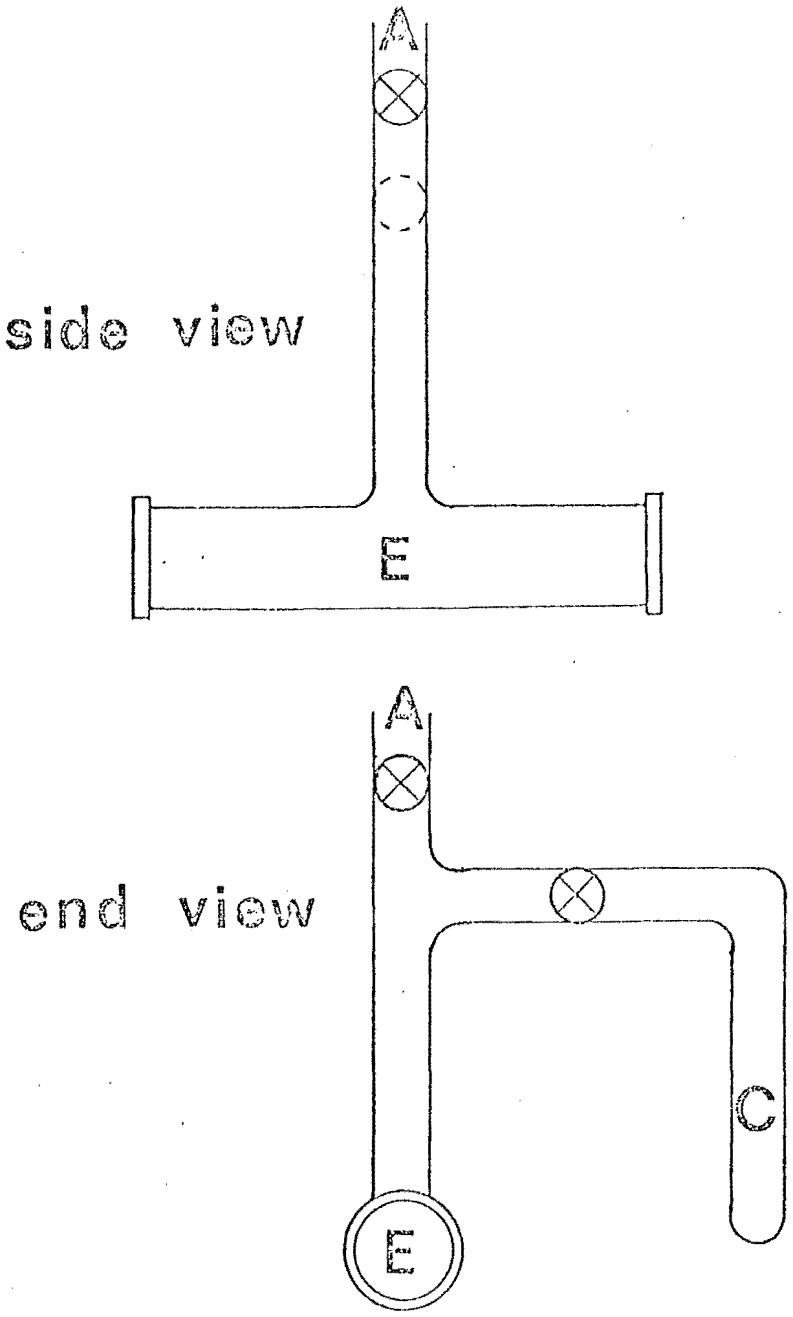

Figure III.2 Schematic Diagram of Static Reaction Vessel

(2) Static Reaction System

The reactions of the alkyl nitrites with ozone were carried out in a 7.5cm long 15mm I.D. black-painted cell with sodium chloride windows which was clamped in the sample beam of a Perkin Elmer Model 421 dual beam spectrophotometer set to operate in the range 600 cm^{-1} to 2000 cm^{-1}. The cell, shown in Figure III.2 consisted of two sections, the sampling cell (E) in the spectrophotometer beam and the side arm (C). The two regions were separated by a stopcock which enabled the reagents to be admitted to the cell without prior contact. Pressures in the cell of between 0 and 300 Torr were measured by a Texas Instruments model 144 quartz spiral gauge and higher pressures by an Edwards Speedivac Model CG3 diaphram gauge, both attached to the cell via A. Relative volumes of different sections of the cell were calibrated using standard gas expansion, pressure-volume techniques.

A second cell was used for the higher temperature runs which was identical to that described above but had a water jacket around the cell and side arm with only the taps and a minimal amount of lagged tubing outside of the jacket. Water from a thermostatically controlled water bath was pumped through this jacket to heat the gases in the cell.

The cell could be pumped out to better than 10^{-5} Torr by a two stage oil diffusion pump backed by an Hitachi model 4VP-C3 two stage 100l.min^{-1} rotary pump.

2. MATERIALS

Methyl and ethyl nitrites were prepared by the dropwise addition of 33% sulphuric acid to a saturated solution of sodium nitrite in 50-50 mixtures of either methanol-water or ethanol-water respectively. The nitrite vapour was swept by a stream of nitrogen through a concentrated sodium hydroxide solution followed by columns of calcium chloride and soda asbestos and finally collected in a trap at 195K. When sufficient nitrite had been collected the taps to the preparation system were shut, the trap surrounded by liquid air and the remaining nitrogen pumped off. The nitrite was distilled into a blackened bulb with only the central third of the distillate being retained. The nitrite was stored in this bulb or in a trap at liquid air temperatures until required.

Liquid methyl nitrate was prepared and purified as described in Organic Synthesis by nitrating methanol with a mixture of nitric and sulphuric acid.(100) Before being used in the vacuum system it was repeatedly frozen, pumped and thawed to ensure it was completely degassed.

Nitrogen dioxide was prepared and purified as described by Nightingale et al. (141) by reacting Matheson 98.5% pure nitric oxide with an excess of industrial grade oxygen, trapping the product at liquid air temperature and pumping off the excess oxygen.

Methane was prepared by fractionating a sample

of natural gas with methane content > 90% to give a sample whose purity was estimated to be > 98% by mass spectrometric analysis.

Argon, welding grade 99.99%, was passed through a trap packed with 5A molecular sieve held at 195K before entering the flow tube and industrial grade hydrogen was similarly treated except that the trap was held at 77K.

Deuterium gas was made by reacting metallic sodium with Aldrich gold label 99.8 atom percent deuterium oxide as described by Melville and Gowenlock.(142)

Hydrogen atoms were generated by passing a 15-20% mixture of hydrogen in argon through the microwave discharge.

Ozone was produced from industrial grade oxygen using a Welsbach ozonator which produced 3% ozone in the oxygen stream. The ozone was trapped on to silica gel at 195K, the trap closed off and the residual oxygen pumped away. The ozone was then stored on the silica gel at 77K until required when the temperature was raised until the desired amount of ozone had been liberated. Extreme care was taken to ensure that no ozone condensed directly onto the glass of the trap as this ozone explodes on warming, three such explosions occurred in this work. At one stage an argon-ozone mixture was stored in a bulb which exploded when the bulb was opened to the handling line. Notes on the purification and safe handling of ozone are presented in

Appendix II. It was found that even at 77K some decomposition of ozone occurred and it was necessary to use the infrared spectrophotometer to check the purity of the ozone liberated.

All stopcocks in the ozone preparation and handling system, the static reaction system and the discharge flow system, were Young Action greaseless stopcocks with teflon o-ring seals. These rings tended to become hard and brittle in the presence of nitrite, nitrogen dioxide and ozone and many had to be replaced. The grease stopcocks in the gas preparation lines and ground glass joints were lubricated with Apiezon N and M greases respectively and for joints where ozone was present Kel-F no 90 fluorocarbon grease was used.

3. CALIBRATION AND MEASUREMENT PROCEDURES - STATIC SYSTEM

In a typical kinetic run the complete cell system was pumped out and the nitrite distilled from a reservoir at 77K into the cell and the side arm. The pressure was monitored by the Texas Gauge and the purity checked by monitoring a nitrite absorption with the spectrophotometer. Once the desired pressure, usually 2-3 Torr, had been admitted, the stopcock to the side arm was shut and the rest of the nitrite pumped from the cell. Argon was then admitted to the cell from a 10l bulb at a pressure between 300 and 600 Torr. Rapid opening and closing the stopcock to the side arm allowed the argon to be admitted to the side arm with

negligible loss of nitrite. Once this was completed the excess argon was pumped from the sample cell.

Ozone from a reservoir absorbed on to silica gel at 77K was distilled into the sample cell, its pressure and purity being monitored in a similar manner to the nitrite. The check on ozone purity was more important than for the nitrite since ozone readily decomposed to oxygen and an accurate ozone pressure was necessary for the rate constant determination. Under no conditions where the pressure was monitored was there any evidence for ozone decomposition in the cell. When the required pressure of ozone, usually about 20 Torr, had been admitted the tap to the cell was closed.

The spectrophotometer was set to the correct frequency, the required chart speed and either the x5 or x10 expanded absorbance range. The reaction commenced with the opening of the stopcock between the sample cell and the side arm. The large pressure difference between the two sections ensured rapid reactant mixing. The chart recorder indicated the decrease in nitrite concentration during the course of the reaction and the time scale was deduced by concurrent calibration of the chart speed.

Attempts were made to quantitatively relate absorbance to concentration and although they were linearly related there were large day to day fluctuations in absolute sensitivity so that only relative nitrite concentrations could be obtained from the spectrophotometer. For this reason the reaction was

generally studied under pseudo first order conditions with ozone in greater than 10 fold excess and the rate constant was calculated from the disappearance of nitrite. The reaction was studied over a narrow concentration range, however this was enforced by the detection limit of nitrite, the necessary ozone excess and the need to maintain a safe concentration of ozone.

4. CALIBRATION AND MEASUREMENT PROCEDURES - DISCHARGE FLOW SYSTEM

(1) Calibrations

To determine concentrations of species within the flow tube from the height of mass peaks it was necessary to know the sensitivity of the mass spectrometer towards each compound. For simplicity all sensitivities were determined in separate experiments and defined relative to that of argon so that during a given kinetic run only the absolute sensitivity of argon was required. This together with the relative sensitivity values gave the absolute sensitivities of all compounds. Since the mass spectrometer had a sensitivity which varied with resolution, calibrations were carried out at the lowest resolution setting which gave clearly resolved peaks in order to maximise the sensitivity.

For the unreactive gases (argon and hydrogen) the sensitivities were found directly by closing off the flow tube from the pumps, admitting the gas to the flow

tube, measuring the appropriate peak height and simultaneously using the micromanometer to determine the pressure. The sensitivity was found to be pressure independent (within 2-3%) over the pressure range 0 - 0.5 Torr. The sensitivity of hydrogen was expressed relative to that of argon where the hydrogen and argon sensitivities were determined in alternate experiments.

To prevent possible damage to the stainless steel diaphram of the micromanometer head the sensitivities of the nitrites, methane and nitrogen dioxide relative to that of argon were determined indirectly. A previously prepared mixture of known composition of the gas and argon was admitted to the flow tube and the ratio of peak heights measured. The mixture composition then enabled the relative sensitivity to be calculated. The partial pressures of the components of these mixtures were measured by a Texas Instruments Model 144 quartz spiral gauge.

With all sensitivities expressed relative to that of argon only this sensitivity needed to be determined daily. However the relative sensitivities were checked regularly particularly whenever a change was made to the ion source of the mass spectrometer, such as filament replacement or cleaning. As the ion source became contaminated the absolute sensitivity dropped but the relative sensitivities remained constant over many months showing the stability of the mass spectrometer. Since the quadrupole mass spectrometer

does not have constant resolution the relative sensitivities applied only to a particular resolution setting which was kept constant for subsequent measurements.

In making up the nitrogen dioxide/argon mixture for relative sensitivity calibration, allowance was made for the presence of a large proportion of dimeric dinitrogen tetroxide. (143) However at the pressures in the flow tube no dimer would exist at equilibrium and as the breakdown of the dimer is rapid only nitrogen dioxide would be present in the flow tube. (144)

For most gases the peak due to the parent ion was used to monitor the gas concentration, however for ethyl nitrite the parent peak at M75 (mass peak 75) was too small to be used. Preliminary experiments showed that during reaction with hydrogen atoms the fragment ion peak M60 (CH_2ONO^+) remained strictly proportional to the parent at M75 showing that there were no complications due to reaction products contributing to M60. For this reason M60 was used to monitor ethyl nitrite concentration during reaction.

Typical sensitivities relative to argon with resolution settings in brackets were:

NO_2 (7.0)		0.200
CH_3ONO (9.0)		0.467
CH_4 (5.0)		0.803
C_2H_5ONO	mass 75 (9.5)	0.070
	mass 60 (9.0)	0.720
H_2 (1.0) relative to Ar (7.0)		0.84

Typical absolute sensitivities for argon expressed as amps of ion current per Torr of argon in the flow tube were:

Ar (7.0) 6.40×10^{-9} amps $Torr^{-1}$

Ar (9.0) 1.10×10^{-9} amps $Torr^{-1}$

The argon flowmeter was calibrated against a moving bubble meter. The gas passed from the cylinder through a di-n-butyl phthalate bubbler to maintain the line pressure at 1 atmosphere. Between this and the needle valve a soap bubble meter was inserted. After the needle valve the gas passed through the capillary flow meter and into the flow system. The time required for a soap bubble to sweep out a given volume in the bubble meter was recorded for various values of the pressure difference across the capillary as measured by a mercury manometer. The flow rates were then graphed against the pressure difference. Since the flowmeter was used only in the determination of flow velocity it was not necessary to convert the flow rates to standard conditions but to record the temperature and pressure, after making allowance for the presence of water vapour, and to incorporate these into the flow velocity expression. For a full description of the calculation of flow velocities see Appendix IV.

(2) Procedure for Flow Experiments

Immediately prior to the beginning of each flow run the argon sensitivity was determined using a range of pressures within the flow tube but under static

conditions. These measurements were continued until constant sensitivity (<5%) was obtained and then the flow was set up and the peak heights of argon and hydrogen were measured immediately along with the temperature and argon flow. The argon sensitivity together with the measured peak height under flow conditions gave the argon concentration at the sampling inlet and this along with the temperature and argon flow enabled the flow velocity at the sampling inlet to be calculated. At the end of a flow run this procedure was reversed i.e. argon peak height measured, the flow cut off and the argon sensitivity redetermined immediately. The argon pressure under flow conditions and the flow velocity were then recalculated. Generally there was no long term change in flow or sensitivity over the three to six hours for which the experiments lasted. It was found that in the short term nitrogen dioxide degraded and nitrite enhanced the sensitivity of the mass spectrometer and for this reason the argon peak height was regularly monitored under flow conditions. Since the argon flow and pressure remained constant, variations in argon peak height represented real changes in sensitivity. All sensitivities were corrected for these changes before calculation of concentrations.

The hydrogen atom concentration was measured by titration with nitrogen dioxide (see Section III.4(3)), the nitrite admitted, the experiment performed and the atom concentration redetermined. This procedure was

repeated as many times as required.

In some cases a long term sensitivity change was observed and the run was discarded if this variation was not monitored by the regular peak height checks.

(3) Titration for Atom Concentration

The hydrogen atom concentration was determined using the titration reaction with nitrogen dioxide. (64) The initial reaction is

$$H + NO_2 \longrightarrow OH + NO$$

followed by

$$OH + OH \longrightarrow H_2O + O$$

and $O + NO_2 \longrightarrow NO + O_2$

in the presence of excess nitrogen dioxide,

or $O + OH \longrightarrow H + O_2$

The overall reaction using either of the last two reactions as the major sink for oxygen atoms is

$$2H + 3NO_2 \longrightarrow 3NO + H_2O + O_2$$

This stoichiometry has also been confirmed by esr (60,145) measurements. It was calculated that all the above reactions are sufficiently rapid for the stoichiometry to reach 2:3 in the distance allowed for the titration.

In an experimental run the atom concentration was obtained by admitting nitrogen dioxide to the flow tube via the fixed inlet and measuring the average decrease in nitrogen dioxide peak height upon activation of the microwave discharge, ensuring always that nitrogen dioxide was in excess. The atom concentration was calculated using the known nitrogen

dioxide sensitivity and the 2:3 stoichiometry. The atom concentration was determined before and after a rate constant or stoichiometry experiment and the average taken, or, if values differed by more than 10% the experiment was discarded.

(4) Primary Rate Constant Determination

The rate constant was determined under conditions where there was a measurable variation in nitrite consumption with reaction time. To minimise the errors involved in concentration measurement it was aimed to keep the variations in consumption between 10 and 80%. The conditions were also chosen so there was a large, generally greater than 10 fold, excess of hydrogen atoms for four reasons. Firstly, with this large atom excess nearly all the loss of nitrite would be due to the primary reaction with hydrogen atoms, the reactions of secondary products with the nitrite being insignificant. Secondly, any subsequent reactions of secondary products with hydrogen atoms would not significantly alter the atom concentration, thus in a large excess of atoms the effects of secondary reactions on the calculated rate constant are small. Thirdly, since the atom concentration remains almost constant the second-order reaction becomes pseudo first-order and the sensitivity of the mass spectrometer towards nitrite is required only to ensure that the atoms are in excess. It is not however required in the calculation of the rate constant thus removing a possible source of error. Finally, provided the movable

inlet is moved entirely within the heated section of the flow tube and the rate constant obtained from a log concentration/time plot, any variation in temperature in the unheated 3cm of flow tube will have no effect on the calculated rate constant. This result only applies for first-order or pseudo first-order reactions and the proof of this statement can be found in Appendix IV.

In addition to having a large atom excess it was found that to avoid complications due to secondary reactions it was necessary to use low nitrite concentrations and to restrict the extent of reaction to below 25%. This was done by operating the flow system under the fastest flow conditions to keep the reaction times short. This low extent of reaction introduced errors into the nitrite concentration measurement but the method of analysis which involved least squares fitting to a log concentration/reaction time line ensured this was not a significant error.

It was often necessary to use up to 20cm lengths of the flow tube to obtain significant reaction at low concentrations in which case the viscous pressure drop down the tube became a major source of error. In extreme cases this pressure drop was up to 30% of the total pressure. The analysis to give the rate constant under these conditions is given in Appendix IV and this method was used to calculate all rate constant values under fast flow conditions. Under slow flow conditions the pressure drop is much less than this

and it was neglected for those rate constants determined under these conditions.

After the atom concentration had been determined less than one tenth of this concentration of nitrite was added to the gas stream. The mass spectrometer was set on the nitrite mass peak, the discharge activated and the nitrite shut off to give the background level. The nitrite was then added through the movable inlet system and measurements commenced once the signal had become stable. The inlet jet was moved back and forward within the flow tube and at each point the distance between inlet and sampling jets and the peak height were measured. This was done for at least one and a half cycles once it was clear that the concentration measurements were reproducible. The background and atom concentration were redetermined and net signals, namely the signal minus background, were used in the calculations.

Checks were made regularly to ensure there was no consumption of nitrite or nitrogen dioxide in the absence of hydrogen atoms by performing all the above procedures in the absence of hydrogen. Checks were also made to show there was no major loss in atoms down the tube in the absence of nitrite by performing the nitrogen dioxide atom titration procedure using the movable inlet and checking that the nitrogen dioxide consumption did not vary as the inlet was moved down the tube.

One major problem did appear in this work. It was

found that at very low hydrogen atom and nitrite concentrations there was a significant decrease in nitrite concentration when the discharge was activated. Using the previously determined value for the rate constant it was calculated that under these conditions no observable reaction should occur. Furthermore, this concentration decrease was independent of reaction time. The probable explanation is that the nitrite was being lost by photolysis by the Lyman α radiation produced in the discharge despite the measures taken to prevent this occurring. At the higher concentrations used when the rate constant was determined this decrease was about 10% of the total nitrite but since it was independent of reaction time the method of analysis meant it could safely be ignored when calculating the rate constant.

(5) Stoichiometry Determination

To determine the stoichiometry the same preliminaries were carried out as for the rate constant determination. To obtain the stoichiometry one reactant must be completely reacted and it was chosen to react the atoms to completion. To ensure complete reaction the flow velocity was lowered, the nitrite inlet was placed as far from the sampling jet as possible and a large excess of nitrite used. The consumption of nitrite when the discharge was activated was measured, additional nitrite added and the consumption again measured. This procedure continued until addition of

more nitrite had no effect on the nitrite consumption. The atom concentration was again measured and the average value used to calculate the stoichiometry.

The pressure drop down the tube would not be a source of error in this determination since the two inlets, for nitrite and nitrogen dioxide, were in similar positions and thus the pressure drop would be the same for both. The stoichiometry is the ratio of the consumption of the two gases and so the pressure drop correction will cancel.

(6) Product Analysis

Product searches were carried out at all possible conditions of flow, reaction time and concentration. The determination of products was difficult because many background peaks increased in the presence of hydrogen atoms. This effect was not noted in new flow tubes but became apparent within a short time of running the reaction in the tube and was ascribed to the presence of formaldehyde polymer on the flow tube walls. Neither heating the flow tube to 830K nor extended periods of conditioning with atoms were successful in removing the coating although washing with hot, concentrated sodium hydroxide lowered the effect somewhat. Furthermore the small decrease in nitrite ascribed to Lymanα photolysis in Section II4.(4) produced an increase in several of the peaks which was independent of reaction time.

The criterion used for a change in mass peak height

to indicate a reaction product was that an increase in reaction time produced a corresponding increase in the mass peak height.

Generally no quantitative yield could be assigned to a particular product because mass spectrometric sensitivities for intermediates were not known or the products could not be observed independently. The exception was methane in the methyl nitrite/hydrogen atom reaction. Preliminary experiments showed the above complications were small for M16 and the yield was obtained by measuring the increase in M16 when the discharge was activated along with the decrease in M61.

(7) Temperature

The temperature was measured using a -10 to 110°C mercury in glass thermometer which was hung beside the flow tube for the room temperature runs, or, used to measure the temperature of water entering and leaving the water jacket in the variable temperature system. The average temperature was used in the calculations. It was found that the temperature drop was less than 1°C in the water jacket at the highest temperatures and immeasurably small at all others.

CHAPTER IV

THE PRODUCTION AND MASS SPECTRUM OF GASEOUS NITROUS ACID

1. INTRODUCTION

The aim of this section was to produce gaseous nitrous acid (HONO) and to attempt to detect it mass spectrometrically with a view to studying some of its gas phase reactions.

In the gas phase, nitrous acid is known to exist in equilibrium with nitrogen dioxide, nitric oxide and water with an equilibrium constant of 1.67×10^{-3} $Torr^{-1}$. (146)

$$NO_2 + NO + H_2O \rightleftharpoons 2HONO \quad \ldots\ldots\ldots (1)$$

Attempts to study nitrous acid reactions using conventional kinetic techniques would be impossible since the low reagent concentrations required, generally below 1 Torr, would favour the dissociation to water and nitrogen oxides leaving very low nitrous acid concentrations. However some studies have found nitrous acid present at above equilibrium concentrations (147-150) suggesting that there may be a degree of kinetic control to the above equilibrium resulting in stable nitrous acid.

An extensive study of nitrous acid photolysis has been carried out by Cox (149,150) who produced above equilibrium concentrations of gaseous nitrous acid by removing the vapour over aqueous nitrous acid solutions. He found that when the mixture of 10ppm (parts per million) nitrous acid in an atmosphere of air was stored in a

teflon bag there was little change in composition over a period of hours. From this he concluded that the reverse of reaction 1, the decomposition of nitrous acid, is most probably heterogeneous and occurs by multilayer absorption of water on a surface. The initial reaction being

$$2HONO + n\,H_2O \longrightarrow N_2O_3 + (n+1)H_2O \quad . \; . \; . \; . \; (2)$$

The difficulty in producing nitrous acid led inevitably to problems in determining its mass spectrum. It is not listed in tables of mass spectra [151] and it has been suggested that it has neither a parent (M47) or a parent minus one (M46) peak. [152] One piece of evidence supporting a detectable nitrous acid parent peak comes from Spokes and Benson. [153] They made a mixture of NO, NO_2 and H_2O which they calculated to contain about 1% nitrous acid and found the mixture contained peaks at M30, M46 and M47 indicating a parent peak exists for nitrous acid.

It was planned to make above equilibrium concentrations of nitrous acid at low pressures, below 10 mTorr, and by taking the mass spectrum soon after production it was hoped that the acid would be sufficiently stable for it to be detected. Once the acid could be produced and detected its reactions could be studied.

2. PRODUCTION OF NITROUS ACID BY THE NITROGEN OXIDE - WATER EQUILIBRIUM

As one possibility it was planned to use the equilibrium reaction

$$NO_2 + NO + H_2O \rightleftharpoons 2HONO \quad \ldots\ldots\ldots\ldots (1)$$

to produce the nitrous acid. A mixture of initial concentrations 9 Torr NO_2, 11 Torr H_2O and 300 Torr NO would contain upon equilibration about 5 Torr of nitrous acid. If this mixture was suddenly expanded to a total pressure of 0.1 Torr, and if the nitrous acid was stable with respect to the reverse of reaction 1, then the nitrous acid concentration immediately after expansion would be about 1.6×10^{-3} Torr compared with the new equilibrium value of 4×10^{-5} Torr.

A mixture of this composition was made up and left in a 5l bulb for 24 hours to equilibrate. Samples of this mixture were then admitted to the flow system (described in Section III.1.(1)) under static conditions to total pressures of around 0.1 Torr. The mass spectrum in each case was taken as soon as practicable, which was generally about one minute after expansion. Under these conditions there was no apparent peak at M47 (mass peak 47) corresponding to the parent peak of nitrous acid. If the nitrous acid concentration was 1.6×10^{-3} Torr and nitrous acid possessed a parent peak of similar size to the other nitrogen oxides, such as nitric oxide and nitrogen dioxide, then the acid should have been detectable. However the equilibrium value of 4×10^{-5} Torr represents the limit of detection of the mass spectrometer towards species in the flow tube, thus nitrous acid at equilibrium concentration would be unlikely to be detected.

The reasons for the failure to detect nitrous acid could have been threefold. Firstly, the homogeneous rate of decomposition could have been sufficiently fast to lower the nitrous acid concentration below detectable limits before the mass spectrum was taken. Secondly, heterogeneous processes could have been responsible for the fast decomposition, or, thirdly, the nitrous acid could have been present but the absence of a strong parent peak at M47 may have prevented its detection.

3. PRODUCTION OF NITROUS ACID BY THE REACTION OF HYDROXYL RADICALS WITH NITRIC OXIDE

Nitrous acid can be formed in the gas phase by the termolecular reaction of hydroxyl radicals with nitric oxide.

$$OH + NO + M \longrightarrow HONO + M \quad . . . . . (3)$$

The rate constant for this reaction lies between 3 and 6×10^{-31} $cm^6 molec.^{-2} s^{-1}$. (154,155) In any system containing hydroxyl radicals one of the most important reactions is the radical combination

$$OH + OH \longrightarrow H_2O + O \quad . . . . . (4)$$

which has a rate constant of $2.3 \times 10^{-12} cm^3 molec.^{-1} s^{-1}$. (156) It may be calculated that for the rate of reaction 3 to exceed the rate of reaction 4 that:

$$\frac{[NO][M]}{[OH]} > 100 \text{ Torr}$$

The discharge flow system described in Section III.1.(1) was capable of producing hydroxyl radical concentrations

of 5×10^{-3} Torr in which case the above expression reduces to

$$[NO][M] > 0.5 \text{ Torr}^2$$

Concentrations of, for example, 0.5 Torr and 1.0 Torr for NO and M respectively would be required to achieve this condition, although higher total pressures and a greater fraction of nitric oxide in the total pressure would favour reaction 3 over reaction 4.

By partially closing the tap between the flow tube and the vacuum pump the flow velocity could be lowered with a simultaneous increase in flow tube pressure. By admitting high concentrations of nitric oxide under these conditions it was calculated that the above criterion could readily be exceeded in the discharge flow system available.

The major chemical problem was still the decomposition of the nitrous acid to nitrogen oxides and water. Since the homogeneous rate of this reaction appears to be slow there would be little decomposition in the 100-200 milliseconds between production of the nitrous acid and sampling by the mass spectrometer. In an attempt to reduce the rate of heterogeneous decomposition the walls of the flow tube were coated with orthophosphoric acid. This coating has been shown to inhibit heterogenous reactions of atomic and radical species [47] and it was hoped it would do the same for nitrous acid. This may not have been the case if all the water was not pumped from the orthophosphoric acid, in which case the damp coating

could have aided the decomposition by providing a water layer on the walls.

The experiments were carried out in flow tubes attached to three different mass spectrometers. The first was the magnetic deflection instrument described by Dunn, [68] the second was an E.A.I. QUAD. 150A residual gas analyser used as supplied but because of the age of the particle multiplier it had a sensitivity about the same as the first. The third was the E.A.I. QUAD. 1210 residual gas analyser described in Section III1.(1) which had a sensitivity over an order of magnitude higher than the other two.

(1) Production of Hydroxyl Radicals by the Reaction of Hydrogen Atoms with Nitrogen Dioxide

In the initial experiments, with the first two mass spectrometers, concentrations of hydrogen atoms of about 5 mTorr were generated as described in Section III.2.. Nitrogen dioxide was added through the titration inlet to generate hydroxyl radicals by the reaction: [64]

$$H + NO_2 \longrightarrow OH + NO$$

A large concentration of nitric oxide was then added less than 1cm downstream via the movable inlet.

When a slight excess of hydrogen atoms was used to ensure complete consumption of the nitrogen dioxide it was found that, at high nitric oxide flows, increasing the flow of nitric oxide increased the height of the peak at M46 but no peak at M47 was observed. The flow tube pressure when this increase occurred was

estimated to be between 1 and 2 Torr with probably greater than 60% of the total gas flow being nitric oxide. Attempts to use the mass spectrometer to accurately measure these concentrations gave absurdly low values and it was concluded that the sensitivity of the mass spectrometer had been severely degraded. This meant that the absolute and relative sensitivities, which were determined at pressures below 0.5 Torr, were no longer valid. A possible explanation for this was that the ion source was being run at a pressure at which ion molecule reactions became important and could have resulted in the lowered sensitivity. Also low concentrations of nitrogen dioxide were found to slightly degrade the sensitivity of the mass spectrometer, (Section III4.(2)) and it appears possible that nitric oxide may do the same. If this is the case then the very high nitric oxide concentrations in this study would greatly affect the sensitivity. To check that the hydroxyl radicals were not being lost by reaction 4 before contacting with the nitric oxide, the nitrogen dioxide was admitted through the moveable inlet and the nitric oxide admitted slightly upstream through the titration inlet so that the hydroxyl radicals were produced in the presence of a large excess of nitric oxide. The same results were obtained in this case as in that above indicating that nitrous acid if present does not possess a detectable parent peak.

The increase in the M46 peak could have been due to a fragment ion from the nitrous acid (NO_2^+). However

the large increase in the flow of nitric oxide would have increased the flow tube pressure. This could have lowered the efficiency of the discharge thereby decreasing the hydrogen atom concentration, so that not all the nitrogen dioxide was consumed. This unreacted nitrogen dioxide could then have caused the increase in M46. Increasing the microwave power to increase the atom concentration under these conditions decreased the peak at M46. This is consistent with reaction of the additional atoms with nitrogen dioxide or perhaps nitrous acid. It proved impossible to distinguish between nitrogen dioxide and nitrous acid contributions to M46 in this study.

This work was later repeated using the Quad 1210 and gave essentially the same results, but because of the greater sensitivity of this mass spectrometer a small peak at M47 was noted. This peak increased relative to M46 upon activation of the discharge and also on increasing the nitric oxide flow, although both M46 and M47 signals increased on quenching the discharge. In the presence of large concentrations of nitric oxide the ratio of peak height M47 to M46 varied from 0.02 with the discharge off, to a maximum of 0.06 with the discharge on. These results implied the presence of a small M47 parent peak for nitrous acid. However the variation in M47 to M46 peak height ratio with nitric oxide flow indicated nitrous acid production was not the only process occurring.

(2) Production of Hydroxyl Radicals by the Reaction of Hydrogen Atoms with Ozone

The reaction of hydrogen atoms with ozone was also used as a source of hydroxyl radicals. (64)

$$H + O_3 \longrightarrow OH + O_2$$

The experiment was performed using the lower sensitivity mass spectrometers in the same manner as in Section IV.2.(1) with the same results. At high nitric oxide flows an increase in nitric oxide flow increased the M46 peak with no M47 peak apparent. However the explanation of the increase in M46 was still ambiguous. If the hydrogen atom concentration was to drop as suggested in the previous section there would then be some unreacted ozone, which would rapidly oxidise the nitric oxide to nitrogen dioxide and increase the peak at M46

$$NO + O_3 \longrightarrow NO_2 + O_2$$

(3) Production of Hydroxyl Radicals by Discharging Water Vapour

To remove the possibility of a nitrogen dioxide contribution to M46 an alternative source of hydroxyl radicals was required. Discharged water vapour contains hydroxyl radicals (157) although this method of production has been shown to be unsatisfactory for kinetic purposes. (158,159) In addition to hydroxyl radicals, hydrogen and oxygen atoms, and hydroperoxy radicals are produced. Furthermore, it has been shown that the hydroxyl radicals are produced at low concentrations, less than 1% dissociation of water, and

that the radicals are not all produced in the discharge region. It appears as if the hydroxyl radicals may be produced by secondary reactions down the tube so that an almost constant concentration is maintained down the flow tube. (158) This contrasts with the production by hydrogen atom reactions with nitrogen dioxide or ozone. These reactions generate much higher initial hydroxyl radical concentrations but the radical reaction (4) causes a rapid subsequent decrease. Since this was only a preliminary qualitative study the disadvantages of using discharged water vapour as the hydroxyl radical source were outweighed by the lack of an M46 peak.

The argon carrier gas was saturated with water vapour at 273K (4.5 Torr) before admission to the flow system where the water vapour pressure was about 2 mTorr. This low concentration along with the low yield of radicals meant that the maximum hydroxyl radical concentration was less than in Sections IV.2.(1),(2). When a high flow of nitric oxide was added to the flow of discharged water vapour the mass spectrum obtained on the more sensitive Quad 1210 was much different to that obtained when the hydrogen atom reactions were used as radical sources. The peak at M47 increased as the nitric oxide flow was increased, whereas the M46 peak showed a much smaller increase. The results of a series of experiments are given in Table IV.1..

These results suggest that the mass spectrum of nitrous acid possesses a parent peak at M47 with perhaps a small peak at M46.

TABLE IV.1

Experiments to Detect Gaseous Nitrous Acid

Conditions Gas Mixture	Discharge	Mass Spectrometric Intensity * M46	M47
H_2O/Ar	Off	0	0
H_2O/Ar	On	1	1
H_2O/Ar/NO[a]	On	3	12
H_2O/Ar/NO[b]	On	7	14
H_2O/Ar/NO[b]	Off	13	6
H_2O/Ar/NO[c]	On	3	10

* Unit of mass spectrometric sensitivity 1 x 10^{-14} amps. Nitric oxide flow a~c>b.

4. DISCUSSION

The differences between mass spectra obtained with different sources of hydroxyl radicals could have several interpretations. The most likely is that considered earlier, where the large nitric oxide flow reduces the hydrogen atom concentration producing an excess of either nitrogen dioxide or ozone. The excess ozone would rapidly oxidise nitric oxide to nitrogen dioxide and in both cases the peak at M46 would increase. Another possibility would be the reverse of this situation where an excess of hydrogen atoms was produced

and these atoms could possibly react rapidly with any nitrous acid produced to give nitrogen dioxide

$$H + HONO \longrightarrow H_2 + NO_2$$

This nitrogen dioxide would also increase the height of the peak at M46.

In the experiments using water vapour as a hydroxyl radical source, in the presence of the large excess of nitric oxide, the peak at M46 decreases on activation of the discharge. This peak is at least 3 orders of magnitude less than the nitric oxide signal and could be due to a small nitrogen dioxide impurity in the nitric oxide. The hydrogen and oxygen atoms produced in the discharge would rapidly remove this nitrogen dioxide. This level of impurity is however far too low to explain the increase in M46 peak with nitric oxide flow found in experiments described in Sections IV. 2.(1),(2).

Before the reaction of hydroxyl radicals with nitric oxide can be used as a source of nitrous acid for kinetic experiments another method of hydroxyl radical production is required. Discharged water vapour has been shown to be generally unsatisfactory for kinetic experiments since the radicals are not produced entirely within the discharge region and other atoms and radicals are also present. The most common hydroxyl radical sources, viz. the reactions of hydrogen atoms with nitrogen dioxide or ozone, have been shown to be unsatisfactory in this particular study. Discharging hydrogen peroxide (H_2O_2) suffers from the

same problems as discharging water vapour. (157) The bimolecular reactions of atomic oxygen with molecular hydrogen, and atomic hydrogen with molecular oxygen

$$O + H_2 \longrightarrow OH + H$$

$$H + O_2 \longrightarrow OH + O$$

are both too slow to produce significant hydroxyl radical concentrations. (28) One possible source of hydroxyl radicals which would require a much higher pressure than was possible in this study would be to react hydrogen atoms with molecular oxygen at pressures of several Torr. The initial reaction would be the termolecular combination of the hydrogen atoms with the oxygen molecules to give the hydroperoxy radical which would react with additional hydrogen atoms to produce the hydroxyl radicals

$$H + O_2 + M \longrightarrow HO_2 + M$$

$$H + HO_2 \longrightarrow OH + OH$$

The rate constants for these reactions are

1.8×10^{-32} $cm^6 molec.^{-2} s^{-1}$ and

1.8×10^{-11} $cm^3 molec.^{-1} s^{-1}$ respectively. (28)

The other problem encountered in this study which must be overcome is the inability to use the mass spectrometer to accurately measure concentration. As discussed earlier this is due to either high total pressures or high nitric oxide concentrations in the ion source. Whatever the cause, the problem can be overcome by decreasing the size of the sampling inlet from the flow tube into the mass spectrometer ion source. This would lower the sensitivity of the mass spectrometer to species in the flow tube by increasing the pressure

differential between the sections, but as the currents measured in this study were well above the detectable limit a small reduction in sensitivity could be accommodated.

CHAPTER V

THE REACTIONS OF OZONE WITH METHYL AND ETHYL NITRITES

1. INTRODUCTION

In this section a study was made of the reactions of ozone with methyl and ethyl nitrites for two reasons. Firstly, the nitrites were used as model compounds for nitrous acid whose oxidation by ozone could be significant in the nitrogen oxide balance in the stratosphere (see Section II.2.(1)). Secondly, the alkyl nitrites have been postulated as intermediates in photochemical smog and computer mechanistic models consider only their loss by photolysis. [7] If their reaction with ozone were of comparable rate to their photolysis then this reaction should be included in future smog models, if not, then its exclusion could be justified.

2. FLOW SYSTEM STUDY

An attempt was made to study the reaction of methyl nitrite with ozone using the flow system described in Section III.1.(1). A mixture of ozone and oxygen was used as the carrier gas and the nitrite admitted through the movable inlet system. Under the slowest flows and at the highest concentration possible no reaction was observed. It was estimated that as little as 5% reaction could have been reliably detected

and using this value an upper limit for the rate constant of 10^{-18} $cm^3 molec.^{-1} s^{-1}$ was estimated.

When the reagents were admitted to the static system formed by isolating the flow tube from the pumps, the ozone concentration was found to decrease showing that the reaction, although slow, did proceed. To study the kinetics of the reaction it was necessary to admit the reagents to a static rather than flowing reaction vessel where they would react at a measurable rate. The flow system could not be used under static conditions since the geometry introduced mixing problems, nor could it be used as a stopped flow reactor. Attaching a small static reaction vessel to the mass spectrometer was possible but the sampling leak size would have severely restricted the pressures available in the reaction vessel. Ultimately the use of a mass spectrometer was rejected in favour of an infrared spectrophotometer to measure reagent concentrations and to facilitate product identification.

3. INFRARED SPECTRA

The infrared spectra of methyl and ethyl nitrites are shown in Figures V.1.a and 2.a respectively. The major absorptions are due to the terminal N-O stretch at 1600-1700 cm^{-1}, the methoxy nitrogen O-N stretch at around 800 cm^{-1} and the carbon oxygen stretch at around 1000 cm^{-1}. These absorptions are all doubled, the most pronounced being the N-O stretch at 1600-1700 cm^{-1}. This doubling is due to the presence of cis-trans

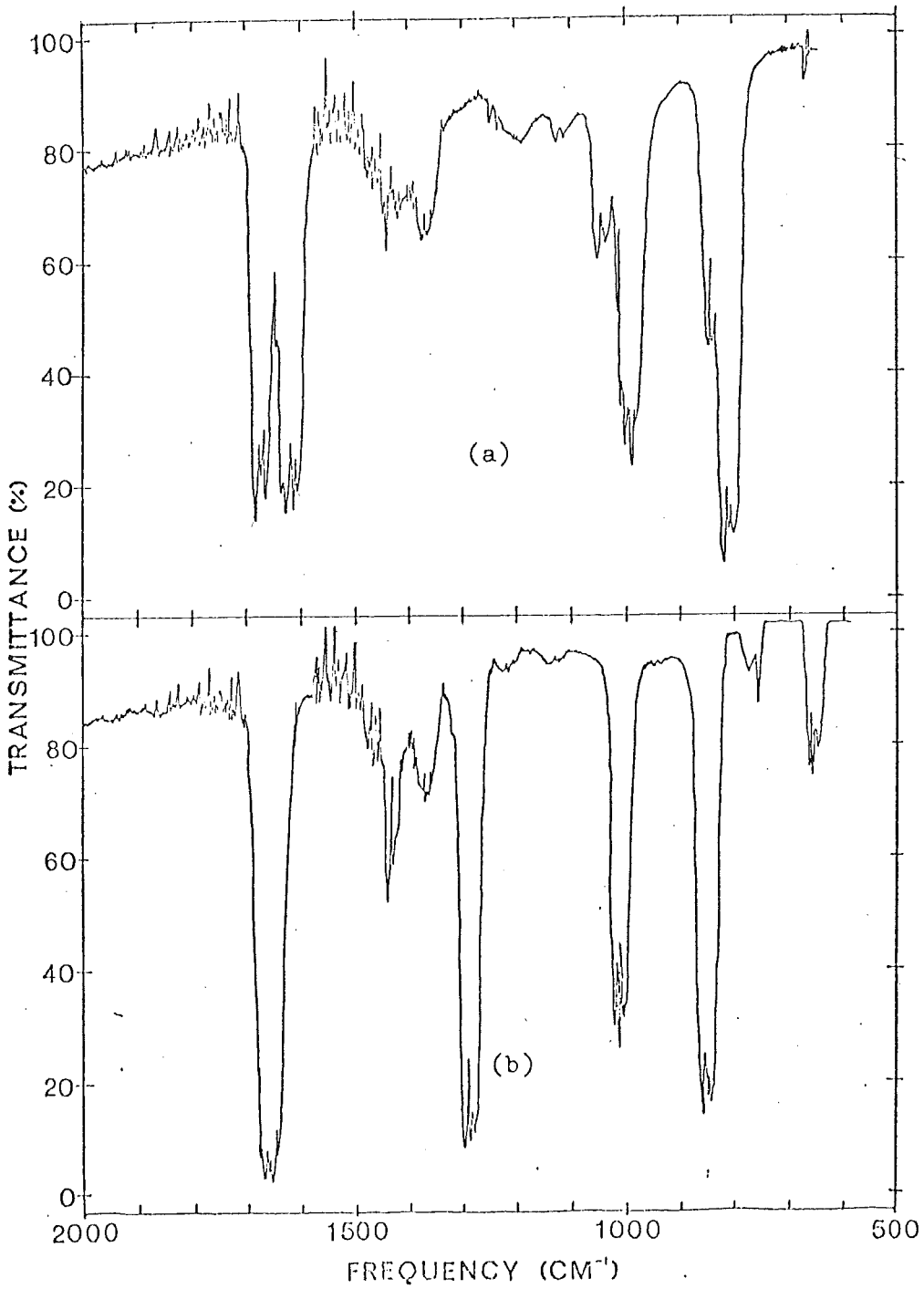

FIGURE V.1. (a) Infrared Spectrum of Methyl Nitrite

(b) Infrared Spectrum of Methyl Nitrate

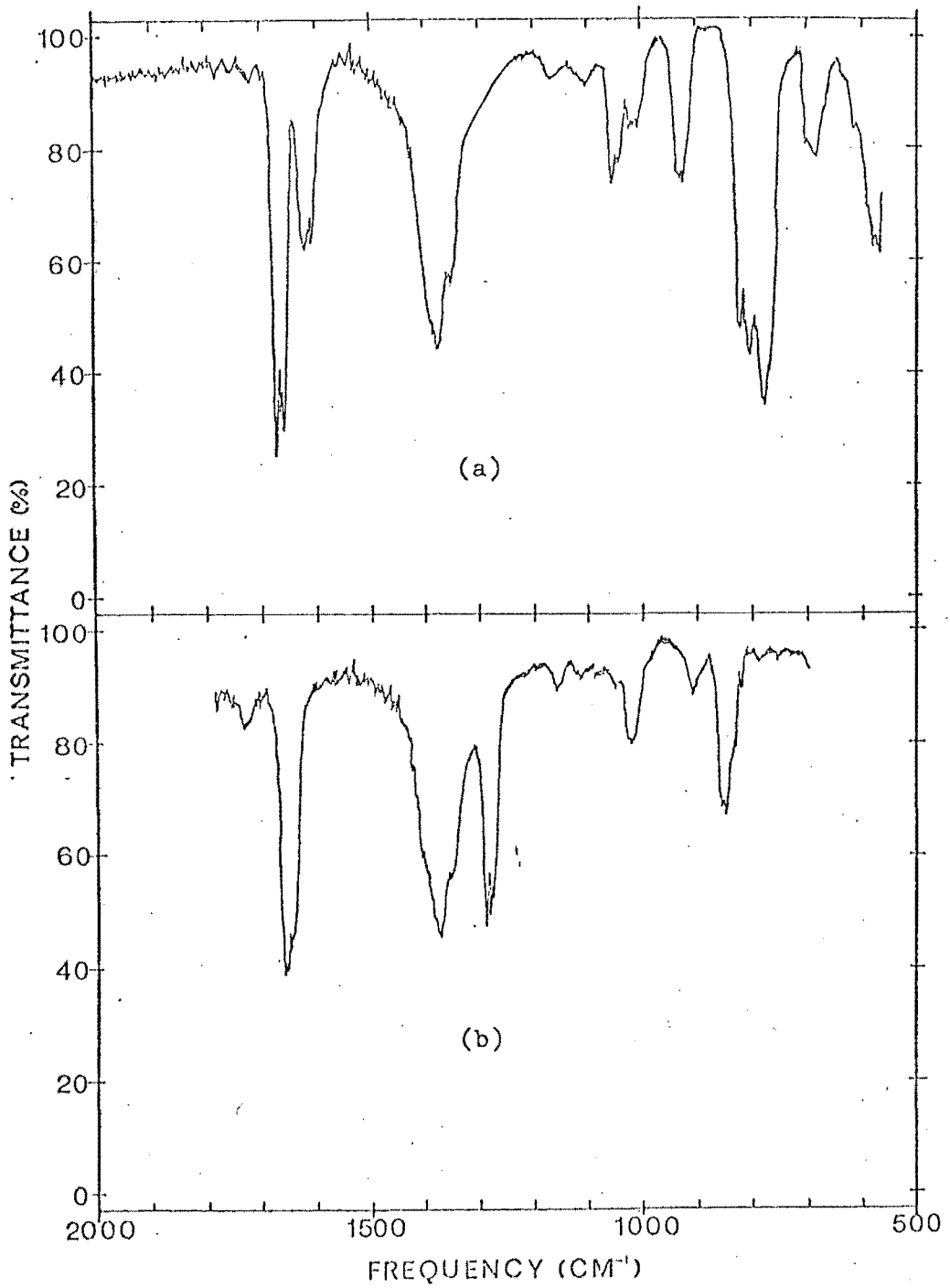

FIGURE V.2. (a) Infrared Spectrum of Ethyl Nitrite

(b) Infrared Spectrum of the Product of the Ethyl Nitrite-Ozone Reaction.

isomers produced by the hindered rotation about the CH_3O-NO bond. (5)

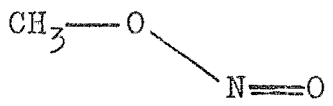

trans

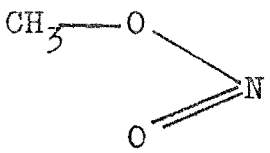

cis

Figure V.1.b shows the infrared spectrum of a specially prepared sample of methyl nitrate. The two major differences between the nitrate and nitrite spectra are the appearance of a strong absorption at 1270-1300 cm^{-1} being the symmetrical stretch of the nitrate group, and the condensing of the double absorptions of the nitrite into single absorptions as there is free rotation about all bonds in the nitrate. (160)

Ozone was found to have a single absorption system centred at 1000 cm^{-1} consistent with its simple structure.

4. PRODUCTS AND STOICHIOMETRY

The infrared spectrum of the product of the reaction of ethyl nitrite and ozone is shown in Figure V.2.b. This shows the features of a nitrate, viz. the nitrate absorption at 1270-1300 cm^{-1} and single absorptions due to the other major vibrations. These latter features contrast with the doublets observed in the nitrite spectra. The infrared spectrum of the product of the reaction of methyl nitrite and ozone showed the same features as that of the ethyl nitrite reaction and the spectrum was identical to that of the specially prepared sample of methyl nitrate.

This showed the nitrate to be a product of the ozonolysis of the nitrite. The other probable product from this reaction, oxygen, could not be detected as its vibrations are infrared inactive. There was no evidence for any other products.

As outlined in Section III.3 it proved difficult to relate infrared absorbances to absolute concentrations of nitrite and nitrate in the cell so only relative concentrations could be measured. However it was possible to determine the stoichiometry by measuring the relative consumptions of nitrite and ozone. On reaction with an excess of ozone the absorbance of methyl nitrate measured by the nitrate absorption at 1280 cm^{-1} was 0.084 $\pm$ 0.010 per Torr of reacted nitrite, and on reaction with an excess of methyl nitrite the absorbance of methyl nitrate was 0.071 $\pm$ 0.010 per Torr of reacted ozone. It was therefore concluded that one mole of ozone reacted with one mole of nitrite.

An experiment was performed in which there was no large excess of argon present and it was found that on reaction there was no pressure change. This showed that there was no change in the number of moles of gas on reaction.

The known product, the stoichiometry and the constant number of moles led to the conclusion that the reaction was

$$RONO + O_3 \longrightarrow RONO_2 + O_2$$

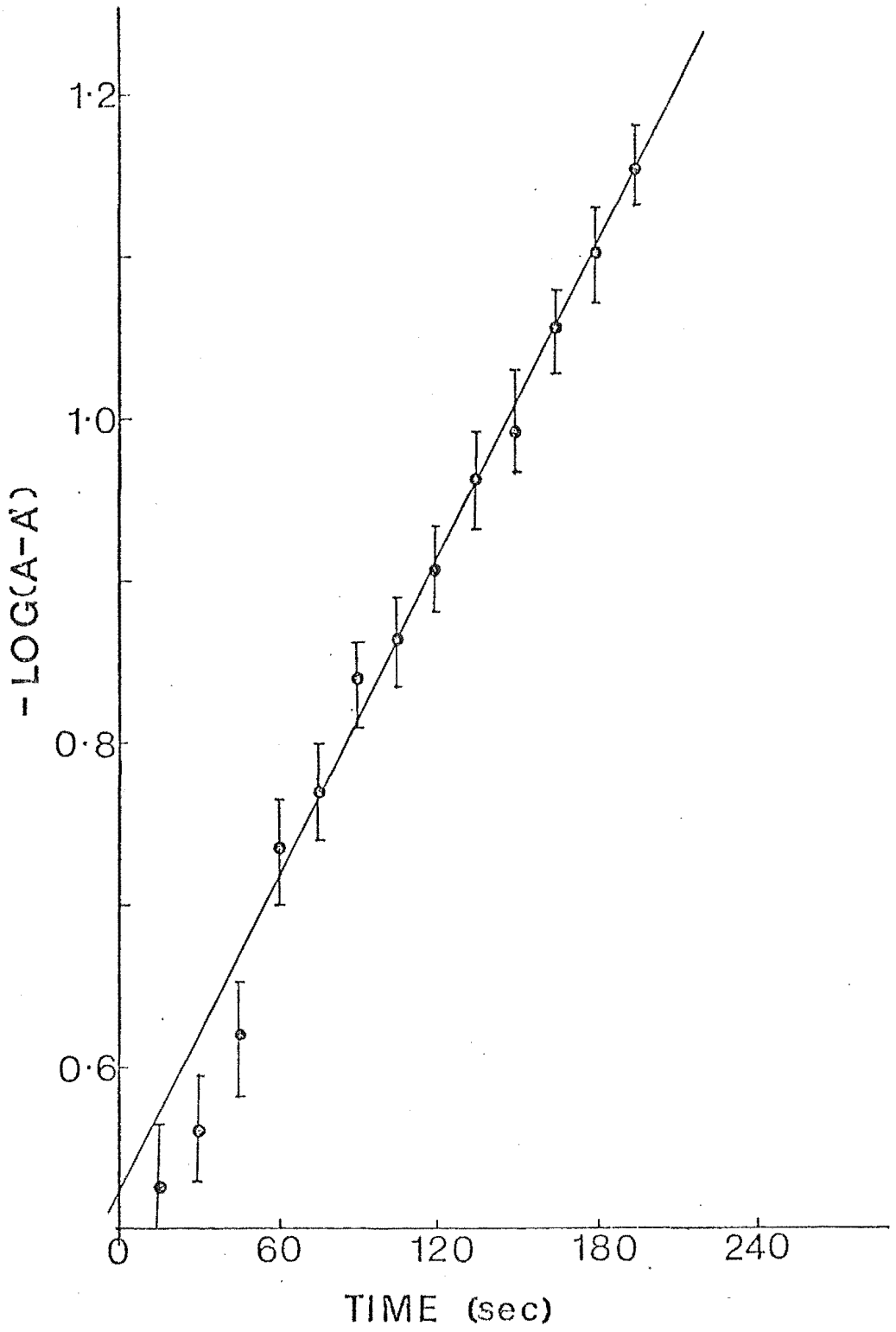

FIGURE V.3 Typical Guggenheim Plot for the Reaction of Methyl Nitrite with Ozone

5. RATE CONSTANT DETERMINATION

In most kinetic experiments the rate constants were determined under pseudo first-order conditions, using an excess of ozone, and measuring the disappearance of the nitrite using the RO-NO absorptions at 805 and 798 cm^{-1} for methyl and ethyl nitrite respectively. At these frequencies there was found to be negligible interference due to absorption bands from other species present. These results were analysed using the Guggenheim method [161] (see Appendix IV) and a typical Guggenheim plot is shown in Figure V.3. The first three points lie off the line because the reagents take a finite time to completely mix.

Since practical considerations limited the concentration range over which the reaction could be studied two other tests involving the rate constant were carried out to confirm that the reaction proceeded as determined in Section V.2. In one kinetic experiment the appearance of methyl nitrate was monitored and the rate constant for its appearance determined. This rate constant was within experimental error of that determined from methyl nitrite disappearance which confirms that methyl nitrate must be the major product of the reaction. The assumption that the reaction followed simple second-order kinetics was tested by using a much lower excess of ozone (approximately 4 fold) and the rate constant calculated using the full second-order rate equation. Absolute nitrite concentrations were obtained from the absorbance. The extinction coefficient was obtained by

extrapolating the absorbance-time curve to zero time. This extrapolation covered no more than 10% of the total absorbance and the initial absorbance so obtained was equated to the product of the extinction coefficient and the known initial nitrite concentration. This determination gave a rate constant within the experimental error of the other measurements verifying the assumption of second-order kinetics. The results of the rate constant determinations are given in Tables V.1 and 2.

It was estimated that the error in each rate constant determination, from the sum of the errors in the slope of the Guggenheim plot and the measurement of ozone concentration, amounted to 7% of the total rate constant.

The standard deviation of a group of results at a given temperature is generally about 7% of the average, showing the scatter of the results to be within the experimental error. In only two of the eight averaged rate constant determinations did the standard deviation exceed 7%. The uncertainties quoted with the averaged values and plotted in Figure V.4 are twice the standard deviation.

Activation energies (E_a) and Arrhenius parameters (A) were obtained from a least squares analysis of the Arrhenius plot, $\log_{10}k$ verses $^1/T$ shown in Figure V.4. This plot results from the Arrhenius equation expressed in the form

$$\log_{10}k = \log_{10}A - \frac{E_a}{2.303RT}$$

TABLE V.1

RATE CONSTANTS FOR THE REACTION OF METHYL NITRITE AND OZONE

Temp. K	$[CH_3ONO]_0$ Torr	$[O_3]_0$ Torr	(pseudo 1st order rate const) $x10^3$ s^{-1}	$kx10^{20}$ $cm^3 molec.^{-1} s^{-1}$	
298	0.879	14.76	6.78	1.42	
298	1.451	18.65	7.45	1.24	
298	0.925	18.23	7.68	1.31	
298	1.237	18.06	7.68	1.31	
298[a]	1.169	16.09	6.46	1.24	
298	0.748	14.26	6.02	1.30	
298[b]	4.574	19.75	-	1.25	$1.30 \pm .12$
316	1.10	12.60	9.12	2.36	
316	1.06	13.11	15.4	3.83	
316	1.05	14.33	13.7	3.13	
316	0.56	9.72	8.62	2.90	3.06 ± 1.06
338	0.56	11.52	28.0	8.40	
338	0.54	9.63	29.6	10.8	
338	0.89	12.07	44.2	12.8	10.67 ± 3.60
352	0.69	11.25	59.7	19.3	
352	0.82	10.53	56.9	19.7	
352	0.82	12.16	60.0	18.0	
352	0.86	11.83	70.0	21.7	19.70 ± 3.06

a Reaction followed by the appearance of methyl nitrate

b Rate constant determination by second-order analysis

TABLE V.2

RATE CONSTANTS FOR THE REACTION OF ETHYL NITRITE AND OZONE

Temp. K	$[C_2H_5ONO]_0$ Torr	$[O_3]_0$ Torr	(pseudo 1st order rate const)$\times 10^2$ s^{-1}	$k \times 10^{19}$ $cm^3 molec.^{-1} s^{-1}$	
298	1.08	13.61	4.72	1.07	
298	0.782	9.34	3.42	1.13	
298	1.07	12.69	5.04	1.22	
298	0.600	13.19	4.97	1.17	
298	1.61	12.75	5.12	1.24	1.17 ± 0.14
310	1.00	13.44	6.54	1.56	
310	0.88	14.60	7.59	1.67	
310	1.11	11.94	5.39	1.45	
310	0.82	12.19	6.63	1.75	
310	0.92	12.17	5.88	1.55	1.60 ± 0.23
324	1.02	12.92	8.47	2.20	
324	0.86	12.53	7.38	1.97	
324	0.89	12.61	7.71	2.05	
324	1.00	13.45	8.91	2.21	
324	1.00	12.46	8.02	2.16	2.12 ± 0.20
328	1.02	12.15	8.96	2.50	
328	1.02	11.90	9.67	2.76	
328	0.83	11.64	8.05	2.35	
328	0.90	12.67	9.22	2.46	2.52 ± 0.35

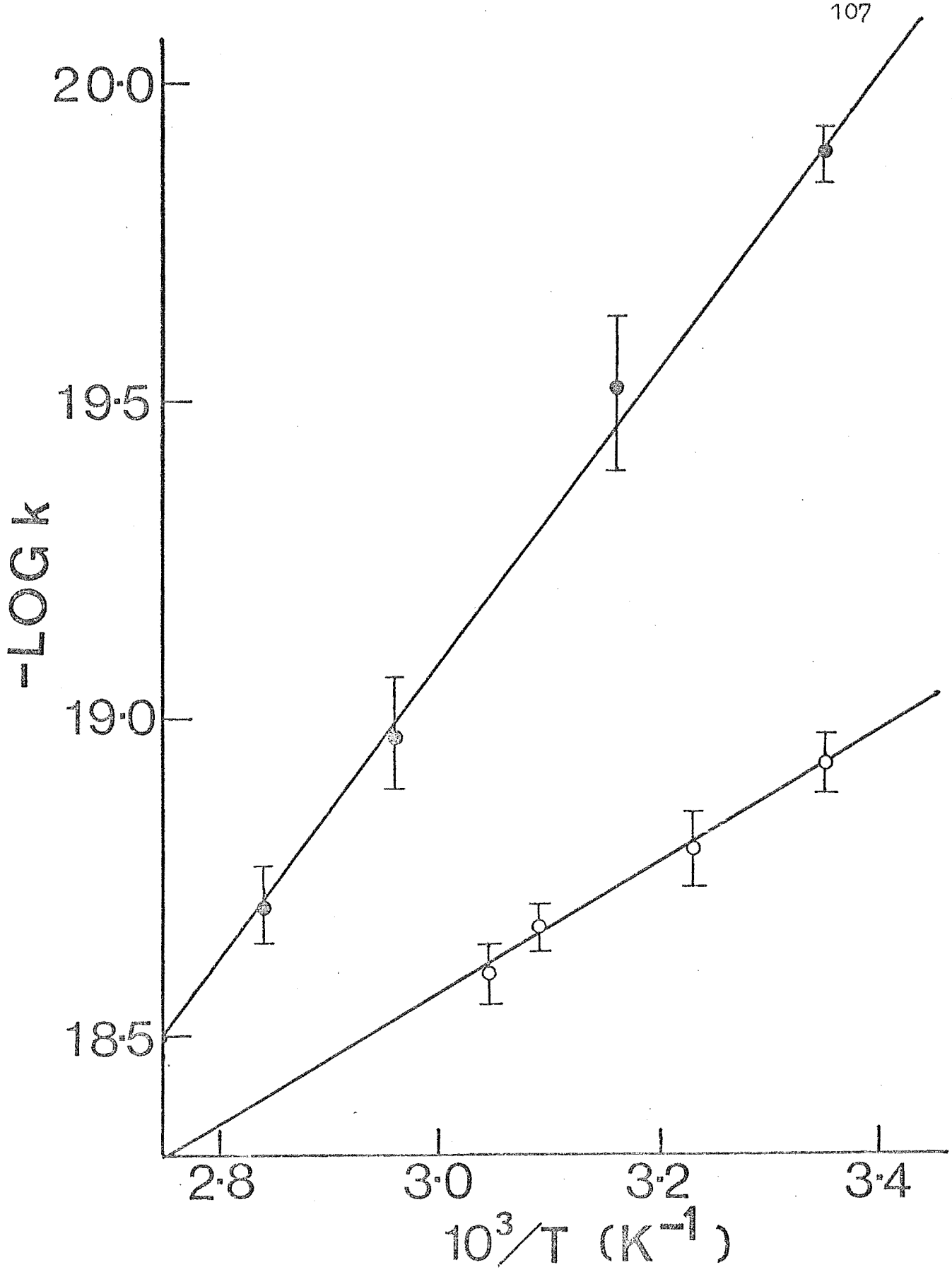

FIGURE V.4. Arrhenius Plots for the Reactions of Methyl Nitrite (filled circles) and Ethyl Nitrite (open circles) with Ozone.

The slope and intercept of these plots gave the following expressions for the rate constants.

$$\log_{10}k = (-12.17\pm0.46) - \left(\frac{44.19\pm2.87}{2.303\ RT}\right)$$

for methyl nitrite and

$$\log_{10}k = (-15.50\pm0.32) - \left(\frac{19.55\pm1.94}{2.303\ RT}\right)$$

for ethyl nitrite. The units of k and A are $cm^3 molec.^{-1} s^{-1}$ and E_a is in $kJ.mol^{-1}$. The uncertainties quoted represent twice the standard errors of the slope and intercept as obtained from the least squares analysis.

6. DISCUSSION

The product analysis, stoichiometry and rate determination experiments show the reaction to be the simple oxidation

$$RONO + O_3 \longrightarrow RONO_2 + O_2 .$$

The enthalpies of these reactions being 198 and 195 $kJ.mol^{-1}$ for R = methyl and R = ethyl respectively. The reactions appear to be uncomplicated with activation energies in the normal range for bimolecular gas phase reactions (0-100$kJ.mol^{-1}$). [76] There appears, however, to be an anomaly in the magnitudes of the Arrhenius parameters with that of the ethyl nitrite ozone reaction being extremely low.

The simple collision theory relates the Arrhenius parameter (A) to the collision frequency (Z) by the steric factor (P). $A = PZ.$

TABLE V.3

Arrhenius parameters, collision frequencies and steric factors for ozone reactions. The orders of magnitude of the values are given in brackets.

Reactant	A / $cm^3 molec.^{-1} s^{-1}$	$Zx10^{10}$ / $cm^3 molec.^{-1} s^{-1}$	P
methane [a]	2.7(-13)	3.46	7.8(-4)
ethylene [a]	6.0(-15)	3.19	1.9(-5)
propene [a]	7.0(-15)	4.18	1.6(-5)
nitrogen dioxide [a]	1.1(-13)	2.47	4.4(-4)
nitric oxide [a]	9.0(-13)	2.59	3.5(-3)
1 butene [b]	2.94(-15)	3.16	9.3(-6)
2 methyl propene [b]	3.18(-15)	3.16	1.0(-5)
2 butene [b]	5.98(-15)	3.16	1.9(-5)
cis 2 butene [b]	3.11(-15)	3.16	9.8(-6)
2 methyl 2 butene [b]	6.37(-15)	3.70	2.0(-5)
2,3 dimethyl butene [b]	2.83(-15)	3.65	9.0(-6)
methyl nitrite [c]	6.76(-13)	3.03	2.2(-3)
ethyl nitrite [c]	3.16(-16)	4.27	7.4(-7)

a) Reference 28

b) Reference 162

c) This work

Table V.3 lists values of A, P and Z obtained from a number of ozone reactions. The most noticeable feature of the table, excluding the ethyl nitrite result, is that for the simpler, smaller reactants such as methane and nitric oxide the steric factors are in the range $0.8\text{-}3.5\times10^{-3}$, whereas for the reactions of the more complex olefins the steric factor is much lower, in the range $0.9\text{-}2\times10^{-5}$. The steric factor for the nitrogen dioxide reaction lies between these values. The values obtained for the steric factors for the more complex molecules are consistent with the simplest form of the transition state theory which predicts that for the reaction of two non linear molecules the steric factor will be related to the partition functions for vibration (q_{vib}) and rotation (q_{rot}) by

$$P = \left(\frac{q_{vib}}{q_{rot}}\right)^5$$

Taking typical values for these functions a probable value for P is $\sim 10^{-5}$. (163)

The value of the steric factor for the methyl nitrite ozone reaction lies within the range for the simpler reactions, but that for the ethyl nitrite reaction is an order of magnitude lower than either the predicted value or the values listed. It is unlikely that the lower steric factor is due to the alkyl group shielding the molecule from ozone attack as an increase in alkene size had no effect on the Arrhenius parameters observed for the ozonolysis of the alkenes.

The other possible explanation is that the relatively small temperature range covered in these experiments coupled with the long extrapolation could produce an error in the Arrhenius parameter much higher than that estimated. If this is the case then the value of 3.16×10^{-16} may well be in error and attempts to explain its anomalously low value unnecessary.

Alkyl nitrites have been postulated as intermediates in photochemical smog, and have been included in smog models. The nitrites are produced by the reaction of alkyoxy radicals with nitric oxide

$$RO + NO + M \longrightarrow RONO + M$$

These species have not been detected although the nitrates formed by the analogous reaction with nitrogen dioxide have been found in a smog chamber. (104)

$$RO + NO_2 + M \longrightarrow RONO_2 + M$$

The only mode of nitrite decomposition considered in the models is the photolysis

$$RONO + h\upsilon \longrightarrow RO + NO$$

which is assumed to have a quantum yield of unity below 400nm and a rate of photolysis in sunlight of $2 \times 10^{-3} s^{-1}$.(7) Consider now the possible competing reaction of the oxidation of the nitrite by ozone. The rate constants at 298K for this reaction have been determined as $1.3 \times 10^{-20} cm^3 molec.^{-1} s^{-1}$ and $1.2 \times 10^{-19} cm^3 molec.^{-1} s^{-1}$ for R = methyl and ethyl respectively. The maximum value of the ozone concentration on a smoggy day from Section II.2.(2) is 4.9×10^{12} molecules per cm^3 (0.20ppm). Calculation of the

pseudo first order rate constants for nitrite removal by this reaction yields $6.4 \times 10^{-8} s^{-1}$ and $5.7 \times 10^{-7} s^{-1}$ for methyl and ethyl nitrite respectively compared with the value of $2 \times 10^{-3} s^{-1}$ for the photolysis. Hence the rate of removal of nitrite by ozone oxidation is over four orders of magnitude slower than the photolysis and can safely be ignored as a removal step for nitrites in photochemical smog.

The oxidation of nitrous to nitric acid by ozone

$$HONO + O_3 \longrightarrow HONO_2 + O_2 + 200 kJmol^{-1}$$

is analogous to the nitrite oxidation to nitrate. Considering the results of this study it appears unlikely that the rate constant for this reaction would exceed $10^{-18} cm^3 molec.^{-1} s^{-1}$. In Section II.2.(1) it was shown that if the rate constant of this reaction exceeded $10^{-17} cm^3 molec.^{-1} s^{-1}$ then the reaction should be included in model calculations on the chemistry of nitrogen in the stratosphere. This study suggests that the rate of this reaction is too low for the reaction to play a significant part in determining the nitrogen balance in the stratosphere.

CHAPTER VI

THE REACTIONS OF HYDROGEN ATOMS WITH METHYL AND ETHYL NITRITES

The aim of this section was to use the discharge flow-mass spectrometer system to examine the reactions between hydrogen atoms and methyl and ethyl nitrites. For each nitrite the study involved the determination of the primary rate constant, the primary and secondary products and the stoichiometry, and led to a postulated mechanism. Of greatest importance among the reaction products were the alkoxy radicals which are important species in photochemical smog. To date however no reactions of these radicals have been directly studied. It was hoped that the alkoxy radicals could be detected as a product of these reactions and an investigation of their reactions undertaken.

1. MASS SPECTRA OF METHYL AND ETHYL NITRITES

References to the mass spectra of these nitrites in the literature usually state that they have negligible parent and parent minus one peaks. (152) In the listed mass spectrum of methyl nitrite the parent peak is 0.1% and the parent minus one peak 2.6% of the largest peak. (151) However in this study it was found that both methyl and ethyl nitrites have parent peaks, although in the latter case it proved too small to use for kinetic studies. The mass spectra of the two nitrites

are presented in Tables VI.1 and VI.2 and were recorded on an A.E.I. M.S. 902 high resolution mass spectrometer at a source pressure of 1.5×10^{-6} Torr using an electron energy of 70eV (as used in the Quad 1210). It was not possible to use the Quad 1210 attached to the flow system to obtain these spectra as the Quad did not have constant resolution between mass ranges, and a single resolution setting could not encompass a sufficiently wide mass range.

The most noticeable feature of the spectra is the large number of fragment ions produced under electron bombardment. In both nitrites the major peak is at M30 (mass peak 30) corresponding to NO^+ and CH_2O^+ which is consistent with the RO-NO bond being the weakest in both molecules. The bond energies D(RO-NO) are 174.9 and 175.7 $kJ.mol^{-1}$ for R = methyl and R = ethyl respectively, [134] compared with typical values of 395kJ for a C-H bond and 330kJ for a C-C bond. [164] This weak bond also explains the large peaks corresponding to the RO^+ ions. Most other possible fragment ions are observed, in particular the peak at M60 (CH_2ONO^+) in the ethyl nitrite spectrum was important as this, rather than the small parent ion was used to monitor ethyl nitrite concentration.

The relatively large H_2O^+ peak in the methyl nitrite spectrum was most probably due to water impurities in the handling line to the mass spectrometer as it was not observed in the ethyl nitrite spectrum. Furthermore spectra taken over the low mass range using the Quad 1210 showed no M18 peak of this relative magnitude.

TABLE VI.1

MASS SPECTRUM OF METHYL NITRITE

Mass No	Species	Relative Peak Intensity *
14	CH_2^+, N^+	1.24
15	CH_3^+	7.50
17	OH^+	0.86
18	H_2O^+	4.21
27	($C_2H_3^+$,HCN^+)?	1.63
28	CO^+	15.11
29	CHO^+	17.89
30	CH_2O^+, NO^+	100.00
31	CH_3O^+	5.66
32	O_2^+	2.55
46	NO_2^+	1.71
60	CH_2ONO^+	5.53
61	CH_3ONO^+	11.97

(all other peaks $<$ 0.5% of mass 30)

* Relative peak intensity expressed as % of the most abundant peak (mass 30).

Contributions to the above peaks from the background mass spectrum have been subtracted.

TABLE VI.2

MASS SPECTRUM OF ETHYL NITRITE

Mass No	Species	Relative Peak Intensity *
13	CH^+	0.56
14	CH_2^+, N^+	2.08
15	CH_3^+	10.00
26	$C_2H_2^+$	2.32
27	$C_2H_3^+$	12.00
28	$C_2H_4^+, CO^+$	11.92
29	$C_2H_5^+, CHO^+$	28.00
30	CH_2O^+, NO^+	100.00
31	$^{13}CH_2O^+, {}^{15}NO^+, CH^{18}O^+$	3.12
32	O_2^+	1.32
42	$C_2H_2O^+$	1.20
43	$C_2H_3O^+$	11.20
44	$C_2H_4O^+$	2.80
45	$C_2H_5O^+$	13.60
46	NO_2^+	1.12
60	CH_2ONO^+	39.60
74	$C_2H_4ONO^+$	0.96
75	$C_2H_5ONO^+$	0.64

(all other peaks $< 0.5\%$ of mass 30)

* Relative peak intensity expressed as % of the most abundant peak (mass 30).

Contributions to the above peaks from the background mass spectrum have been subtracted.

2. REACTION PRODUCTS

Products were determined using as wide a variation in reaction conditions as possible. Since the carbon-carbon bond in ethyl nitrite is one of the strongest in the molecule (bond energy about 339kJ.mol^{-1}) (164) it was initially assumed and later shown that this bond was not broken on reaction and so the products from the two reactions were considered to be similar.

In the methyl nitrite reaction with hydrogen atoms, the peaks at M2, M16, M18, M28 and M30 increased as the extent of reaction increased under all reaction conditions. To help elucidate the reaction products, several experiments were performed with deuterium atoms in place of hydrogen atoms. In these experiments peaks at M3, M4, M17, M18, M19, M20, M28 and M30 increased under all reaction conditions. In the ethyl nitrite reaction the same peaks, with the exception of M16 and M17, increased and of the other peaks only M31 in the reaction with deuterium atoms showed a consistent increase.

The increase in M30 could only be discerned at high extents of reaction because of the large contribution to this peak from the nitrite. Little information can be gained from this observation as nitric oxide has a higher mass spectrometric sensitivity at M30 than either of the alkyl nitrites. This means that if all the consumed nitrite is converted to nitric oxide, which will be shown to be the case, the peak at M30 will rise solely due to differences in mass

spectral sensitivity. This makes the identification of other products at M30 impossible.

The production of nitric oxide was definitely established by the presence of the characteristic green-white "air glow" which results from the reaction of oxygen atoms with nitric oxide

$$O + NO \longrightarrow NO_2^*$$

$$NO_2^* \longrightarrow NO_2 + h\nu$$

The increases at M2, M3 and M4 showed that molecular hydrogen was a product, both of the hydrogen atom abstraction from the alkyl group, and, of a series of reactions causing net recombination of atoms.

The peak at M16 in the methyl nitrite reaction was found to increase proportionally to nitrite destruction at short and long reaction times (see Table VI.3). This observation shows that the atomic oxygen is not a contributor to this peak as its yield would be expected to drop at long times due to the reaction with methyl nitrite. [9] This also excludes molecular oxygen as a possible major long term product as this would increase the yield at M16 at longer times. Methane was the most likely product because its subsequent low reactivity would ensure a constant yield. Further evidence for methane production came from the increase in M17 (CH_3D) in the reaction of deuterium atoms with methyl nitrite.

It was impossible to detect ethane directly by means of its parent peak in the ethyl nitrite reaction with hydrogen atoms because of the large changes already present at M30 due to NO. However the small

increase in M31 on reaction with deuterium atoms confirmed that ethane was formed.

Water and heavy water were detected in the hydrogen and deuterium reactions by the peaks at M18 and M20 respectively, and HDO in the deuterium atom reaction at M19. These signals were erratic and irreproducible at short times, but at longer times and greater extents of reaction the increases became more stable and sizeable.

The changes at M28 (CO^+) seemed to bear no relation to changes in the parent alkyl nitrite peaks and could not readily be explained as any species with a carbon-oxygen bond would contribute to this peak. The only conclusion that could be reached was that there are carbon and oxygen containing products present at all times.

In the ethyl nitrite reaction the peaks at M60 (CH_2ONO^+) and M75 ($C_2H_5ONO^+$) were compared to see if there was any evidence for carbon-carbon bond rupture on reaction, but under a wide variety of conditions these peaks behaved in parallel. This showed that M60 had no contribution from a product of the reaction and could be used as a monitor of ethyl nitrite concentration.

In the ethyl nitrite reaction M44 (CO_2^+,$C_2H_4O^+$) showed an increase in height on reaction at short times with low atom concentration. However at longer times and higher concentrations this peak, which has a small contribution from the ethyl nitrite mass spectrum, behaved as a fragment ion of the nitrite decreasing with the extent of reaction. The initial increase was attributed to acetaldehyde (CH_3CHO) which must be produced

at short times but then removed by secondary reactions.

Methanol and ethanol appear to be likely products from these reactions. The parent peak of methanol is at M32 and in the methyl nitrite reaction this peak was studied for evidence of the alcohol. Unfortunately this peak is a fragment in the nitrite spectrum and decreased on reaction. This decrease, however, was less than expected from the parent decrease at M61 but attempts to reconcile this difference with methanol production were unsuccessful. Operating the ion source at low electron energies to lower the contribution of the nitrite to the M32 peak gave no additional information. However when the total pressure was raised above 2 Torr, by throttling the flow down, the M32 peak increased as the extent of reaction increased showing either methanol or molecular oxygen to be a product. When deuterium atoms were used there was no increase in M33 until the total pressure was raised above 2 Torr confirming methanol to be a product at higher total pressures and higher reactant concentrations. In the reaction of ethyl nitrite with hydrogen atoms the ethanol peak at M46 also increased only when the total pressure was raised. This implies that the alcohols are formed but probably by secondary processes and their presence only at higher pressures implies they may be formed by termolecular reactions.

The peak at M46 was examined to see if nitrogen dioxide, NO_2, could be detected as a reaction product. At all reaction times under all reaction conditions and

at a wide range of electron energies M46, which is a fragment peak of the nitrite spectrum, showed parallel behaviour to the parent M61 giving no evidence for nitrogen dioxide.

Examination of the peak at M47 showed no evidence for nitrous acid (HONO) production.

Searches were carried out for the alkoxy radical (RO) and nitroxyl molecule (HNO) in both reactions. It was not possible to look for these species at reaction times less than 1ms because imperfect mixing gave anomalous results. In the methyl nitrite reaction both CH_3O and HNO have parent peaks at M31 which is also a large fragment peak of the nitrite spectrum. By working at low electron energies (about 12eV), low atom and high nitrite concentrations the signal at M31 was found to pass through a maximum with increasing reaction time. This indicated the presence of one or both of these species although the problems encountered in their detection showed their concentrations to be very low. The two corresponding intermediates (C_2H_5O and HNO) no longer have the same mass in the ethyl nitrite reaction and by using similar conditions to those described above the ethoxy radical and nitroxyl molecule were similarly detected independently at M45 and M31 respectively.

A search was made for the hydroxyl radical (OH) at M17 but this was complicated by OH^+ formed from water as a reaction product. Although the appearance potentials of OH^+ from the two sources differ by 5eV it was not possible to unambiguously identify the OH radical,

possibly because the electron gun in the mass spectrometer produces electrons with a range of energies in excess of this difference.

An attempt was made to detect the CH_2ONO radical in the methyl nitrite reaction by measuring the ratio of heights of M60 and M61 under a wide range of reaction conditions,but this ratio was found to be constant. Since the M60 peak was about half the height of M61 peak the detection limit for this radical was quite high so it must be discounted as a major long-lived product.

In Section III.4.(6). it was stated that a polymer adhered to the walls of the flow tube and in the presence of atoms gave rise to several peaks in the mass spectrum. This effect was most marked with masses M30, M46 and M60 but persisted with many mass numbers up to the limit of the mass spectrometer (M100). The high masses observed suggested that a polymer was responsible and with M30 showing the biggest effect followed by M46 and M60 it was concluded that the offending polymer was probably one of the polymeric forms of formaldehyde $(CH_2O)_n$. This then gave fragments CH_2O, CH_2O_2, $(CH_2O)_2$, $(CH_2O)_3$ etc. either directly on reaction with atoms or in the mass spectrometer ion source. Since the methyl nitrite/hydrogen atom reaction was the first to be run in all the flow tubes used in this work formaldehyde can only be assigned a product of this reaction. Qualitative observations however suggested that the effect of the polymer was also present with the ethyl nitrite reaction and

formaldehyde was also tentatively assigned as a product of this reaction.

Of the primary products only methane in the methyl nitrite reaction was stable to further atom or radical attack and had a mass peak relatively uncomplicated by other species so that a yield could be measured quantitatively. The results of 14 yield determinations are shown in Table VI.3 and the yield of methane from the reaction of hydrogen atoms with methyl nitrite is (8.7 ± 1.5) % assuming that all the increase in M16 is due to methane. The absence of a trend in the calculated yield shows that atomic and molecular oxygen do not contribute substantially to this peak and that methane is formed solely by the primary reaction.

In conclusion, the products detected for the methyl nitrite/hydrogen atom reaction were hydrogen, nitric oxide, methane, water and formaldehyde. Methanol was detected at higher pressures with either methoxy radicals or nitroxyl molecules (or perhaps both) detected as intermediates. The products detected for the ethyl nitrite reaction were hydrogen, nitric oxide, ethane, water and possibly formaldehyde. Ethanol was detected at higher pressures and acetaldehyde, the ethoxy radical and nitroxyl molecule detected as intermediates.

TABLE VI.3

METHANE YIELD FROM METHYL NITRITE HYDROGEN ATOM REACTION

Reaction Time ms	CH_3ONO mTorr	CH_4 mTorr	Yield %
4.5	0.53	0.049	9.2
7.9	0.73	0.077	10.5
15.0	1.20	0.091	7.6
6.0	0.80	0.070	8.8
10.0	1.13	0.083	7.3
28.0	14.7	1.20	8.2
28.0	23.2	2.07	8.9
28.0	23.3	2.07	8.9
10.6	14.0	1.21	8.6
10.6	13.3	1.16	8.7
10.6	10.6	0.94	8.9
10.6	4.65	0.41	8.8
48	31.3	2.56	8.2
48	36.7	3.23	8.8
	Mean with estimated error		8.7 ± 1.5

TABLE VI.4

STOICHIOMETRY OF THE RONO + H REACTION

R = METHYL

[H]	$[CH_3ONO]$	$\Delta[CH_3ONO]$	$\Delta[CH_3ONO]$	[H]
mTorr	mTorr	mTorr	[H]	$\Delta[CH_3ONO]$
3.25	24.43	0.92	0.28	3.53
6.17	39.09	1.63	0.26	3.79
7.93	27.30	2.04	0.26	3.89
9.56	17.10	2.44	0.26	3.92
10.17	42.76	3.05	0.30	3.33
14.04	20.36	3.37	0.24	4.17
16.95	41.13	4.48	0.26	3.78
			0.27 ± 0.02	3.78 ± 0.50

R = ETHYL

[H]	$[C_2H_5ONO]$	$\Delta[C_2H_5ONO]$	$\Delta[C_2H_5ONO]$	[H]
mTorr	mTorr	mTorr	[H]	$\Delta[C_2H_5ONO]$
4.61	79	4.83	1.05	0.95
6.78	189	4.94	0.73	1.37
10.31	127	8.87	0.86	1.16
13.29	79	10.9	0.82	1.22
16.07	285	14.2	0.88	1.13
23.73	82	18.2	0.77	1.30
28.55	353	25.6	0.90	1.12
			0.86 ± 0.20	1.17 ± 0.28

3. STOICHIOMETRY OF THE REACTION

The stoichiometry was determined at times greater than 100ms and at total pressures of about 400m Torr. The results of the stoichiometry determinations are shown in Table VI.4. The overall consumption of hydrogen atoms per molecule of nitrite is 3.78 ± 0.50 for methyl nitrite and 1.17 ± 0.28 for ethyl nitrite. The uncertainties quoted represent twice the standard deviation of the results averaged.

4. KINETIC DATA FOR THE PRIMARY REACTION

Preliminary experiments indicated that the reaction was quite slow so initially the rate constant was determined under slow flow conditions at total pressures around 400 mTorr with 35-60 mTorr of atoms, 0.5-5.5 mTorr of nitrite and reaction times of 10-100ms. Calculation of the rate constant from the slope of the log concentration/time plot gave rate constants that increased as the concentrations were lowered. This trend suggested that secondary reactions were occurring to a significant degree and first order kinetics were not being followed. To minimise the effect of these reactions it was necessary to decrease the reaction time by operating under fast flow conditions and the reagent concentrations were lowered to the point where the calculated rate constant was found to be independent of concentration. Typical conditions were total pressure 120 mTorr with 10 mTorr of atoms, 0.5 mTorr of nitrite and reaction times of 2-15ms.

The results of the determination of the primary rate constants are given in Tables VI.5 and VI.6 for the methyl nitrite and ethyl nitrite reactions respectively. Allowance has been made in each determination for the effect of the pressure drop down the tube on the rate constant and the full description of the analysis used to obtain the rate constant can be found in Appendix IV. The uncertainty in each determination arising from the errors in flow velocity, atom concentration and the standard error of the log concentration/reaction time plot is 15% of the calculated value. The uncertainties quoted for the averaged result for a given temperature are two standard deviations which is in the range 10-20% consistent with the estimated uncertainties.

Activation energies (E_a) and Arrhenius parameters (A) were obtained from a least squares analysis of the Arrhenius plot of $\log_{10}k$ against $^1/T$ shown in Figure VI.1. This plot comes from the Arrhenius equation expressed in the form

$$\log_{10}k = \log_{10}A - \frac{E_a}{2.303RT}$$

The slope and intercept of these plots gave the following expressions for the rate constants

$$\log_{10}k = (-10.61 \pm 0.20) - \left(\frac{16.2 \pm 1.0}{2.303RT}\right)$$

for the methyl nitrite reaction and

$$\log_{10}k = (-11.06 \pm 0.20) - \left(\frac{13.8 \pm 1.0}{2.303RT}\right)$$

for the ethyl nitrite reaction. The rate constants and

TABLE VI.5

RATE CONSTANTS FOR THE REACTION OF METHYL NITRITE WITH HYDROGEN ATOMS

T / K	[Argon] / mTorr	[H] / mTorr	$[CH_3ONO]_0$ / mTorr	$kx10^{14}$ / $cm^3 molec.^{-1} s^{-1}$	
298	128	12.6	0.78	3.52	
"	"	"	0.35	3.78	
"	"	"	0.69	3.73	
"	"	7.35	0.39	3.74	
"	"	"	0.31	3.91	
"	"	"	0.17	3.62	
"	"	"	0.97	3.58	
"	"	"	1.40	3.27	
"	"	"	1.94	3.47	
"	115	23.9	0.19	3.61	
"	"	"	0.37	3.70	
"	"	"	0.090	3.54	
"	"	"	1.69	3.46	3.61 ± 0.33
285.5	122	6.13	0.35	2.08	
"	"	"	0.17	2.73	
"	"	4.21	0.39	2.77	
"	"	"	0.17	2.67	
"	"	"	0.10	2.87	2.62 ± 0.62
314.5	120	4.29	0.36	5.10	
"	"	"	0.32	4.89	
"	"	"	0.30	4.80	
"	"	"	0.14	5.06	
"	"	2.19	0.13	5.21	
"	"	"	0.50	4.73	4.97 ± 0.38

TABLE VI.5 CONTD

T	[Argon]	[H]	$[CH_3ONO]_0$	$kx10^{14}$	
K	mTorr	mTorr	mTorr	$cm^3 molec.^{-1} s^{-1}$	
328	119	5.10	0.34	6.24	
"	"	"	0.23	6.82	
"	"	"	0.15	6.83	
"	"	3.81	0.48	6.68	
"	"	"	0.52	6.07	
"	"	"	0.29	6.79	6.57 ± 0.66
341.5	115	3.79	0.52	7.88	
"	"	"	0.32	8.59	
"	"	"	0.17	8.83	
"	"	5.19	0.20	7.21	
"	"	3.79	0.33	7.92	8.09 ± 1.28

TABLE VI.6

RATE CONSTANTS FOR THE REACTION OF ETHYL NITRITE WITH HYDROGEN ATOMS

T	[Argon]	[H]	$[C_2H_5ONO]_0$	$kx10^{14}$	
K	mTorr	mTorr	mTorr	$cm^3 molec.^{-1} s^{-1}$	
298	98.1	15.69	0.99	3.03	
"	"	"	0.68	3.03	
"	"	"	0.26	3.46	
"	"	7.32	0.62	3.81	
"	119	13.55	0.40	3.40	
"	"	"	1.12	3.10	
"	"	"	0.68	3.28	
"	"	"	0.36	3.53	
"	107	10.15	1.07	3.08	
"	"	"	1.62	3.09	
"	"	"	0.49	3.30	
"	"	"	0.21	3.63	
"	"	18.09	0.78	3.34	
"	"	"	1.72	3.33	
"	"	"	0.53	3.38	
"	"	"	0.21	3.57	3.34 ± 0.46
283.5	113	6.30	0.28	2.33	
"	"	"	0.16	2.46	
"	"	"	0.15	2.50	
"	"	"	0.094	2.40	2.41 ± 0.15
315.5	116	5.96	0.24	4.32	
"	"	"	0.14	4.36	
"	"	"	0.10	4.47	
"	"	3.28	0.20	4.86	4.50 ± 0.48

TABLE VI.6 CONTD

T	[Argon]	[H]	$[C_2H_5ONO]_0$	$kx10^{14}$	
K	mTorr	mTorr	mTorr	$cm^3 molec.^{-1} s^{-1}$	
327.5	107	5.07	0.15	4.99	
"	"	"	0.090	5.68	
"	"	6.16	0.16	5.90	
"	"	"	0.095	6.07	
"	"	"	0.25	5.24	5.58 ± 0.90
341.5	108	6.80	0.25	6.12	
"	"	"	0.24	6.29	
"	"	"	0.25	6.92	
"	"	"	0.16	7.37	6.68 ± 1.15

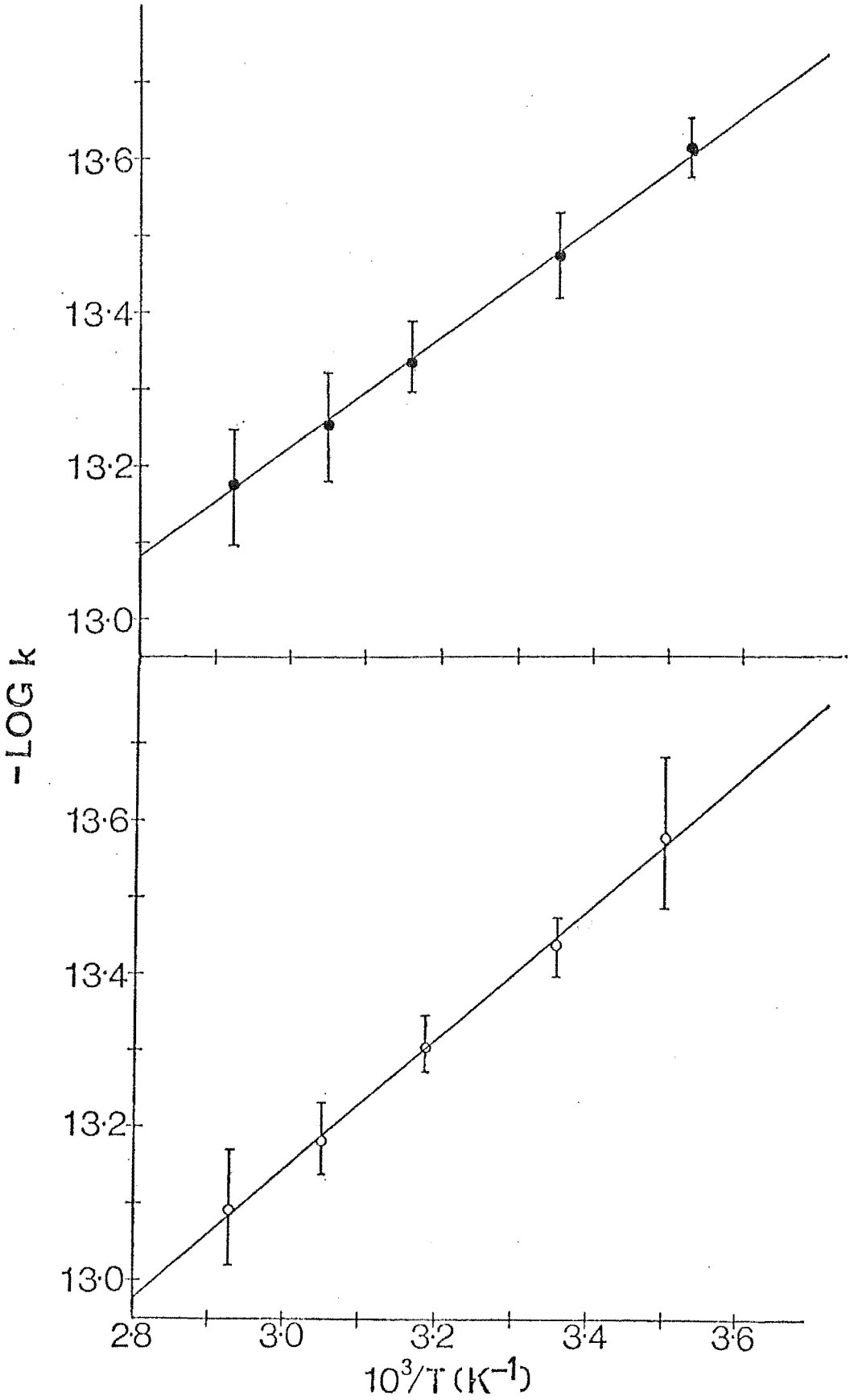

FIGURE VI.1 Arrhenius Plots for the Reactions of Methyl Nitrite (open circles) and Ethyl Nitrite (filled circles) with Hydrogen Atoms

Arrhenius parameters are in $cm^3 molec.^{-1} s^{-1}$ and the activation energies in $kJ.mol^{-1}$. The errors quoted represent twice the standard errors in the slope and intercept of the Arrhenius plot as determined from the least squares analysis.

5. DISCUSSION

The reactions between hydrogen atoms and the alkyl nitrites are too complex for a complete analysis of their mechanisms to be made on the basis of the present measurements. Nevertheless, much useful information can be deduced from the product analysis and stoichiometry.

(1) The Primary Reactions

There are six possible exothermic pathways for the primary reaction of methyl nitrite with hydrogen atoms. They are:

$$H + CH_3ONO \longrightarrow CH_3OH + NO + 261.9 \quad (1a)$$

$$\longrightarrow CH_2ONO + H_2 + 40.8 \quad (1b)$$

$$\longrightarrow CH_3O + HNO + 31.0 \quad (1c)$$

$$\longrightarrow CH_2O + H_2 + NO + 176.7 \quad (1d)$$

$$\longrightarrow CH_4 + NO_2 + 192.9 \quad (1e)$$

$$\longrightarrow CH_3 + HONO + 83.7 \quad (1f)$$

The reaction enthalpies are given in $kJmol^{-1}$ and have been calculated from the data in Appendix I except for reaction channel 1b. In this case the bond dissociation energy $D(H\text{-}CH_2ONO)$ has been taken as $395.2 kJ.mol^{-1}$ which is the average of $D(H\text{-}CH_2OCH_3)$, $392.4 kJ.mol^{-1}$ and $D(H\text{-}CH_2OH)$, $397.9 kJ.mol^{-1}$. (165)

Reaction channel (1a) can be discounted as a primary reaction as methanol was not detected early in the reaction. It was however detected only at higher pressures (>2 Torr) and long reaction times (150ms) implying the alcohol could be a secondary product formed by a termolecular reaction.

The CH_2ONO radical produced in reaction channel (1b) was not detected indicating that it is not a major long-lived product. The unimolecular decomposition of this radical to formaldehyde and nitric oxide is exothermic by 135.9kJ.mol^{-1} and the radical may decompose to give these products. If this is the case then the products are identical with those of channel (1d) which cannot be discounted as a possible reaction pathway. This channel will be considered further in the following discussion and channel (1b) ignored since it is impossible to distinguish between the two channels. The presence of HD among the reaction products of the deuterium atom reaction is evidence that channel (1d) operates.

That no mass peak was found at M47 is probably sufficient reason to discount channel (1f) as a major reaction channel since the results discussed in Chapter IV showed nitrous acid to have a parent peak.

Reaction channel (1c) proceeds since either nitroxyl or the methoxy radical were detected at M31 in the methyl nitrite reaction and both nitroxyl and the ethoxy radical in the ethyl nitrite reaction.

Channel (1e) proceeds since methane was identified as a primary product. The green-white "air glow" which was observed to accompany the reaction results from the reaction of oxygen atoms with nitric oxide. The following series of reactions initiated by the reaction of nitrogen dioxide, the other product from channel (1e), could be responsible for the observed "air glow".

$$H + NO_2 \longrightarrow OH + NO \quad \ldots\ldots\ldots\ldots (2)$$

$$OH + OH \longrightarrow H_2O + O \quad \ldots\ldots\ldots\ldots (3)$$

$$O + NO \longrightarrow NO_2^*$$

$$NO_2^* \longrightarrow NO_2 + h\nu)$$

Hence the major primary reaction channels are (1c), (1d) and (1e) with channel (1e) accounting for $(8.7\pm1.5)\%$ of the total reaction.

The analogous exothermic reactions which are possible for the reaction of ethyl nitrite with hydrogen atoms are:

$$H + C_2H_5ONO \longrightarrow C_2H_5OH + NO + 260.3 \quad \ldots (1'a)$$

$$\longrightarrow C_2H_4ONO + H_2 + 40.8 \quad \ldots (1'b)$$

$$\longrightarrow C_2H_5O + HNO + 30.2 \quad \ldots (1'c)$$

$$\longrightarrow CH_3CHO + H_2 + NO + 191.4 \quad (1'd)$$

$$\longrightarrow C_2H_6 + NO_2 + 167.1 \quad \ldots (1'e)$$

$$\longrightarrow C_2H_5 + HONO + 77.6 \quad \ldots (1'f)$$

Reaction channels (1'a), (1'b) and (1'f) can be discounted for the same reasons as the analogous reactions (1a), (1b) and (1f) were discounted in the methyl nitrite reaction. Furthermore the absence of ethanol as a product at short times and the detection of acetaldehyde support the omission of (1'a) and the inclusion of (1'd)

respectively.

(2) Secondary Reactions

(a) The Methyl Nitrite Reaction: The primary products methane, nitric oxide and molecular hydrogen will undergo no further significant reaction in the time available before sampling. All other primary products are reactive and will react with either methyl nitrite or atomic or molecular hydrogen since these species have the highest concentrations in the flow tube, after unreactive argon.

Nitrogen dioxide reacts rapidly with hydrogen atoms with a rate constant of 1.3×10^{-10} $cm^3 molec.^{-1} s^{-1}$. (176) The failure to detect nitrogen dioxide can be explained by its low steady state concentration brought about by its low yield ($8.7 \pm 1.5\%$) from the slow reaction and its rapid rate of reaction with hydrogen atoms.

The reactions involved are:

$$H + NO_2 \longrightarrow OH + NO \quad \ldots\ldots\ldots (2)$$

$$OH + OH \longrightarrow H_2O + O \quad \ldots\ldots\ldots (3)$$

$$O + NO_2 \longrightarrow O_2 + NO \quad \ldots\ldots\ldots (4)$$

$$O + OH \longrightarrow O_2 + H \quad \ldots\ldots\ldots (5)$$

This series of reactions would explain the production of water in the reaction and heavy water in the deuterium atom reaction.

The nitroxyl molecule is known to react with hydrogen atoms to produce nitric oxide and hydrogen, the rate constant being in the range 10^{-12}-10^{-13} $cm^3 molec.^{-1} s^{-1}$. (28) The observed maximum in the nitroxyl signal with increasing reaction time supports this as a rapid

secondary reaction.

$$H + HNO \longrightarrow H_2 + NO \quad \ldots\ldots\ldots (6)$$

Hence all nitrogen is converted to nitric oxide.

At the pressures used in this work (<0.5 Torr) the methoxy radical can react with hydrogen atoms via two channels.

$$H + CH_3O \longrightarrow CH_3 + OH \quad \ldots\ldots\ldots (7a)$$

$$\longrightarrow CH_2O + H_2 \quad \ldots\ldots\ldots (7b)$$

It has been estimated [166] that reaction (7b) comprises 31% of the total reaction and provides a secondary source of formaldehyde. The other channel produces hydroxyl radicals which can react as in reactions (3) and (5). If the hydrogen atom concentration is low then the methoxy radical may attack the methyl nitrite as observed in the photolysis. [133]

$$CH_3O + CH_3ONO \longrightarrow CH_3OH + CH_2O + NO \quad \ldots\ldots (8)$$

Methanol was not detected under the normal conditions of this study even at high excesses of nitrite over atoms, showing this reaction does not occur to a significant extent. At higher pressures (above 2 Torr) the termolecular reaction of methoxy radicals with hydrogen atoms to generate methanol may become important.

$$CH_3O + H + M \longrightarrow CH_3OH + M \quad \ldots\ldots\ldots (9)$$

Compared with most of the other secondary reactions the reaction between hydrogen atoms and formaldehyde is relatively slow with a rate constant of 5.4×10^{-14} cm^3 $molec^{-1}$ s^{-1}. [44]

$$H + CH_2O \longrightarrow H_2 + HCO \quad \ldots\ldots\ldots (10)$$

The subsequent reaction of the HCO radical would be

expected to be much faster

$$H + HCO \longrightarrow H_2 + CO \quad \ldots\ldots\ldots\ldots (11)$$

The other likely reaction of formaldehyde is with hydroxyl radicals

$$OH + CH_2O \longrightarrow H_2O + HCO \quad \ldots\ldots\ldots\ldots (12)$$

This reaction has a rate constant of $1.4\times10^{-11}cm^3molec.^{-1}s^{-1}$ (167) so at low hydrogen atom concentrations where $[OH] \sim 0.01[H]$ reaction (12) will compete with reaction (10) but yield the same product radical. Since formaldehyde polymer was found on the walls of the flow tube an additional reaction for formaldehyde must be the wall catalysed polymerisation

$$n\,CH_2O + wall \longrightarrow (CH_2O)_n.\ wall \quad \ldots\ldots\ldots (13)$$

A major reaction of the hydroxyl radical will be with methyl nitrite which has a rate constant of $1.3\times10^{-12}cm^3molec.^{-1}s^{-1}$ (136) but for which the products are not known.

$$OH + CH_3ONO \longrightarrow \text{products} \quad \ldots\ldots\ldots\ldots (14)$$

The bimolecular reactions of hydroxyl radicals with atomic and molecular hydrogen

$$OH + H \longrightarrow H_2 + O \quad \ldots\ldots\ldots\ldots (15)$$

$$OH + H_2 \longrightarrow H_2O + H \quad \ldots\ldots\ldots\ldots (16)$$

are unlikely to be significant in hydroxyl radical removal as their respective rate constants are 7×10^{-16} and $6\times10^{-15}cm^3molec.^{-1}s^{-1}$. (28)

The fate of the methyl radicals is uncertain. The most common reactions for the small alkyl radicals (methyl and ethyl) are combination reactions,

$$R + R \longrightarrow R - R$$

and atom transfer equilibria of the form

$$R + H - X \longrightarrow RH + X. \quad (168)$$

The atom transfer in this system would most likely involve methyl nitrite in the reaction

$$CH_3 + CH_3ONO \longrightarrow CH_4 + CH_2ONO \quad (17)$$

If this reaction proceeded to a significant extent an increase in the methane yield would be observed at long times. This was not the case and hence this reaction must be of minor importance only. Methyl abstraction of nitric oxide from methyl nitrite has been observed in pyrolysis experiments (169)

$$CH_3 + CH_3ONO \longrightarrow CH_3NO + CH_3O \quad (18)$$

but there was no evidence for this reaction in this system. It must be concluded that the methyl radicals are long lived being lost by termolecular or perhaps heterogeneous combination with themselves to form ethane or hydrogen atoms to form small amounts of methane.

$$CH_3 + H + M \longrightarrow CH_4 + M \quad (19)$$

The overall observed stoichiometry of 3.8 hydrogen atoms per methyl nitrite molecule is consistent with hydrogen atoms reacting with CH_3ONO, CH_3O, HNO, CH_2O, CHO and NO_2. The stoichiometry would be lowered by the consumption of methyl nitrite by hydroxyl radicals and the loss of formaldehyde to the flow tube walls. The system is too complex for any further rationalisation of the observations.

(b) The Ethyl Nitrite Reaction: In the reaction between hydrogen atoms and ethyl nitrite the primary products NO_2 and HNO are identical with those of the methyl nitrite reaction and will react as they did in that reaction. Similarly in this reaction system

ethane, hydrogen and nitric oxide can be considered unreactive.

The reaction of the ethoxy radical with hydrogen atoms could follow pathways analogous to those of the methoxy radical reaction with the additional pathway to form methane and formaldehyde

$$H + C_2H_5O \longrightarrow C_2H_5 + OH \quad \ldots\ldots\ldots \quad (20a)$$
$$\longrightarrow CH_3CHO + H_2 \quad \ldots\ldots\ldots \quad (20b)$$
$$\longrightarrow CH_4 + CH_2O \quad \ldots\ldots\ldots \quad (20c)$$

The ethoxy radical could alternatively undergo the unimolecular decomposition

$$C_2H_5O \longrightarrow CH_3 + CH_2O \quad \ldots\ldots\ldots \quad (21)$$

The rate constant for this reaction is $4.5 s^{-1}$ at room temperature [170] so for the rate of this reaction to equal the rate of removal of the radical by reaction (20) the rate constant k_{20} would need to be $1.5 \times 10^{-14} cm^3 molec.^{-1} s^{-1}$ for a hydrogen atom concentration of 10 mTorr. The rate constant for an atom/radical reaction of this type is likely to be of the order of 10^{-11} to $10^{-12} cm^3 molec.^{-1} s^{-1}$ so at high or excess hydrogen atom concentrations the unimolecular decomposition is unlikely. In the stoichiometry determination these conditions do not apply as the hydrogen atom concentration is markedly lowered. Thus the unimolecular decomposition may become a significant removal process for the radical under these circumstances.

If reaction (20b) did not occur and reactions (20a) and (20c) proceeded at a relative rate of 70:30 then the products of the reaction of the ethoxy radical

with hydrogen atoms would be virtually identical to those of the reaction of hydrogen atoms with methoxy radicals. Each reaction would produce an alkyl radical, a hydroxyl radical, formaldehyde and an unreactive species (H_2 or CH_4). If this were the case then the overall reactions would be virtually identical and hence the stoichiometries approximately equal. However the stoichiometries are 3.8 for the methyl nitrite reaction and 1.2 for the ethyl nitrite reaction. This would imply that reaction (20c) is responsible for less than 30% of reaction (20) as if this is the case more hydroxyl radicals would be produced and less formaldehyde produced compared to the methoxy radical reaction. Both of these changes would lower the overall observed stoichiometry in the ethyl nitrite reaction from that of the methyl nitrite reaction.

The rate constant for the reaction of hydrogen atoms with acetaldehyde is $3.2\times10^{-14}cm^3molec^{-1}s^{-1}$ (171) which is almost the same as that for the reaction with formaldehyde ($5.4\times10^{-14}cm^3molec^{-1}s^{-1}$) both reactions ultimately yielding carbon monoxide. The difference between the two reactions is that while formaldehyde yields carbon monoxide after a two step reaction sequence, acetaldehyde has a three step sequence

$$H + CH_3CHO \longrightarrow H_2 + CH_3CO \quad \ldots\ldots\ldots (22)$$

$$H + CH_3CO \longrightarrow H_2 + CH_2CO \quad \ldots\ldots\ldots (23)$$

$$H + CH_2CO \longrightarrow CH_3 + CO \quad \ldots\ldots\ldots (24)$$

The rate constant for reaction (23) has been estimated as 5×10^{-12} and the reaction of hydrogen atoms with

ketene (24) has a rate constant of $1.3 \times 10^{-13} cm^3 molec.^{-1} s^{-1}$. (172) Where the hydrogen atom concentration is low the initial attack on the acetaldehyde may be made by the hydroxyl radical

$$OH + CH_3CHO \longrightarrow H_2O + CH_3CO \quad \ldots\ldots\ldots (25)$$

This reaction is much faster than the reaction with hydrogen atoms its rate constant being $1.5 \times 10^{-11} cm^3 molec.^{-1} s^{-1}$. (173) These reactions are consistent with the maximum observed in the acetaldehyde concentration as the reaction time was increased.

Depending on the involvement of reaction (25), each acetaldehyde molecule would remove between two and three hydrogen atoms with the production of no other reactive species. However the stoichiometry of the ethyl nitrite hydrogen atom reaction is close to 1:1 atom:nitrite compared with 3.8:1 in the methyl nitrite reaction. Since formaldehyde consumes between one and two hydrogen atoms and acetaldehyde between two and three, the lower stoichiometry in the ethyl nitrite reaction implies that little acetaldehyde is produced either by primary or secondary reactions. This ties in well with the argument that reaction (20a) is the major channel for the reaction of hydrogen atoms with ethoxy radicals.

The differences between the two overall reactions seems to be due to the modes of decomposition of the alkoxy radical. The methoxy radical is lost by reaction with hydrogen atoms, the reaction proceeding via two channels. This work suggests that at high hydrogen atom concentrations the reaction of ethoxy radicals with

hydrogen atoms removes the radicals but largely via the single reaction (20a). At low atom concentrations the unimolecular decomposition of the ethoxy radical can become an important reaction. The net effect of these two differences is to lower the stoichiometry of the hydrogen atom/ethyl nitrite reaction compared to that of the methyl nitrite reaction by increasing the hydroxyl radical concentration and decreasing the number of hydrogen atoms required for the removal of ethoxy radicals.

(3) The Rate Constants

Unlike the reaction between the nitrites and ozone the Arrhenius parameters obtained from the reaction of the nitrites with hydrogen atoms are as expected. For the reaction of an atom with a complex molecule the steric factor is less than that for the reaction of 2 molecules and is related to the partition functions for vibration and rotation by

$$P = \left(\frac{q_{vib}}{q_{rot}}\right)^2$$

This has a likely value of $\sim 10^{-2}$. Calculating the collision frequencies for these reactions one obtains 1.15×10^{-9} and 1.40×10^{-9} $cm^3 molec.^{-1} s^{-1}$ for the methyl and ethyl nitrite reactions respectively. These yield steric factors of 2×10^{-2} and 6×10^{-3} which are both within the range of the predicted values. The Arrhenius parameters also lie within the range of values for other hydrogen atom reactions as do the activation energies (see Table VI.7.)

TABLE VI.7

ARRHENIUS PARAMETERS AND ACTIVATION ENERGIES FOR HYDROGEN ATOM REACTIONS

Reactant	A	Ea
	$cm^3 molec.^{-1} s^{-1}$	$kJ.mol^{-1}$
MeONO[a]	2.47(-11)	16.22
EtONO[a]	8.80(-12)	13.84
H_2O_2[b]	5.2 (-12)	11.63
CH_2O[c]	2.2 (-11)	15.71
NO_2[c]	5.8 (-10)	6.15
NO_2[f]	7.1 (-10)	4.2
HCl[d]	3.8 (-11)	14.6
C_2H_4S[e]	9.5 (-11)	8.13
ONCl[f]	7.6 (-11)	3.8

(a) This work

(b) Ref 174

(c) Ref 28

(d) Ref 58

(e) Ref 175

(f) Ref 176

(4) Comparison with Other Work

The only other reported work on either of these reactions has been a study of the methyl nitrite reaction with hydrogen atoms undertaken by Moortgat et al.. [137] They used a discharge flow system attached to a photoionisation mass spectrometer, ran the flow system at total pressures of around 4 Torr and used reagent concentrations an order of magnitude higher than this work. The main discrepancies between the two studies are that Moortgat et al. assigned methanol to be a primary product with a yield of 47% and showed that methane could not be a primary product, the opposite conclusions to those obtained in this study. The other difference is in the rate expressions which are shown below, that of Moortgat et al. being listed first.

$$\log_{10}k = (-12.37\pm0.09) - \left(\frac{7.96\pm0.47}{2.303RT}\right)$$

$$\log_{10}k = (-10.61\pm0.20) - \left(\frac{16.22\pm1.00}{2.303RT}\right)$$

The rate constants and Arrhenius parameters have units of $cm^3molec.^{-1}s^{-1}$ and the activation energies $kJ.mol^{-1}$. The higher precision of the first expression is artificial as Moortgat et al. quoted one standard deviation as their uncertainty whereas this study quotes two. Moortgat et al. used the nitrogen dioxide titration to obtain hydrogen atom concentrations but assumed 1:1 stoichiometry at ~3ms. This could lead to an overestimation of the hydrogen atom concentration by a factor of $^3/_2$ and a corresponding underestimation of the rate constant. Figure VI.2 shows the Arrhenius plots

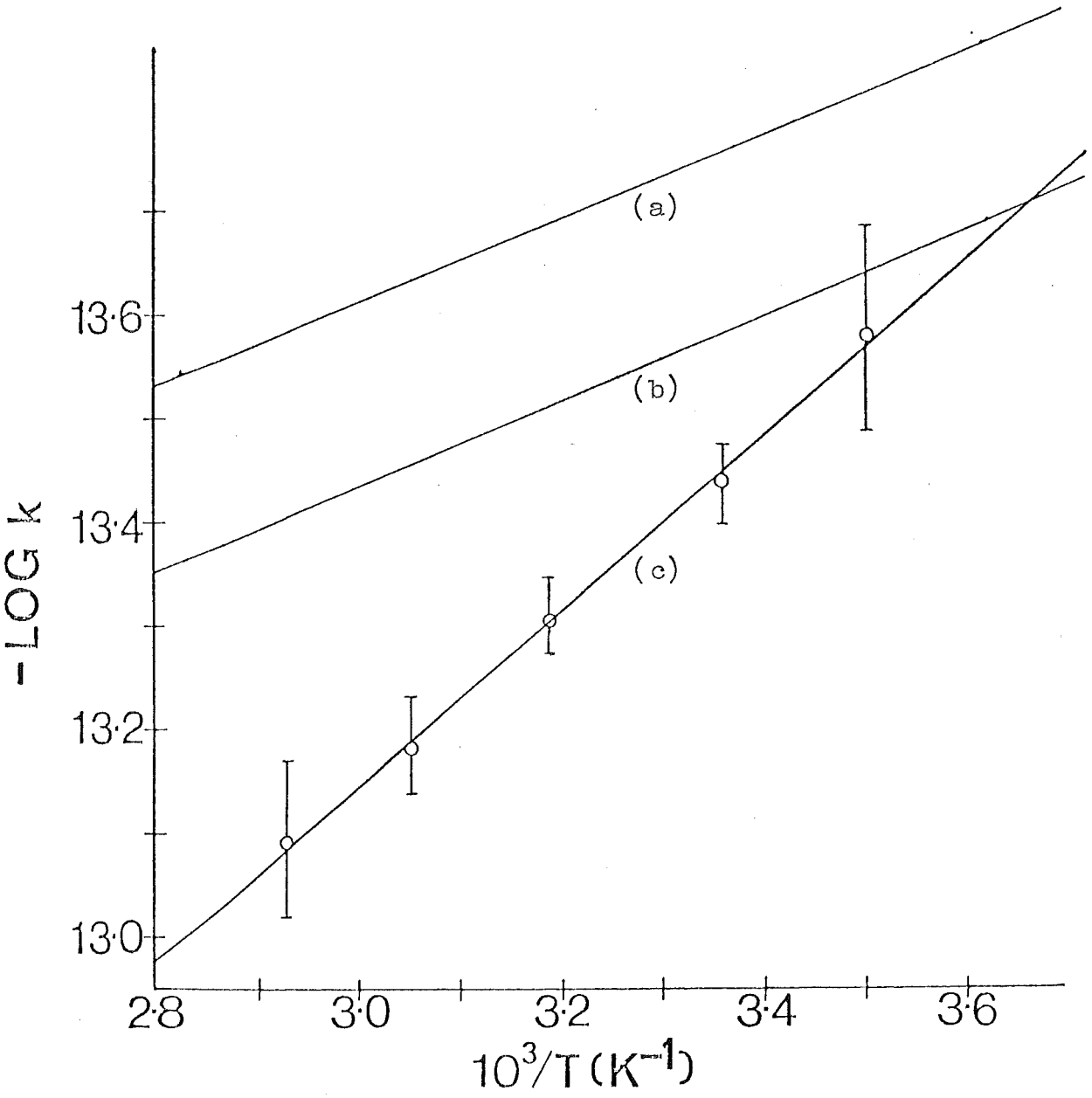

FIGURE VI.2 Comparison of Arrhenius Plots for the Methyl Nitrite-Hydrogen Atom Reaction.

for both studies, line (a) representing the above expression of Moortgat et al., line (b) this value multiplied by $^{3}/_{2}$ and (c) the results from this study. The room temperature rates are, for Moortgat's study $1.65 \pm 0.21 \times 10^{-14}$ which corrects to $2.48 \pm 0.32 \times 10^{-14}$ compared with the value of $3.61 \pm 0.71 \times 10^{-14}$ $cm^{3}molec.^{-1}s^{-1}$ obtained in this study. Thus the two determinations are in satisfactory agreement at room temperature. While the rate constants agree at around room temperature the difference in activation energies is significant. The most likely explanation for this discrepancy results from the higher pressures and higher reagent concentrations used by Moortgat et al.. It is possible that the observed rate of methyl nitrite removal under their conditions was not governed solely by the rate constant of the primary reaction but was affected by secondary reactions.

The room temperature results of Moortgat etal. are listed in Table VI.8 and it may be significant that even at constant total pressure the highest atom concentration produces the lowest rate constant and the lowest nitrite concentration gives the highest rate constant. This trend was observed in this study when operating at reagent concentrations slightly less than those of Moortgat et al., viz., 40-50 mTorr of atoms and 1-4 mTorr of nitrite, where the rate constant calculated ranged upwards from 6×10^{-15} $cm^{3}molec.^{-1}s^{-1}$. Some of these results are also shown in Table VI.8. In this study it has been assumed that such a trend indicated that

secondary reactions were complicating the analysis and the concentrations were lowered until the trend was no longer observed, at which point it was assumed that secondary reactions were not significantly complicating the reaction. If the primary reaction is followed by fast secondary reactions the effect of which cannot be minimised, then the normal method of obtaining the rate constant involves determining the overall stoichiometry and making an allowance for additional reagent consumption in calculating the rate constant. [9] This was not done by Moortgat et al. and as a result their rate constants could be in error especially if the atom excess is low. The atom excess employed by Moortgat et al ranged from 6 to 36 fold but was generally around 10 fold and a pseudo first order analysis was used to calculate the rate constant. If the calculated hydrogen atom concentrations are in error by a factor of $^{2}/_{3}$ this excess reduces to 7 fold and for an overall stoichiometry of 4 H atoms/methyl nitrite molecule , as found in this study, the atom excess would not exceed 4 fold. In this case the pseudo first-order analysis would be invalid.

The conclusion is that Moortgat et al. are not studying the primary reaction alone but that a number of reactions all contribute to the nitrite loss. The observed rate constant is therefore a composite value made up of the rate constants of several reactions, although the validity of the method of analysis must also be questioned in some runs. The apparent temperature dependence of the composite rate constant will differ from

TABLE VI.8

COMPARISON OF THE RATE CONSTANTS OBTAINED BY MOORTGAT ET AL. WITH REDUNDANT CALCULATED RATE CONSTANTS FROM THIS STUDY

T / K	P / Torr	[H] / mTorr	$[CH_3ONO]_0$ / mTorr	$kx10^{14}$ / $cm^3 molec^{-1} s^{-1}$
a) Moortgat et al.				
298	1.50	59.6	2.89	1.94
"	2.13	102.7	3.77	1.52
"	2.40	83.3	12.97	1.62
"	3.48	107.3	10.37	1.63
"	3.49	92.7	9.20	1.64
"	3.50	90.3	7.40	1.71
"	3.52	102.0	5.63	1.69
"	3.53	151.7	7.00	1.24
"	3.53	53.3	5.10	1.50
"	3.68	89.3	4.70	1.58
"	3.68	118.7	3.30	2.03
b) This study				
298	0.490	56.4	3.12	0.844
"	"	"	3.06	1.06
"	"	"	2.83	0.965
"	"	"	1.55	1.19
"	"	"	0.91	1.30
"	"	"	0.70	1.32
"	"	38.3	4.61	0.963
"	"	"	3.19	1.05
"	"	"	1.45	1.45
"	"	"	0.46	1.90
"	0.435	44.2	4.97	0.617
"	"	"	2.70	0.829

that of the primary reaction leading to values for the Arrhenius parameter and activation energy which differ from those of the primary reaction. Some evidence to support this explanation comes from the Arrhenius parameter of 4×10^{-13} which is over an order of magnitude below the predicted value ($\sim1.2\times10^{-11}$) and any other measured value (see Table VI.7).

Methane was detected in this work, positively identified by the detection of d_1 methane in the deuterium atom reaction and found to have a yield of $(8.7\pm1.5)\%$. Moortgat et al. claimed to be able to detect a yield of 2% methane but detected no d_1 methane in the deuterium atom reaction although methanes up to d_4 were detected. It is unlikely the difference could be due to an error in the estimation of the methane sensitivity. A more likely explanation, in view of the presence of higher deuterated methanes, is that the d_1 methane produced on reaction could react further with deuterium atoms, decreasing the d_1 methane concentration to below the 2% level before sampling. The reactions involved are:

$$D + CH_3D \longrightarrow CH_2D_2 + H \quad \ldots\ldots\ldots \quad (1a)$$

$$D + CH_2D_2 \longrightarrow CHD_3 + H \quad \ldots\ldots\ldots \quad (1b)$$

$$D + CHD_3 \longrightarrow CD_4 + H \quad \ldots\ldots\ldots \quad (1c)$$

The rate constants for these reactions appear to be below $10^{-17}cm^3molec.^{-1}s^{-1}$ (177,178) and so the reactions would be unlikely to proceed significantly in the system. However there appears to be no other source of these methanes as they are generally unreactive so reaction (1) must be faster than stated, and included in the

reaction sequence.

The major problem encountered in explaining the differences observed in methanol production results from the lack of kinetic data on the reactions of methyl and methoxy radicals with other species in the system. Methanol was detected by Moortgat et al. who assigned it to be a primary product accounting for 47% of the consumed methyl nitrite, whereas it was detected in this study only when the conditions of Moortgat's study were simulated, viz. when the pressure was raised. The evidence from the present study points to methanol being a secondary product produced at high total pressures and high reagent concentrations.

The abstraction of a hydrogen from methyl nitrite by the methoxy radical

$$CH_3O + CH_3ONO \longrightarrow CH_3OH + CH_2O + NO \quad \ldots\ldots (2)$$

can be discounted completely. In both studies d_1 methanol was detected in the deuterium atom reaction and when Moortgat et al. reacted hydrogen atoms with d_3 methyl nitrite d_3 methanol was the product. The reaction of methoxy radicals with molecular hydrogen could be the methanol source through the reaction

$$CH_3O + H_2 \longrightarrow CH_3OH + H \quad \ldots\ldots\ldots (3)$$

but this process would be in competition with the reaction of methoxy radicals with hydrogen atoms

$$H + CH_3O \longrightarrow CH_2O + H_2 \quad \ldots\ldots\ldots (4a)$$

$$\longrightarrow CH_3 + OH \quad \ldots\ldots\ldots (4b)$$

There is no rate constant for reaction (3) but the analogous reaction of hydroxyl radicals with hydrogen

has a rate constant of 6×10^{-15} $cm^3 molec.^{-1} s^{-1}$. (28) Using this value for the rate constant of reaction (3) and assuming the atom concentration to be 1/5th the molecular concentration then for the rates of the two reactions (3 and 4) to be equal the rate constant for reaction (4) would need to be 3×10^{-14} $cm^3 molec.^{-1} s^{-1}$ which is some two orders of magnitude less than the expected value of 10^{-11} to 10^{-12} $cm^3 molec.^{-1} s^{-1}$. The other bimolecular reaction which could produce methanol is the reaction between the methoxy radical and the nitroxyl molecule.

$$CH_3O + HNO \longrightarrow CH_3OH + NO \quad \ldots\ldots\ldots \quad (5)$$

If the rate constant for this reaction were the same as that for reaction (4) the reaction would be unimportant as the atom concentration would greatly exceed the HNO molecule concentration. Similarly the fast reaction of nitroxyl molecules with hydrogen atoms

$$H + HNO \longrightarrow H_2 + NO \quad \ldots\ldots\ldots \quad (6)$$

which has a rate constant between 10^{-12} and 10^{-13} cm^3 $molec.^{-1} s^{-1}$ (28) would keep the nitroxyl concentration low so that reaction (5) can be discounted.

The high pressure required to produce methanol in this study suggests a termolecular reaction may be responsible for methanol production. The direct addition of methoxy radicals and hydrogen atoms

$$CH_3O + H + M \longrightarrow CH_3OH + M \quad \ldots\ldots\ldots \quad (7)$$

must also compete with reaction (4). Using the rate constant for the addition of hydroxyl radicals to hydrogen atoms of 6.8×10^{-31} $cm^6 molec.^{-2} s^{-1}$ (28) as an

estimate for the rate constant of reaction (5) and taking a typical pressure from Moortgat's work of 4 Torr the pseudo second-order rate constant for reaction (7), k[M], is 8×10^{-14} $cm^3 molec.^{-1} s^{-1}$. This is between 1 and 2 orders of magnitude slower than the estimate for the rate constant for reaction (4) and thus reaction 7 is unlikely to be significant. The combination of methyl and hydroxyl radicals is also a likely source of methanol as reaction (4) is fast and produces both these radicals although their concentrations are much less than that of the hydrogen atoms.

$$CH_3 + OH + M \longrightarrow CH_3OH + M \quad \ldots\ldots\ldots (8)$$

The rate constant for this reaction is not known but the same estimate of the pseudo second-order rate constant can be used as was used for reaction (7), viz. 8×10^{-14} $cm^3 molec.^{-1} s^{-1}$. Even at 50% nitrite consumption, where the nitrite and methyl radical concentrations are approximately equal, reaction (8) *is* still an order of magnitude slower than the hydroxyl radical reaction with methyl nitrite

$$OH + CH_3ONO \longrightarrow \text{products} \quad \ldots\ldots\ldots (9)$$

which has a rate constant of 1.3×10^{-12} $cm^3 molec.^{-1} s^{-1}$. However at these high extents of reaction many of the hydroxyl radicals will react with the formaldehyde produced by reaction (4) since the rate constant for this reaction is 1.4×10^{-11} $cm^3 molec.^{-1} s^{-1}$ (167) and the formaldehyde concentration at least 3/7th's of that of the methyl radical. Thus reaction (8) is also unlikely to produce significant concentrations of methanol.

Throughout the above discussions it has been necessary to use, as estimates, rate constants from hydroxyl radical and hydrogen atom reactions in place of those of the corresponding methoxy radical and methyl radical processes. No reaction stood out as being a likely source of methanol with the rate constants of all reactions considered, being too low. Unless the rates of some of the alkoxy radical reactions are orders of magnitude faster than the corresponding hydroxyl radical reactions then the production of methanol cannot be explained by this mechanism.

It must therefore be concluded that the reaction system is so complex that the method used to study it in this work is unable to provide sufficient information for the mechanism to be fully determined.

(5) The Reaction's Use as an Alkoxy Radical Source

The difficulty of the detection of the alkoxy radicals in this study suggests they have a low steady state concentration. This can be explained by the slow rate of production of the radical which will be somewhat less than the rate of nitrite removal which has a rate constant of 3.6 and 3.3 x 10^{-14} $cm^3 molec.^{-1} s^{-1}$ for methyl and ethyl nitrite respectively. Also the reactions of the alkoxy radical are fast with that with hydrogen atoms estimated to be between 10^{-11} and 10^{-12} $cm^3 molec.^{-1} s^{-1}$. Using the steady state approximation and the simplified reaction sequence

$$H + CH_3ONO \xrightarrow{k_1} CH_3O + HNO$$

$$H + CH_3O \xrightarrow{k_2} \text{products}$$

one obtains $$[CH_3O]_{ss} = \frac{k_1 [CH_3ONO]}{k_2}$$

$$\sim 10^{-2} [CH_3ONO]$$

This explains the low steady state concentration of the radical which would be further lowered if other fast alkoxy radical reactions were included.

In conclusion the low steady state concentration of alkoxy radicals makes this reaction an unsatisfactory source of the radical for kinetic studies.

CHAPTER VII

SUMMARY AND CONCLUSIONS

1. GASEOUS NITROUS ACID

Gaseous nitrous acid has been postulated as an intermediate in many hydrogen, oxygen, nitrogen reaction systems but because of problems in its production and detection there have only been indirect studies of its reactions. In this work a discharge flow-mass spectrometer system was used in an attempt to make and detect the acid. It was found that gaseous nitrous acid could be formed in the discharge flow system at total pressures of 1-4 Torr by the reaction of hydroxyl radicals with nitric oxide

$$OH + NO + M \longrightarrow HONO + M$$

Using discharged water vapour as the hydroxyl radical source a parent peak at M47 (mass peak 47) was observed indicating that nitrous acid was formed and possessed a detectable parent peak. This showed that the apparatus used in this study could be used to make and detect nitrous acid and only slight modifications to the flow tube would be required before reactions of the acid could be studied.

Future work on nitrous acid reactions using this reaction as the nitrous acid source will be possible only if a more satisfactory source of hydroxyl radicals is found. Discharges through water vapour and hydrogen peroxide are generally regarded as unsatisfactory sources

of the radical and the normal sources, the hydrogen atom reactions with nitrogen dioxide or ozone, were found to present insurmountable problems in this study. The most promising source appears to be the reaction of molecular oxygen with an excess of hydrogen atoms at pressures sufficiently high for the first reaction to be the termolecular production of the hydroperoxy radical

$$H + O_2 + M \longrightarrow HO_2 + M$$

This would be followed by the rapid reaction of the hydroperoxy radical with hydrogen atoms to give hydroxyl radicals

$$H + HO_2 \longrightarrow OH + OH$$

This seems to be a sufficiently clean source of hydroxyl radicals that the nitrous acid could be easily produced, detected and its reactions followed.

2. THE REACTIONS OF OZONE WITH METHYL AND ETHYL NITRITES

The reactions of ozone with methyl and ethyl nitrites were studied in a static reaction vessel under conditions of excess ozone using an infrared spectrophotometer to follow concentration changes and to detect products. The reaction was shown to be the simple oxidation

$$RONO + O_3 \longrightarrow RONO_2 + O_2$$

The rate constant expressions obtained with k in units of $cm^3 molec^{-1} s^{-1}$ and activation energies in $kJmol^{-1}$ were

$$\log_{10} k = (-12.17 \pm 0.46) - \left(\frac{44.2 \pm 2.9}{2.303RT} \right)$$

for R = methyl, and

$$\log_{10}k = (-15.50\pm0.32) - \left(\frac{19.6\pm1.9}{2.303RT}\right)$$

for R = ethyl. The only unusual feature of this reaction is the abnormally low Arrhenius parameter in the ethyl nitrite reaction which could not be satisfactorily explained.

This reaction was studied because of its possible importance in photochemical smog but the room temperature reaction rate values of 1.30×10^{-20} and 1.17×10^{-19} $cm^3molec.^{-1}s^{-1}$ for R = methyl and R = ethyl show that this reaction is too slow to compete with the photolysis of the nitrite.

That these reactions are slow implies the analogous reaction of nitrous acid

$$HONO + O_3 \longrightarrow HONO_2 + O_2$$

is also slow and is unlikely to be a significant reaction in the nitrogen balance in the stratosphere.

3. THE REACTIONS OF HYDROGEN ATOMS WITH METHYL AND ETHYL NITRITES

(1) Results of this Study

The reactions of hydrogen atoms with methyl and ethyl nitrites were studied using a discharge flow-mass spectrometer system. Products detected in the methyl nitrite reaction were hydrogen, nitric oxide, methane, water and formaldehyde. Methanol was detected at higher pressures with either methoxy radicals or nitroxyl molecules (or perhaps both) detected as intermediates. The products detected for the ethyl nitrite reaction

were hydrogen, nitric oxide, ethane, water and possibly formaldehyde. Ethanol was detected at higher pressures with acetaldehyde, the ethoxy radical and nitroxyl molecule detected as intermediates.

The primary reactions were shown to be:

$$H + RONO \longrightarrow RO + HNO$$
$$\longrightarrow RH + NO_2$$
$$\longrightarrow R_{-H}O + NO + H_2$$

where in the methyl nitrite reaction the yield of methane was found to be $8.7 \pm 1.5\%$ of the consumed nitrite.

The overall stoichiometries were found to be 3.8:1 and 1.2:1, H atoms:nitrite for methyl and ethyl nitrite respectively.

On the basis of the observed products and stoichiometries the following secondary reactions were included in the mechanisms for both reactions:

$$H + HNO \longrightarrow H_2 + NO$$
$$H + NO_2 \longrightarrow OH + NO$$
$$OH + OH \longrightarrow H_2O + O$$
$$O + NO \longrightarrow NO_2 + h\nu$$
$$O + OH \longrightarrow O_2 + H$$
$$O + NO_2 \longrightarrow NO + O_2$$

For the methyl nitrite/hydrogen atom reaction other secondary reactions are:

$$H + CH_3O \longrightarrow CH_3 + OH$$
$$\longrightarrow CH_2O + H_2$$
$$H + CH_2O \longrightarrow H_2 + HCO$$
$$OH + CH_2O \longrightarrow H_2O + HCO$$
$$H + HCO \longrightarrow H_2 + CO$$

For the ethyl nitrite/hydrogen atom reaction the secondary reactions are:

$$H + C_2H_5O \longrightarrow C_2H_5 + OH$$
$$H + CH_3CHO \longrightarrow CH_3CO + H_2$$
$$OH + CH_3CHO \longrightarrow CH_3CO + H_2O$$
$$H + CH_3CO \longrightarrow CH_2CO + H_2$$
$$H + CH_2CO \longrightarrow CH_3 + CO$$

To account for the lower overall stoichiometry in the ethyl nitrite reaction compared to the methyl nitrite reaction it is necessary to postulate a low yield of acetaldehyde. Any further rationalisation of the mechanism is impossible as the fragmented nature of the nitrite spectrum made product identification difficult.

The rate constant expressions obtained with k in units of $cm^3 molec.^{-1} s^{-1}$ and the activation energy in $kJ.mol^{-1}$ were:

$$\log_{10}k = (-10.61 \pm 0.20) - \left(\frac{16.2 \pm 1.0}{2.303RT}\right)$$

for the methyl reaction and

$$\log_{10}k = (-11.06 \pm 0.20) - \left(\frac{13.8 \pm 1.0}{2.303RT}\right)$$

for the ethyl nitrite reaction. The Arrhenius parameters and activation energies are consistent with those expected for this type of reaction.

As a source of alkoxy radicals for kinetic experiments these reactions are unsatisfactory as the steady state concentration of the radical is very low. This is brought about by the slow rate for the radical production but its fast rate of removal by reaction.

(2) Future Studies

The two studies of methyl nitrite reaction with hydrogen atoms, namely this study and that of Moortgat et al., show several differences. The products observed differ, with Moortgat et al. claiming methanol to be a major primary product but not methane, the opposite conclusions to those of this work. There is also a marked difference in the temperature dependence of the rate constant expression.

To check on the primary products one method would be to run the reaction under the conditions of this study and bleed off some of the reaction mixture for gas chromatographic analysis. Provided the atoms were destroyed on sampling by passing them over an active surface, this analysis would assist in the identification of the primary reaction products.

An attempt was made to use a computer to simulate the conditions in the flow tube given the initial concentrations and mechanism presented in Chapter VI. The aim was to fit the mechanism to the observations and thus find the most important secondary reactions. It was also planned to use this computer model to attempt to fit the concentration profiles and rate constant expression obtained by Moortgat et al.. Unfortunately the computer package being used in this work (the Burroughs Dynamic Modelling, Dynamo package) proved to be faulty and as the errors could not be readily rectified this approach had to be deferred. Once this package is operable this work should continue as it will

indicate the more important reactions and will enable the two sets of work on the methyl nitrite reaction to be compared.

Most of the problems encountered in trying to rationalise the observations of this study resulted from the lack of kinetic data on alkoxy radical reactions. This problem will continue with all similar systems until a satisfactory method of obtaining kinetic data on the radical can be found. The lack of distinct spectral features of the alkoxy radical indicate that a discharge flow/mass spectrometric system may be one of the best methods available for studying these reactions. The major problem would be in the clean production of the radical.

It may be possible to photolyse a compound in the flow tube to yield the radical. In this case the dialkyl peroxide (ROOR) would possibly be the cleanest alkoxy radical source, [179] although the yield may be too low.

$$ROOR + h\upsilon \longrightarrow RO + OR$$

For a reaction to be used as a radical source it would need to have a rate constant the order of $10^{-11} cm^3 molec.^{-1} s^{-1}$. The reactions of hydrogen and oxygen atoms, [9] and hydroxyl radicals [136] with alkyl nitrites, and the reaction of hydrogen atoms with methylhydroperoxide (CH_3OOH) [166] have all been found to be too slow. The reactions most likely to produce the alkoxy radicals are those where an atom or radical attacks an oxide or peroxide in a reaction of the type:

$$A + ROX \longrightarrow RO + AX$$

where A = O, H, N, OH or CH_3

X = Cl, Br, NO_2, NO, OR or OH

The major problem that would be encountered with many of these reactions is the preference for A to remove a hydrogen from the alkyl group rather than the X group as required.

The reaction of hydroxyl radicals with the alkyl nitrite is an important reaction in the mechanism proposed in Chapter VI and may account for much of the nitrite consumption at long times. The rate constant of the methyl nitrite reaction has been determined (136) but the products have not been identified. If this reaction proceeds to a significant extent as a secondary reaction in the hydrogen atom/nitrite reaction system then the products would need to be included in the mechanism. The identification of the products of the hydroxyl radical nitrite reaction is therefore important if a full understanding of the hydrogen atom/nitrite reaction is to be achieved.

APPENDIX I

THERMO CHEMICAL DATA

Enthalpy changes for chemical reactions were calculated using the following heats of formation obtained from the JANAF Thermochemical Tables [180] unless otherwise indicated.

Species	$\Delta H_f^o 298$ / kJmol^{-1}
H	217.986 ± 0.004
O	249.19 ± 0.13
N	472.8 ± 4.2
OH	39.43 ± 1.26
HNO	102.5
CH_3	145.69 ± 0.84
O_3	143.1. ± 1.7
NO_2	33.10 ± 0.84
NO	90.33 ± 0.17
HNO_2	- 76.73 ± 1.34 (cis)
	- 78.83 ± 1.34 (trans)
HNO_3	-134.30 ± 0.42
CH_4	- 74.87 ± 0.33
CH_3ONO^a	- 66.9 ± 2.1
$C_2H_5ONO^a$	-102.5
$CH_3ONO_2{}^b$	-121.8 ± 1.3
$C_2H_5ONO_2{}^b$	-154.1 ± 1.2
CH_3OH^b	-201.12 ± 0.21
CH_3O^a	17.6 ± 2.9

Species	$\Delta H_f^0 298$ / kJmol^{-1}
C_2H_5O[a]	- 17.2 ± 2.9
CH_2O	-115.9 ± 6.3
C_2H_5OH[c]	-235.10
C_2H_4O[c]	-166.19
C_2H_6[c]	- 84.68
C_2H_5[c]	+104.6

a Reference 134

b Reference 181

c Reference 182

APPENDIX II

PURIFICATION OF OZONE

Ozone is hazardous because it can explode violently and it has a very high toxicity with a threshold limit value (T.L.V.) of 0.1 ppm, compared with 10ppm for hydrogen cyanide. The T.L.V. is the maximum recommended concentration in which humans can safely work for an 8 hour day. (183)

A commercial ozonator running on pure oxygen produces about 3% ozone in the oxygen stream and this concentration will readily attack rubber tubing and hydrocarbons such as grease and pump oil. The ozone can be destroyed by bubbling the ozone/oxygen mixture through a potassium iodide solution where the oxidation of iodide to iodine takes place, and can be used as a quantitative analysis for ozone.

$$O_3 + 2H^+ + 2I^- \longrightarrow H_2O + I_2 + O_2$$

Obtaining pure ozone from this mixture must be carried out with high regard to safety features as ozone readily explodes if it rapidly evapourates from a glass surface, is heated or if a high pressure exists. Pressures of pure ozone greater than 100 Torr are not recommended. (184)

The following method of purification of Cook et al. (185) appears to be the safest. The ozone is trapped from the oxygen by passing the mixture through a "U" tube containing non indicating silica gel held at 195K by a

dry ice bath the level of which is below the level of the silica gel. At this temperature 4.5gm of ozone will be adsorbed per 100gm of silica gel. After passing through the "U" tube the gas should pass through a potassium iodide bubbler to remove traces of ozone before the oxygen is allowed into the room. When the iodide solution is appreciably darkened the silica gel is fully loaded with ozone. To purify the ozone the "U" tube is isolated, surrounded by liquid air and the oxygen pumped off. Once the oxygen is removed the ozone can be stored on the silica gel, although some decomposition will take place, expanded into a bulb by warming, or transferred to another silica gel filled trap. The liquid air trap before the pump should also contain silica gel as the system will need to be pumped out occasionally. The trap can safely be removed from the line as normal and placed in a fume cupboard where, as the trap warms, the ozone will be liberated.

Once it is adsorbed on to silica gel the ozone is quite safe as at 168K a loading of 21gm of ozone per 100gm silica gel was subjected to an electrical discharge with no resultant explosion. (185) Also in the present study a gaseous ozone explosion shattered a trap containing ozone on silica gel but the adsorbed ozone did not explode.

When working with ozone points to note are

(i) Ensure ozone cannot condense on glass above the silica gel as on warming it may explode.

(ii) Use greaseless stopcocks and fluorocarbon greases.

(iii) Do not jar a sample of gaseous ozone either physically or by subjecting it to a sudden pressure change.

APPENDIX III

HEAT TRANSFER FROM THE WALLS OF THE FLOW TUBE INTO THE GAS STREAM

The aim of this section is to show that the heating arrangement described in Section III.1.(1) was sufficient to heat the gases in the flow tube. Equations used in this section can be found in the Chemical Engineers Handbook [186] and the constants used are from this source or the Handbook of Chemistry and Physics. [187]

Consider the case of the flow tube with the wall temperature held at Tw by circulating water. The gas enters the heated portion of the tube with temperature Tg_o and at a distance L down the tube the temperature has changed to Tg. The problem as it applies to this work is how long must L be before Tg is within an acceptable range of Tw.

The solution to this problem depends on the nature of the gas flow, whether it is laminar or turbulent. The test for turbulence is to calculate the dimensionless Reynolds number (N_{Re}). If this number exceeds 2100 the flow is turbulent if not the flow is laminar.

The Reynolds number is given by

$$N_{Re} = \frac{D.v.\rho}{\mu}$$

where D = flow tube diameter

v = gas flow velocity

ρ = gas density

μ = gas viscosity

These constants were calculated for argon at 0.1 Torr and yielded at fast flow velocities

$D = 0.02m$

$v = 10 m.s^{-1}$

$\mu = 2.15 \times 10^{-5} N.s.m^{-2}$

$\rho = 2.14 \times 10^{-4} kg.m^{-3}$

from which $N_{Re} = 1.99$

The flow is therefore laminar. For the slow flow conditions where

$v = 2 m.s.^{-1}$

and $\rho = 8.46 \times 10^{-4} kg.m^{-3}$

the Reynolds number is 1.57 so under all conditions in this work the flow is laminar.

The heat transfer (q) into the gas is given by

$q = h.A.\Delta T$

where h = heat transfer coefficient

A = area of flow tube wall in contact with the gas

ΔT = difference between wall and gas temperature

If the flow is plug then $dA = \pi DdL$ and so

$$dq = h.\Delta T.\pi.D.dL \quad \ldots\ldots\ldots\ldots\ldots\ldots \quad (1)$$

The mass flow of gas per unit time G is given by

$$G = A.v.\rho$$

$$= \frac{\pi.D^2.v.\rho}{4}$$

The heat transfer is related to the heat capacity of the gas by

$dq = G.Cp.dT$

where Cp is the heat capacity per unit mass.

Hence $$dq = \frac{\pi.D^2}{4}.v.\rho.Cp.dT \quad \ldots\ldots\ldots\ldots\ldots\ldots \quad (2)$$

Equating (1) and (2) yields

$$h.\Delta T.\pi.D.dL = \pi.\frac{D^2}{4}.v.\rho.Cp.dT$$

$$\frac{4.h}{D.v.\rho.Cp}.dL = \frac{dT}{\Delta T}$$

Integrating and inserting the boundary condition that when L = 0 Tg = Tg_o gives

$$\frac{4.h.L}{D.v.\rho.Cp} = \log_e\left(\frac{Tg_o - Tw}{Tg - Tw}\right) \quad \ldots\ldots\ldots\ldots(3)$$

The heat transfer coefficient is not known but can be calculated if the Nusselt number (N_{Nu}) is known, because

$$N_{Nu} = \frac{h.D}{k}$$

where k = thermal conductivity

For simple systems equations for determining the Nusselt number have been derived. For a circular tube there is the Hausen equation which can be used provided the dimensionless Graetz number (N_{Gz}) is less than 100. This is defined as

$$N_{Gz} = \frac{N_{Re}.N_{Pr}.D}{L}$$

where N_{Pr} is the Prandtl number defined as

$$N_{Pr} = \frac{Cp.\mu}{k}$$

For argon $Cp = 0.52\ kJ.kg^{-1}K^{-1}$

and $k = 1.73\times10^{-5}\ kJ.s^{-1}m^{-1}K^{-1}$

Hence $N_{Pr} = 0.65$

The Graetz number is therefore

$N_{Gz} = 5.2\times10^{-2}$ for a 50 cm long tube

This value for the Graetz number is well less than 100 so Hausen's equation can be used to calculate the Nusselt number.

$$N_{Nu} = 3.66 + \frac{0.085 . N_{Gz}}{1 + 0.047 . N_{Gz}^{2/3}} . \left(\frac{\mu_b}{\mu_w}\right)^{0.14}$$

where μ_b = viscosity of the bulk gas

μ_w = viscosity of the gas in the layer adhering to the wall

The second term is negligible compared to the first so that

$$N_{Nu} = 3.66$$

and $$h = 3.66 \frac{k}{D}$$

Inserting this expression into equation 3 yields

$$\log_e \left(\frac{Tgo - Tw}{Tg - Tw}\right) = \frac{14.64\ k.L}{D^2 . v . \rho . Cp}$$

If the difference between the initial gas temperature and the wall temperature is 50K and the gas temperature is required to be within 0.5K of the wall temperature then

$$\ln \left(\frac{Tgo - Tw}{Tg - Tw}\right) = 4.60$$

and $$L = \frac{0.31\ D^2 . v . \rho . Cp}{k}$$

Using the values for fast flow conditions

$D = 0.02m$

$v = 10\ ms^{-1}$

$\rho = 2.14 \times 10^{-4} kg.m^{-3}$

$Cp = 0.52\ kJ.kg^{-1}K^{-1}$

$k = 1.73 \times 10^{-5}\ kJ\ s^{-1}m^{-1}k^{-1}$

one obtains $L = 8 \times 10^{-3} m$

Hence within 8mm of entering the heated section of flow tube the gas is within 0.5K of the wall temperature. Since the gas travels at least 5cm before reaching the nitrite inlet it is reasonable to assume the gas temperature is the same as that of the flow tube walls.

APPENDIX IV

CALCULATION OF RESULTS

1. CONCENTRATION OF REAGENTS

(1) Static Reaction System

The initial concentrations of ozone and nitrite were calculated from the pressures of these reagents in their respective parts of the cell and the previously determined ratio of volumes within the cell. In most cases it was not necessary to calculate nitrite concentration during the reaction but where a second order analysis was applied the nitrite absorbance was extrapolated to zero time, the extinction coefficient calculated and the concentrations determined.

(2) Discharge Flow System

The concentration C(X) in Torr of any gas X at the sampling leak could be calculated from its sensitivity S(X) in amps $Torr^{-1}$ and the mass spectrometric peak height A(X) in amps using the relation

$$C(X) = \frac{A(X)}{S(X)}$$

However only the absolute sensitivity of argon was determined daily all other gases having sensitivities expressed relative to argon previously determined. The absolute sensitivity for gas X is given by its relative sensitivity R(X) and the current argon sensitivity S(Ar) by

$$S(X) = S(Ar).R(X)$$

Since the argon concentration remained constant variations in argon peak height meant corresponding changes in the absolute sensitivity. If on calibration the argon peak height was A'(Ar) and later changed to A(Ar) then the sensitivity S(X) can be related to the sensitivity on calibration S'(X) by

$$S(X) = S'(X).\ \frac{A(Ar)}{A'(Ar)}$$

The expression for the concentration of X becomes

$$C(X) = \frac{A(X).A'(Ar)}{A(Ar)S'(Ar).R(X)}$$

where the second term is a constant for a particular run.

2. GAS VELOCITY IN THE DISCHARGE FLOW TUBE

The gas velocity in the discharge flow tube at the point of sampling was calculated from the expression

$$u = \frac{F.T.P'}{A.T'.P} = \frac{K.F.T}{P}$$

where u is the linear flow velocity in cm s^{-1},

T,T' are the temperatures in Kelvin at the time of the experiment and of calibration of the capillary flow meter,

P is the argon gas pressure in Torr at the sampling leak as determined in the experiment

P' is the atmospheric pressure in Torr at the time of calibration of the flowmeter

A is the cross-sectional area in cm^2 of the flowtube

F is the flowrate of argon in $cm^3 sec^{-1}$ as determined

by the flowmeter

and K is a constant incorporating P'T' and A and had the value 1.06 Torr cm^{-2} K^{-1} in the present system. It was only necessary to determine the flow and pressure of the argon to determine the flow velocity.

3. RATE CONSTANT CALCULATIONS

In all cases where the rate constant is calculated the reaction was carried out in an excess of one reagent so that the reaction became pseudo first order. In the reaction between ozone and the nitrites the infinity value of the nitrite sometimes lay outside the range of the recorder and because of the small though finite mixing time, extrapolation of nitrite concentration to zero time was found to be inaccurate so the Guggenheim method which requires neither a zero nor infinity reading was used. The calculations associated with the discharge flow system are generally straightforward however the pressure drop down the tube greatly increased the complexity of the analysis.

(1) Guggenheim Method

Consider the general second order reaction

$$A + B \longrightarrow \text{products}$$

which has the rate expression

$$-\frac{dA}{dt} = k_2 . A . B$$

where A and B are concentrations of species A and B and k_2 is a second order rate constant. If B is in large excess then

$$-\frac{dA}{dt} = k_1.A \quad \ldots\ldots\ldots\ldots\ldots\ldots (1)$$

where k_1 is a pseudo first order rate constant

$$k_1 = k_2.B$$

Solving equation (1) and inserting the boundary condition $A = A_0$ when $t = 0$ gives

$$A = A_0.\exp(-k_1.t)$$

Let A at time t be A_t

and A " " t + T be A_t'

Then $A_t = A_0.\exp(-k_1.t)$

and $A_t' = A_0.\exp(-k_1(t + T))$

Subtracting gives

$$A_t' - A_t = A_0.\exp(-k_1.t).(1-\exp(-k_1T))$$

$$\log_e(A_t'-A_t) = \text{const} - k_1.t \quad \ldots\ldots\ldots (2)$$

Hence a plot of $-\log_e(A_t'-A_t)$ against t will give a straight line of slope k_1 from which k_2 can be calculated.

Furthermore it is not necessary to use the concentration of species A, and a parameter which is proportional to concentration (c) is sufficient. Suppose

$$G = c.A$$

then $\log_e(A_t'-A_t) = \log_e(G_t'-G_t) - \log_e c$

Hence equation 2 becomes

$$\log_e(G_t'-G_t) = \text{const}' - k_1.t$$

and a plot of $-\log_e(G_t'-G_t)$ against t is a straight line of slope k_1.

In the calculation of rates for the ozone/nitrite reactions the absorbance was used as a measure of concentration and if $\underline{A}_t$ is the absorbance of nitrite at time t a plot of $-\log_e(\underline{A}_t'-\underline{A}_t)$ against t was used to

obtain k_1 and hence k_2.

(2) Data Analysis in Discharge Flow System

Consider the second order reaction

$$A + B \longrightarrow \text{products}$$

with rate expression

$$-\frac{dA}{dt} = k_2 . A . B$$

where A and B are the concentrations of species A and B and k_2 is the second order rate constant. If B is in large excess this simplifies to

$$-\frac{dA}{dt} = k_1 . A$$

where k_1 is a pseudo first order rate constant

$$k_1 = k_2 . B$$

Solving this differential equation with the boundary condition the $A = A_0$ when $t = 0$ gives the solution

$$\log_e\left(\frac{A_0}{A}\right) = k_1 . t$$

Under the specified conditions if the gas velocity is u and the reaction distance is x

$$t = \frac{x}{u}$$

and so $k_1 . x = \log_e\left(\frac{A_0}{A}\right) . u$

or $k_2 . x = \log_e\left(\frac{A_0}{A}\right) . \frac{u}{B}$

Hence a plot of either $\log_e\left(\frac{A_0}{A}\right)$ or $-\log_e A$

against x would give a straight line of slope $\frac{k_1}{u} = \frac{k_2 . B}{u}$

from which k_1 and k_2 could be calculated.

However in the case where there is a pressure drop down the tube the analysis changes. If measurements are made at the low pressure end of the tube then the early stages of reaction take place at higher reagent concentrations, because of the pressure drop, and the reaction is therefore faster than if the same quantities of gases passed through a section of tube closer to the low pressure end. This increase in pressure has the same effect as a non linear increase in reaction time up the tube and the following analysis shows the pressure drop correction increases the reaction time from that calculated from

$$t = \frac{x}{u}$$

Consider the second order reaction to be taking place in a flow tube

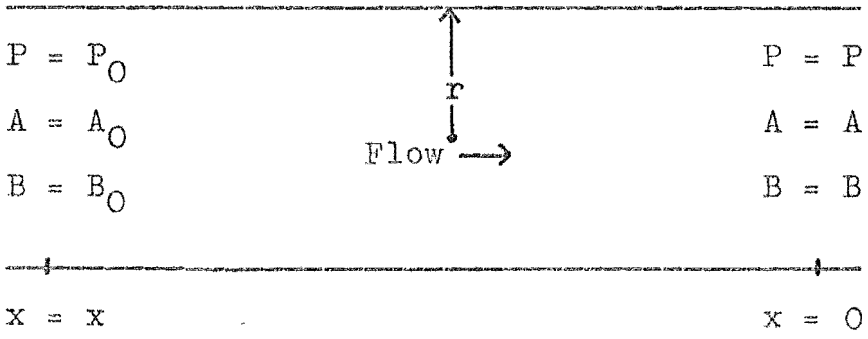

The pressure drop down the tube is given by the Poiseuille expression

$$y = \frac{P}{P_0} = (1-b.x)^{\frac{1}{2}} \quad \ldots\ldots\ldots\ldots\ldots\ldots \quad (1)$$

If B is in large excess the change in concentration of B down the tube is entirely due to the pressure drop so that

$$B = B_0 . \frac{P}{P_0}$$

Consider a volume element of the tube $\pi r^2 dx$, the time a molecule spends in this element is

$$dt = \frac{dx}{u} = \frac{\pi . r^2 . dx}{v} = \frac{P . dV}{R.T.F.} \quad \ldots\ldots\ldots\ldots (2)$$

where u and v are the average linear and volumetric flow velocities, P, V, R, T come from the gas equation and F is the flow of gas in moles per second. The total time a molecule is in the tube is the contact time tc and

$$tc = \frac{P.V}{R.T.F}$$

Substituting for dt in the rate expression $-\frac{dA}{dt} = kAB$

gives $-d(v.A) = \pi . r^2 . k . A . B . dx$

$$\therefore \quad -v.dA - A.dv = \pi . r^2 . k . A . B . dx \quad \ldots\ldots\ldots (3)$$

Let $\pi . r^2 . k = D$ $\qquad v = \frac{R.T.F}{P} = \frac{C}{P}$

obtaining differentials

$$dx = \frac{-2y}{b} . dy \qquad dy = \frac{dP}{P_0} \qquad dv = \frac{C . dP}{P^2}$$

Substitute for v B and dx in equation (3)

$$\frac{-C}{P} . dA + \frac{A . C}{P^2} . dP = D . A . B_0 . \frac{P}{P_0} . \frac{-2 . P}{b \; P_0^2} . dP$$

$$= \frac{-2D . A . B_0}{b} . \frac{P^2 dP}{P_0^3}$$

Hence $$\frac{-C . dA}{A} + \frac{C . dP}{P} = \frac{-2D . B0 . P^3 dP}{b \; P_0^3}$$

Integrate and insert the boundary conditions when

$x = x \quad P = P_0 \qquad A = A_0$

$$-c . \log_e \left(\frac{A}{A_0} \right) + C . \log_e \left(\frac{P}{P_0} \right) = \frac{-2 . D . B_0 . (P^4 - P_0^4)}{4 . b . P_0^3}$$

Substitute back for C, D, b and P/PO

$$\frac{P_0.V.\log_e\left(y.\frac{A_0}{A}\right)}{t_c} = -\tfrac{1}{2}.B_0.\pi.r^2.\frac{k.x.P_0^4(y^4-1)}{(1-y^2)\ P_0^3}$$

Since $V = \pi r^2 x$

$$k.B_0.t_c = 2\ \frac{(1-y^2)}{(1-y^4)}.\log_e\left(y.\frac{A_0}{A}\right)$$

$$= \frac{2}{(1+y^2)}\log_e\left(y.\frac{A_0}{A}\right) \quad \ldots\ldots\ldots (4)$$

The contact time t_c is related to the average linear flow velocity u

$$t_c = \frac{x}{u}$$

where $u = \tfrac{1}{2}(u_{x=0} + u_{x=x})$

The velocity is pressure dependent so

$$u_x = u_0.\frac{P}{P_0} = u_0.y$$

Hence $u = u_0.\ \frac{(1+y)}{2}$

and $t_c = \frac{2x}{u_0.(1+y)}$

$$B_0 = \frac{B}{y}$$

$$A_0 = \frac{A'}{y}$$

where A' is the concentration of A at x = 0 in the absence of reaction

Substitute for t_c B_0 A_0 in equation (4)

$$k.\frac{B}{y}.\frac{2x}{u_0(1+y)} = \frac{2}{(1-y^2)}.\log_e\left(\frac{A'}{A}\right)$$

$$\frac{k.x.(1+y^2)}{y.(1+y)} = \log_e\left(\frac{A'}{A}\right).\frac{u_0}{B}$$

where u B A and A' are all determined at x = 0. Since A' is a constant a plot of either $\log_e\left(\frac{A'}{A}\right)$ or $-\log_e A$ against $\frac{x.(1+y^2)}{y.(1+y)}$ will be a straight line of slope $\frac{k.B.}{u}$

As the pressure drop decreases y tends to unity and $\frac{x.(1+y^2)}{y.(1+y)}$ tends to x and this is the same result as the initial case without the pressure drop.

To calculate the above function of y the Poiseuille expression was used in the form

$$P_0^2 - P^2 = \frac{16F.\eta.R.T.x}{\pi.r^4}$$

where F is the flow rate, η the viscosity, r the tube radius, R the gas constant and T the temperature. In this work the expression reduced to

$$P_0^2 - P^2 = 2.55\times10^{-6}T.x$$

where T is in Kelvin, x is in cm.

The computer programme described in Appendix V found the value of y for each value of x and performed a least squares analysis of the plot of $+\log_e A$ against $\frac{x.(1+y^2)}{y.(1+y)}$ to obtain the rate constant.

The rate constant units used in this work were the same as adopted by the C.I.A.P. programme [28] namely $cm^{3(n-1)}$ $molecule^{(1-n)}$ sec^{-1} where n is the order of the reaction.

(3) The Effect of a Non Constant Temperature Down the Flow Tube

This section examines the effect a variation in

temperature in the unheated end section of the flow tube would have on the calculated rate constant.

Using the same conventions as the previous section consider the pseudo first order reaction with its corresponding rate expression

$$A + B \longrightarrow \text{products}$$

$$-u.\frac{dA}{dt} = k_1.A$$

If there are two sections of the tube at different temperatures then there will be two different rate constants for the two sections of the tube and

$$u.\frac{dA}{dt} = k_1.A + k_1'.A$$

where k_1, is the rate constant at the required temperature and k_1' is that in the variable temperature region. If all measurements are made with the movable inlet jet within the heated section of the tube then the length of the variable temperature section will be constant at x_1. Integrating the rate expression yields

$$-u\left[\log_e A\right]_0^{x_1} - u\left[\log_e A\right]_{x_1}^{x} = \left[k_1 x\right]_{x_1}^{x} + \left[k_1' x\right]_0^{x_1}$$

$$\log_e\left(\frac{A_{x_1}}{A}\right) = k_1.\frac{x}{u} + \left(k'_1.\frac{x_1}{u} - k_1.\frac{x_1}{u} + \log_e\left(\frac{A_0}{A_{x_1}}\right)\right)$$

Hence a plot of $-\log_e A$ against x will give a straight line of slope $\frac{k_1}{u}$ and the variable temperature section has no effect on the calculated rate constant. This result applies only to first-order reactions and for measurements where $x > x_1$.

4. CALCULATION OF COLLISION FREQUENCIES

The collision frequencies (Z) were calculated using the formula

$$Z = \sigma^2 \left(\frac{8.\pi.R.T}{\mu} \right)^{\frac{1}{2}}$$

where σ = average molecular diameter.

μ = reduced mass

The following molecular diameters were used in the calculations. In many cases the molecular diameters for the desired molecules were not known so those of molecules of expected similar size were used. Where this was done the other molecule is shown in brackets.

Molecule	Molecular Diameter * A
H (He)	2.6
$CH_3ONO(nC_4H_{10})$	5.0
$C_2H_5ONO(nC_5H_{12})$	5.8
O_3 (CO_2)	4.0
CH_4	3.8
C_2H_4	4.2
C_3H_6	5.0
C_4H_8	5.0
NO	3.5
NO_2 (N_2O)	3.8

* Reference 188

APPENDIX V

COMPUTER PROGRAMMES

Two computer programmes were used in this work and since they both required least square analyses along with data manipulation it was found convenient to use the Omnitab II data manipulation and statistical [189] package attached to the Burroughs 6718 computer.

The first programme was that used to calculate the rate constant in the discharge flow system study and included allowance for the pressure drop down the tube. The input data was the $\log_e$ of the electrometer reading for the nitrite peak height and the measured reaction distance. The programme calculated the corrected distance expression $\frac{x.(1+y^2)}{y.(1+y)}$ and performed a least squares analysis of the $\log_e$ nitrite concentration against this expression. From the slope and intercept of this line the rate constant, the initial nitrite concentration and the predicted values were calculated. The input data to the least squares analysis and the predicted values were plotted on the same graph to highlight any marked deviation from linearity. The computer output from a typical set of data is shown after the description of the activation energy programme.

Page 1 lists the input data for the least squares analysis along with the output of predicted values and deviations. Pages 2 and 3 show plots of the residuals

against the input order and the two parameters so any trends in the data can be observed. The probability plot of the standardised residuals is also included. Pages 4 and 5 list the statistical information from the least squares analysis, the most important data being the coefficients and their standard deviations on page 5. Term 0 is the intercept and term 1 the slope. Page 6 is a plot of the input data to the least squares analysis (dots) along with the predicted values (asterisks), numbers indicate multiple points on the same print position. Pages 7 and 8 list the input data, the results and the other calculated values required to ensure the programme has run successfully. Pages 9, 10 and 11 list the programme.

The other programme used, was to calculate the activation energies and Arrhenius parameters of a reaction from the temperature and rate constant values by performing a least squares analysis of the $\log_{10}k$ verses $^{1}/T$ plot. A sample output is shown following the rate constant calculation output and the two programmes have the same output format.

SAMPLE OUTPUT OF THE COMPUTER PROGRAMME USED TO CALCULATE RATE CONSTANTS IN THE DISCHARGE FLOW SYSTEM

********** 19/8/76/1 **********

LEAST SQUARES FIT FOR LN NITRITE IN COLUMN 1
AS A POLYNOMIAL OF DEGREE 1 IN DIST CORR IN COLUMN 37
USING 17 NON-ZERO WEIGHTS = 1.0000000

ROW	DIST CORR IN COLUMN 37	LN NITRITE IN COLUMN 1	PREDICTED VALUES	STD. DEV. OF PRED. VALUES	RESIDUALS	STD. RES.	WEIGHTS
1	32.369402	3.5700000	3.4984411	.014315597	.071558925	3.35	1.000
2	20.633498	3.6500000	3.6466276	.0077142924	.0033723604	0.14	1.000
3	12.601620	3.7500000	3.7480443	.0063534378	.0019556722	0.08	1.000
4	8.6099863	3.8000000	3.7984458	.0074263150	.0015542331	0.06	1.000
5	4.2141394	3.8600000	3.8539511	.009491987O	.0060488825	0.25	1.000
6	1.9484010	3.9000000	3.8825601	.0107568823	.017439923	0.75	1.000
7	6.7130372	3.8200000	3.8223981	.0082359750	-.0023981089	-0.10	1.000
8	10.448491	3.7700000	3.7752314	.0068071051	-.0052313940	-0.21	1.000
9	17.676629	3.6800000	3.6839634	.0066981525	-.0039633538	-0.16	1.000
10	26.404872	3.5700000	3.5737538	.0106582265	-.0037538340	-0.16	1.000
11	20.920665	3.6200000	3.6430017	.0078360866	-.0230016051	-0.94	1.000
12	14.694705	3.7100000	3.7216154	.0062499455	-.011615423	-0.47	1.000
13	7.1810289	3.8200000	3.8164889	.0080227292	.0035111154	0.14	1.000
14	3.5548097	3.8600000	3.8622763	.0098502302	-.0022763220	-0.10	1.000
15	9.2163903	3.8000000	3.7907888	.0072017283	.0092111563	0.37	1.000
16	17.815000	3.6800000	3.6822162	.0067344738	-.0022161695	-0.09	1.000
17	27.478608	3.5000000	3.5601960	.0112886389	-.0601960111	-2.60	1.000

STANDARDIZED RESIDUALS VS ROW NUMBER

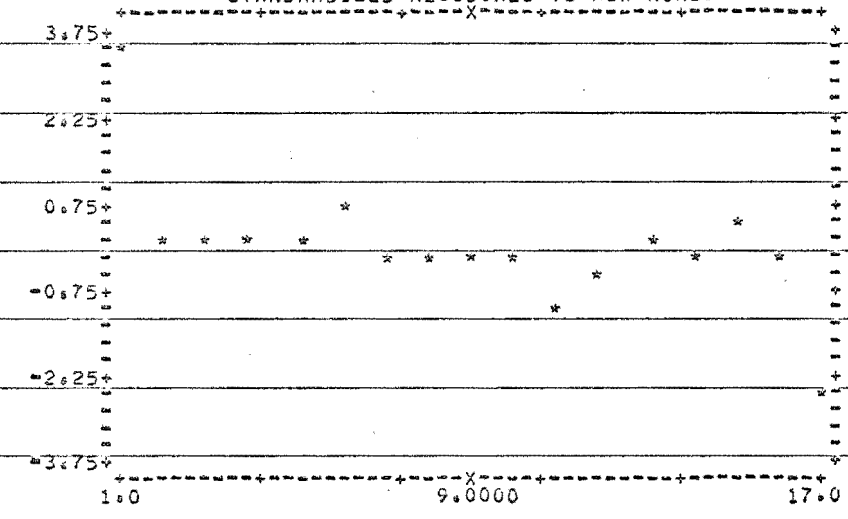

STANDARDIZED RESIDUALS VS PREDICTED VALUES

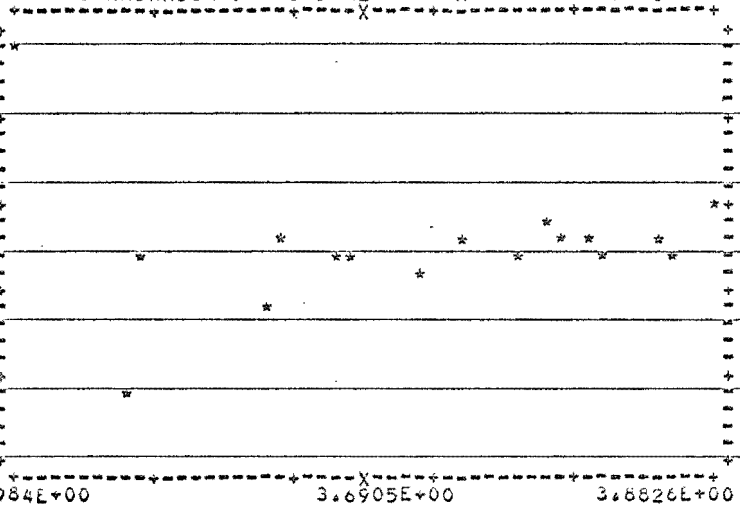

STANDARDIZED RESIDUALS VS DIST CORR

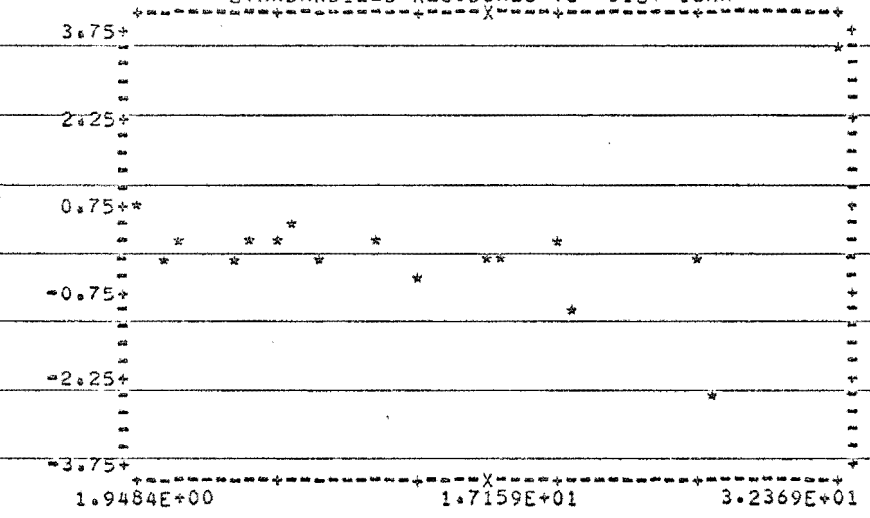

PROBABILITY PLOT OF STANDARDIZED RESIDUALS

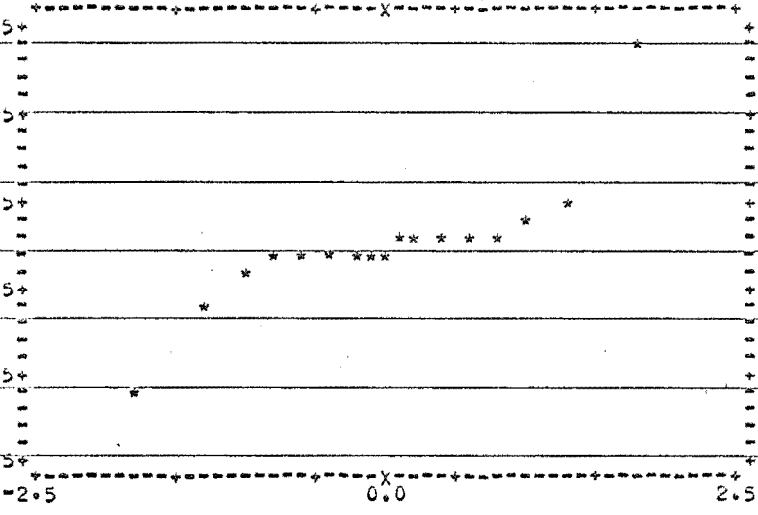

********** 19/8/76/1 **********

LEAST SQUARES FIT FOR LN NITRITE IN COLUMN 1
AS A POLYNOMIAL OF DEGREE 1 IN DIST CORR IN COLUMN 37
USING 17 NON-ZERO WEIGHTS = 1.0000000

VARIANCE-COVARIANCE MATRIX OF THE ESTIMATED COEFFICIENTS

TERM	0	1
0	1.4197057-04	
1	-7.2213754-06	5.0627983-07

ANALYSIS OF VARIANCE
"DEPENDENT ON ORDER VARIABLES ARE ENTERED, UNLESS VECTORS ARE ORTHOGONAL"

TERM	SS=RED. DUE TO COEF.	CUM. MS REDUCTION	D.F.	CUM. RESIDUAL MS	D.F.	F(COEF=0)	P(F)	F(COEFS=0)	P(F)
0	236.14645	236.14645	1	.013659559	16	356473.625	0.000	178394.270	0.000
1	.20861617	118.17753	2	.000-6245139	15	314.915	0.000	314.915	0.000
RESIDUAL	.0099367708		15						
TOTAL	236.36500		17						

19/8/76/1

LEAST SQUARES FIT FOR LN NITRITE IN COLUMN 1
AS A POLYNOMIAL OF DEGREE 1 IN DIST CORR IN COLUMN 37
USING 17 NON-ZERO WEIGHTS = 1.0000000

	ESTIMATES FROM LEAST SQUARES FIT				FIT OMITTING LAST TERM		
TERM	COEFFICIENT	S.D. OF COEFF.	RATIO	*ACC. DIGITS	COEFFICIENT	S.D. OF COEFF.	RATIO
0	3.9071621	.011915140	327.92	10.95	3.7270588	.028346137	131.48
1	-.012626771	.00071153343	-17.75	12.00			
RESIDUAL STANDARD DEVIATION =		.025736131				.11687412	
BASED ON DEGREES OF FREEDOM		17- 2 = 15				17- 1 = 16	

* THE NUMBER OF CORRECTLY COMPUTED DIGITS IN EACH COEFFICIENT USUALLY DIFFERS BY LESS THAN 1 FROM THE NUMBER GIVEN HERE

19/8/76/1

ABS= DIST CORR ,ORD= LN NITRITE (.), COLUMN 12 (*),

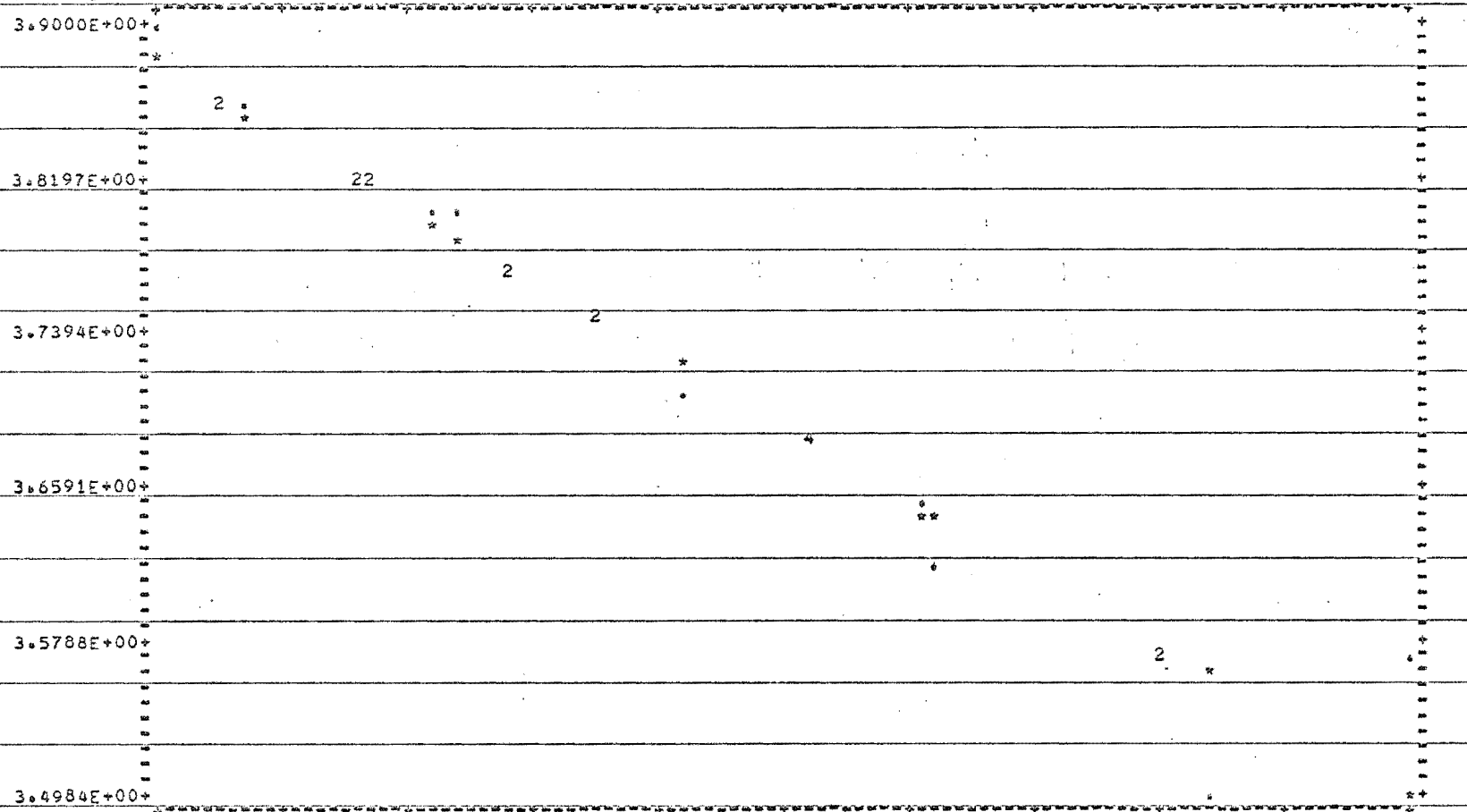

********** 19/8/76/1 **********

LN NITRITE	DIST CORR	DISTANCE	VELOCITY	ATOMS	T	P	P/PO
3.5700000	32.369402	24.600000	1182.0000	13.550000	298.00000	.11900000	.65652197
3.6500000	20.633498	16.900000	1182.0000	13.550000	298.00000	.11900000	.72416655
3.7500000	12.601620	11.000000	1182.0000	13.550000	298.00000	.11900000	.79298274
3.8000000	8.6099863	7.8000000	1182.0000	13.550000	298.00000	.11900000	.83960735
3.8600000	4.2141394	4.0000000	1182.0000	13.550000	298.00000	.11900000	.90735067
3.9000000	1.9484010	1.9000000	1182.0000	13.550000	298.00000	.11900000	.95261566
3.8200000	6.7130372	6.2000000	1182.0000	13.550000	298.00000	.11900000	.86623061
3.7700000	10.448491	9.3000000	1182.0000	13.550000	298.00000	.11900000	.81675462
3.6800000	17.676629	14.800000	1182.0000	13.550000	298.00000	.11900000	.74656190
3.5700000	26.404872	20.800000	1182.0000	13.550000	298.00000	.11900000	.66742593
3.6200000	20.920665	17.100000	1182.0000	13.550000	298.00000	.11900000	.72213724
3.7100000	14.694705	12.600000	1182.0000	13.550000	298.00000	.11900000	.77240588
3.8200000	7.1810289	6.6000000	1182.0000	13.550000	298.00000	.11900000	.85933817
3.8600000	3.5548097	3.4000000	1182.0000	13.550000	298.00000	.11900000	.91962082
3.8000000	9.2163903	8.3000000	1182.0000	13.550000	298.00000	.11900000	.83177605
3.6800000	17.815000	14.900000	1182.0000	13.550000	298.00000	.11900000	.74544797
3.5000000	27.478608	21.500000	1182.0000	13.550000	298.00000	.11900000	.68140488

********** 19/8/76/1 **********

VO	K T-1 S-1	COLUMN 4	P NEUTRAL	K CM3 MOLEC
14.927263	-1.1014644 *	3.9071621	.39500564 *	3.4005291-14
14.927263	-1.1014644	-.012628771	.39500564 *	3.4005291-14
14.927263	-1.1014644	.011915140	.39500564 *	3.4005291-14
14.927263	-1.1014644 *	7.1153343-04	.39500564 *	3.4005291-14
14.927263	-1.1014644 *	17.000000	.39500564 *	3.4005291-14
14.927263	-1.1014644 *	2.0000000	.39500564 *	3.4005291-14
14.927263	-1.1014644 *	15.000000	.39500564 *	3.4005291-14
14.927263	-1.1014644	.025738131	.39500564 *	3.4005291-14
14.927263	-1.1014644 *	6.6245139-04	.39500564 *	3.4005291-14
14.927263	-1.1014644	.95453380	.39500564 *	3.4005291-14
14.927263	-1.1014644 *		.39500564 *	3.4005291-14
14.927263	-1.1014644 *		.39500564 *	3.4005291-14
14.927263	-1.1014644 *		.39500564 *	3.4005291-14
14.927263	-1.1014644 *		.39500564 *	3.4005291-14
14.927263	-1.1014644 *		.39500564 *	3.4005291-14
14.927263	-1.1014644 *		.39500564 *	3.4005291-14
14.927263	-1.1014644 *		.39500564 *	3.4005291-14

LIST OF COMMANDS, DATA AND DIAGNOSTICS

```
TITLE1**********************************9/8/76/1 ********************************
TITLE2*************************************************************************
$      THIS PROGRAM TAKES DATA OF THE FORM LOGE CONCENTRATION AS A FUNCTION
$      OF DISTANCE AND CALCULATES THE RATE CONSTANT ASSUMING EXPONENTIAL
$      DECAY. A PRESSURE DROP CORRECTION  IS INCLUDED WHERE THE POISEUILLE
$      EXPRESSION P**2-PO**2=KXT  IS USED TO CALCULATE Y=PO/P AND THE RATE
$      CONSTANT OBTAINED FROM A LEAST SQUARES PLOT OF LOGE CONCENTRATION
$      AGAINST (1+Y**2)X/(1+Y)
$
$      READ IN DATA
$
SET Y=LN NITRITE  IN COLUMN 1
3.57,3.65,3.75,3.80,3.86,3.90,3.82,3.77,3.68,3.57,3.62,3.71,3.82,3.86,3.60,
3.68,3.50
$
SET X=DISTANCE  IN COLUMN 3
 24.6,16.9,11.0,7.8,4.0,1.9,6.2,9.3,14.8,20.8,17.1,12.6,6.6,3.4,8.3,14.9,21.5
$
$   DEFINE CONSTANTS    PRESSURES IN MTORR
$
DEFINE  VELOCITY AS 1182. IN COL 20
$
DEFINE  ATOM PRESSURE AS 13.55  IN COL 21
$
DEFINE CONVERSION  MV TO MT AS 37.79  IN CUL 22
$
DEFINE  ELECTROMETER SCALE AS 0.3 IN COL 23
$
DEFINE  TEMPERATURE AS 298. K IN CUL 24
$
   DEFINE POISEUILLE CONSTANT K AS 2.55E-6 IN COL 26
$
DEFINE   TOTAL PRESSURE AS 0.119   IN COL 25
$
$ TO OVERCOME PROBLEMS WITH TRUNCATING COLUMNS
$
1/ DEFINE ROW 1 OF COL 26 INTO ALL COL 26
1.1/  DEFINE ROW 1 OF COL 25 INTO ALL COL 25
1.2/  DEFINE ROW 1 OF COL 24 INTO ALL COL 24
$
$ FIND P AT DIST X
$
2/ MULTIPLY COL 26 BY COL 24 PUT ANS IN COL 27
2.5/ MULTIPLY COL 27 BY COL 3 PUT IN COL 28
3/ SQUARE COL 25 PUT IN 38
3.5/ ADD COL 38 TO COL 28 PUT IN COL 29
4/ SQRT COL 29 PUT PRESSURE IN COL 30
$
$ CALCULATE Y FOR X
$
```

LIST OF COMMANDS, DATA AND DIAGNOSTICS

```
5/ DIVIDE COL 25 BY COL 30 PUT Y IN COL 31
$
$ CALCULATE (1+Y**2)/(U+Y)Y
$
6/ SQUARE COL 31 PUT Y*Y IN COL 32
$
7/ ADD 1.0 TO COL 32 PUT IN COL 33
$
 8/ ADD 1.0 TO COL 31 PUT IN COL 34
9/ DIVIDE COL 33 BY COL 34 PUTIN COL 35
10/ DIVIDE COL 35 BY COL 31 PUT FN Y IN COL 36
$
$ OBTAIN CORRECTED DISTANCE FUNCTION
11/ MULTIPLY COL 36 BY COL 3 PUT CURR FN IN COL 37
$
$      PERFORM LEAST SQUARES ANALYSIS
$
12/ POLYFIT LN C IN COL 1,WEIGHTS 1.0,DEGREE 1 TO X CORR IN COL 37 ANS IN COL4
$
$ SLOPE OF THIS LINE IS IN ROW 2 OF COL 4 , THE INTERCEPT IN RUW 1
$      CONVERT SLOPE OF LINE INTO A RATE CONSTANT OF THE RIGHT UNITS
$
13/ MULTIPLY SLOPE *2,4* BY VELOCITY *1,20* PUT ANS INTO COL 5
14/ DIVIDE COL 5 BY ATOMS *1,21* PUT ANS INTO COL 6
$ CONVERT RATE CONST FROM T-1S-1 TO CM3 MOLEC-1 S-1 BY MULTIPLYING BY
$ 10.36E-17*T     NEGATIVE REQUIRED AS SLOPE IS NEGATIVE
15/ MULTIPLY COL 6 BY -10.36E-17 PUT ANS IN 7
16/ MULTIPLY COL 7 BY TEMP *1,24* PUT RATE CONSTANT IN COL 7
$
$      USE INTERCEPT TO FIND THE INITIAL NITRITE PRESSURE
$
17/ EXPONENTIAL OF INTERCEPT *1,4* PUT IN COL 8
18/ MULTIPLY 8 BY  *1,23* PUT IN COL 9
19/ DIVIDE 9 BY *1,22* PUT INITIAL NITRITE PRESSURE IN COL 10
$
$      CALCULATE THE PREDICTED VALUES SO THE LEAST SQUARES LINE CAN BE
$      PLOTTED ALONG WITH THE DATA
$
19.1/ MULTIPLY *2,4* BY COL 37 PUT IN COL 11
19.2/ ADD COL 11 TO *1,4* PUT PREDICTED VALUE OF LN C  IN COL 12
$
$
$      HEAD EACH COLUMN PRIOR TO PRINTING
$
 HEAD 1/ LN NITRITE
  HEAD 3/ DISTANCE
  HEAD 6/ K T-1 S-1
  HEAD 7/ K CM3 MOLEC-1 S-1
  HEAD 9/      VO
 HEAD 10/ P NEUTRAL
```

LIST OF COMMANDS, DATA AND DIAGNOSTICS

```
      HEAD 20/ VELOCITY
       HEAD 21/    ATOMS
        HEAD 24/        T
        HEAD 25/        P
        HEAD 37/ DIST CORR
        HEAD 31/    P/PO
      19.5/ PLOT COLS 1 AND 12 AGAINST COL 37
       20/ PRINT COLS1,37,3,20,21,24,25,31,9,6,4,10,7
       21/ RESET    1
      PERFORM OPERATIONS 1 THROUGH 21
       STOP
```

NATIONAL BUREAU OF STANDARDS, WASHINGTON, D. C. 20234, OMNITAB II VERSION 5.00 MAY 15, 1971

SAMPLE OUTPUT OF THE COMPUTER PROGRAMME USED TO CALCULATE ACTIVATION ENERGIES AND ARRHENIUS PARAMETERS

LEAST SQUARES FIT FOR DATA IN COLUMN 4
AS A POLYNOMIAL OF DEGREE 1 IN VARIABLE X IN COLUMN 3
USING 35 NON-ZERO WEIGHTS = 1.0000000

ROW	VARIABLE X IN COLUMN 3	DATA IN COLUMN 4	PREDICTED VALUES	STD. DEV. OF PRED. VALUES	RESIDUALS	STD. RES.	WEIGHTS
1	.0033557047	-13.453457	-13.448822	.0058384574	-.0046352824	-0.16	1.000
2	.0033557047	-13.422508	-13.448822	.0058384574	.0263138084	0.93	1.000
3	.0033557047	-13.428291	-13.448822	.0058384574	.0205309916	0.72	1.000
4	.0033557047	-13.427128	-13.448822	.0058384574	.0216936886	0.77	1.000
5	.0033557047	-13.407823	-13.448822	.0058384574	.0409988842	1.45	1.000
6	.0033557047	-13.441291	-13.448822	.0058384574	.0075306547	0.27	1.000
7	.0033557047	-13.446117	-13.448822	.0058384574	.0027051107	0.10	1.000
8	.0033557047	-13.485452	-13.448822	.0058384574	-.0363630163	-1.29	1.000
9	.0033557047	-13.459671	-13.448822	.0058384574	-.0108486441	-0.38	1.000
10	.0033557047	-13.442493	-13.448822	.0058384574	.0063292680	0.22	1.000
11	.0033557047	-13.431798	-13.448822	.0058384574	.0170238089	0.60	1.000
12	.0033557047	-13.450997	-13.448822	.0058384574	-.0021746538	-0.08	1.000
13	.0033557047	-13.460924	-13.448822	.0058384574	-.0121016117	-0.43	1.000
14	.0035026270	-13.681937	-13.573256	.0085390661	-.1086680451	-3.93	1.000
15	.0035026270	-13.563837	-13.573256	.0085390661	.0094188603	0.34	1.000
16	.0035026270	-13.557520	-13.573256	.0085390661	.0157359682	0.57	1.000
17	.0035026270	-13.573489	-13.573256	.0085390661	-.0002325528	-0.01	1.000
18	.0035026270	-13.542118	-13.573256	.0085390661	.0311386110	1.13	1.000
19	.0031796502	-13.292430	-13.299715	.0050823429	.0072847599	0.26	1.000
20	.0031796502	-13.310691	-13.299715	.0050823429	-.0109976357	-0.39	1.000
21	.0031796502	-13.318759	-13.299715	.0050823429	-.0190443979	-0.67	1.000
22	.0031796502	-13.295849	-13.299715	.0050823429	.0038665300 7	0.14	1.000
23	.0031796502	-13.283162	-13.299715	.0050823429	.0165522307	0.58	1.000
24	.0031796502	-13.325139	-13.299715	.0050823429	-.0254240075	-0.89	1.000
25	.0030487805	-13.204815	-13.188876	.0066835632 1	-.0159392257	-0.57	1.000
26	.0030487805	-13.166216	-13.188876	.0066835632 1	.0226605928	0.81	1.000
27	.0030487805	-13.165579	-13.188876	.0066835632 1	.0232966857	0.83	1.000
28	.0030487805	-13.175224	-13.188876	.0066835632 1	.0136552816	0.49	1.000
29	.0030487805	-13.216811	-13.188876	.0066835632 1	-.0279351556	-0.99	1.000
30	.0030487805	-13.188130	-13.188876	.0066835632 1	.0207459927	0.74	1.000
31	.0029282577	-13.103474	-13.066801	.0092930807	-.0166730030	-0.61	1.000
32	.0029282577	-13.066007	-13.066801	.0092930807	.0207939916	0.76	1.000
33	.0029282577	-13.054039	-13.066801	.0092930807	.0327614556	1.20	1.000
34	.0029282577	-13.142065	-13.066801	.0092930807	-.0552639837	-2.02	1.000
35	.0029282577	-13.101275	-13.066801	.0092930807	-.0144740066	-0.53	1.000

STANDARDIZED RESIDUALS VS ROW NUMBER

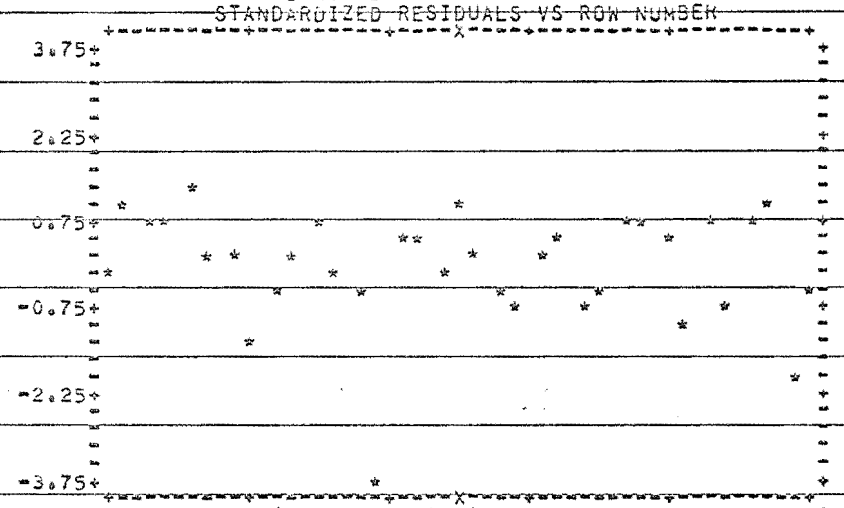

STANDARDIZED RESIDUALS VS PREDICTED VALUES

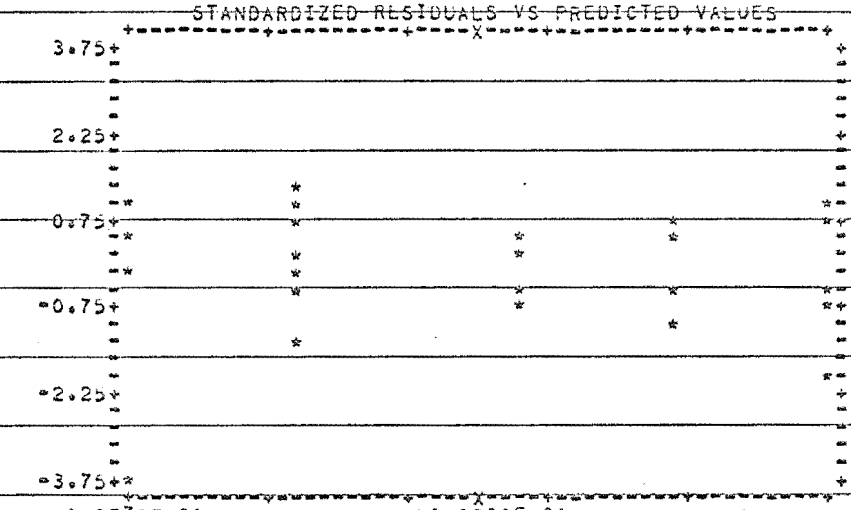

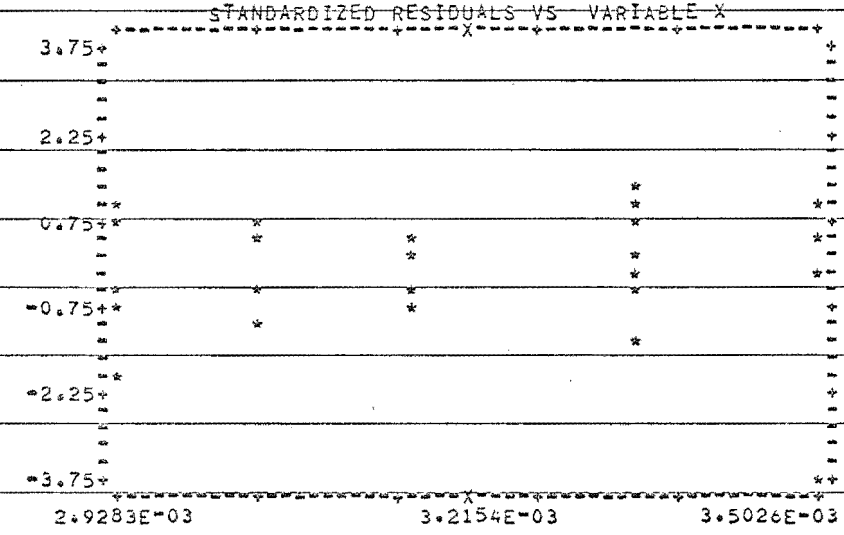
STANDARDIZED RESIDUALS VS VARIABLE X
3.75
2.25
0.75
-0.75
-2.25
-3.75
2.9283E-03
3.2154E-03
3.5026E-03

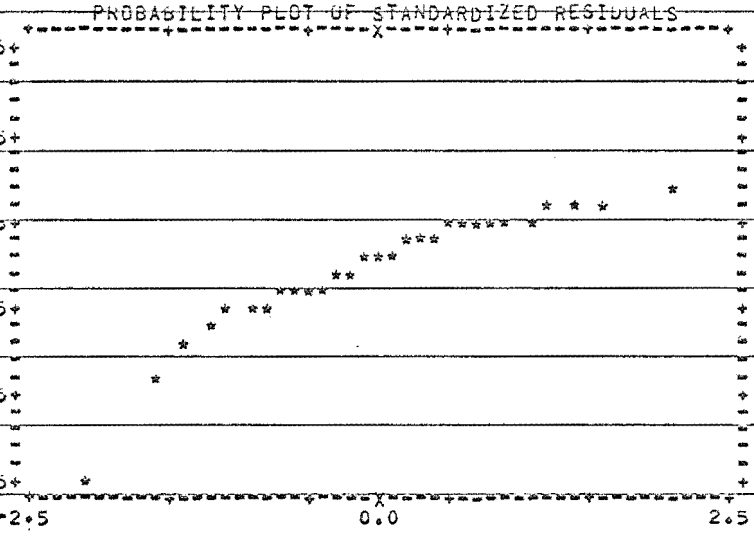
PROBABILITY PLOT OF STANDARDIZED RESIDUALS
3.75
2.25
0.75
-0.75
-2.25
-3.75
-2.5
0.0
2.5

LEAST SQUARES FIT FOR DATA IN COLUMN 4
AS A POLYNOMIAL OF DEGREE 1 IN VARIABLE X IN COLUMN 3
USING 35 NON-ZERO WEIGHTS = 1.0000000

VARIANCE-COVARIANCE MATRIX OF THE ESTIMATED COEFFICIENTS

TERM	0	1
0	.0070579318	
1	-2.1758020	6.7303251+02

ANALYSIS OF VARIANCE
"DEPENDENT ON ORDER VARIABLES ARE ENTERED, UNLESS VECTORS ARE ORTHOGONAL"

TERM	SS=RED. DUE TO COEF.	CUM. MS REDUCTION	D.F.	CUM. RESIDUAL MS	D.F.	F(COEF=0)	P(F)	F(COEFS=0)	P(F)
0	6232.8895	6232.8895	1	.027063284		34744267.032	0.000	372197 1.906	0.000
1	.89251646	3116.8910	2	.00083743002	33	1065.780	0.000	1065.780	0.000
RESIDUAL	.027635191		33						
TOTAL	6233.8096		35						

LEAST SQUARES FIT FOR DATA IN COLUMN 4
AS A POLYNOMIAL OF DEGREE 1 IN VARIABLE X IN COLUMN 3
USING 35 NON-ZERO WEIGHTS = 1.0000000

	ESTIMATES FROM LEAST SQUARES FIT				FIT OMITTING LAST TERM		
TERM	COEFFICIENT	S.D. OF COEFF.	RATIO	*ACC. DIGITS	COEFFICIENT	S.D. OF COEFF.	RATIO
0	-10.606747	.084011498	-126.25	10.96	-13.344758	.027807134	-479.90
1	-846.93850	25.942870	-32.65	10.01			
RESIDUAL STANDARD DEVIATION =		.028938383			.16450922		
BASED ON DEGREES OF FREEDOM		35- 2 = 33			35- 1 = 34		

* THE NUMBER OF CORRECTLY COMPUTED DIGITS IN EACH COEFFICIENT USUALLY DIFFERS BY LESS THAN 1 FROM THE NUMBER GIVEN HERE

ABS= COLUMN 3 ,ORD= COLUMN 4 (.), COLUMN 11 (*),

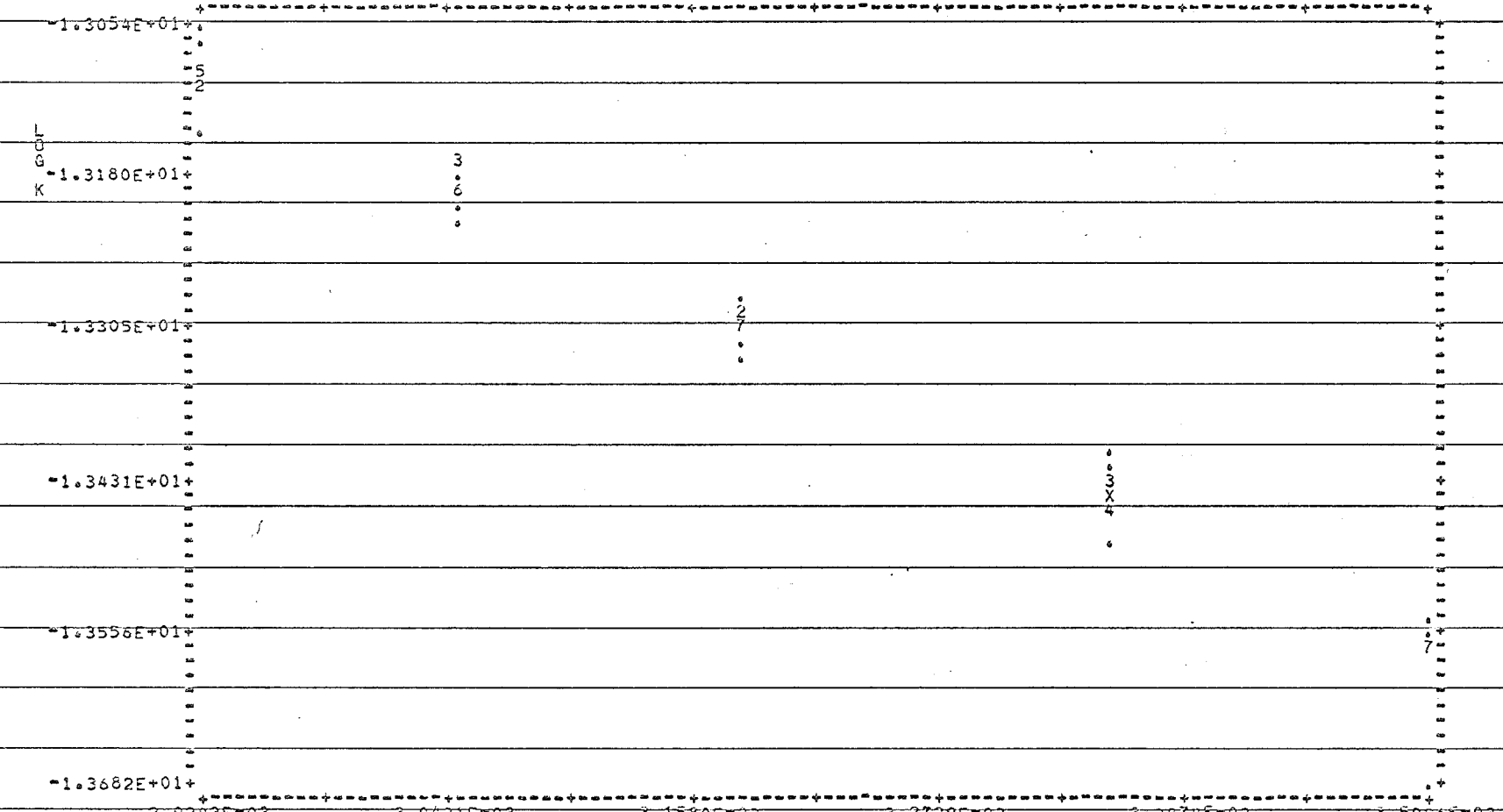

T K	K CC/MOLEC*S	1/T	LOG K	COLUMN 5	COLUMN 6	EA J/MOL	LOG A
298.00000	* 3.5200000-14	.0033557047	-13.453457	*-1.0606747+01	-7041.7008	16217.037	-10.606747
298.00000	* 3.7800000-14	.0033557047	-13.422508	*-8.4693850+02	-7041.7008	16217.037	-10.606747
298.00000	* 3.7300000-14	.0033557047	-13.428291	.0844011498	-7041.7008	16217.037	-10.606747
298.00000	* 3.7400000-14	.0033557047	-13.427128	*25.942870	-7041.7008	16217.037	-10.606747
298.00000	* 3.9100000-14	.0033557047	-13.407823	*35.000000	-7041.7008	16217.037	-10.606747
298.00000	* 3.6200000-14	.0033557047	-13.441291	* 2.0000000	-7041.7008	16217.037	-10.606747
298.00000	* 3.5800000-14	.0033557047	-13.446117	*33.000000	-7041.7008	16217.037	-10.606747
298.00000	* 3.2700000-14	.0033557047	-13.485452	.0289383 83	-7041.7008	16217.037	-10.606747
298.00000	* 3.4700000-14	.0033557047	-13.459671	* 8.3743002-04	-7041.7008	16217.037	-10.606747
298.00000	* 3.6100000-14	.0033557047	-13.442493	.96996670	-7041.7008	16217.037	-10.606747
298.00000	* 3.7000000-14	.0033557047	-13.431798	*	-7041.7008	16217.037	-10.606747
298.00000	* 3.5400000-14	.0033557047	-13.450997	*	-7041.7008	16217.037	-10.606747
298.00000	* 3.4600000-14	.0033557047	-13.460924	*	-7041.7008	16217.037	-10.606747
285.50000	* 2.0800000-14	.0035026270	-13.681937	*	-7041.7008	16217.037	-10.606747
285.50000	* 2.7300000-14	.0035026270	-13.563837	*	-7041.7008	16217.037	-10.606747
285.50000	* 2.7700000-14	.0035026270	-13.557520	*	-7041.7008	16217.037	-10.606747
285.50000	* 2.6700000-14	.0035026270	-13.573469	*	-7041.7008	16217.037	-10.606747
285.50000	* 2.8700000-14	.0035026270	-13.542118	*	-7041.7008	16217.037	-10.606747
314.50000	* 5.1000000-14	.0031796502	-13.292430	*	-7041.7008	16217.037	-10.606747
314.50000	* 4.8900000-14	.0031796502	-13.310691	*	-7041.7008	16217.037	-10.606747
314.50000	* 4.6000000-14	.0031796502	-13.336759	*	-7041.7008	16217.037	-10.606747
314.50000	* 5.0600000-14	.0031796502	-13.295849	*	-7041.7008	16217.037	-10.606747
314.50000	* 5.2100000-14	.0031796502	-13.283162	*	-7041.7008	16217.037	-10.606747
314.50000	* 4.7300000-14	.0031796502	-13.325139	*	-7041.7008	16217.037	-10.606747
328.00000	* 6.2400000-14	.0030487805	-13.204815	*	-7041.7008	16217.037	-10.606747
328.00000	* 6.8200000-14	.0030487805	-13.166216	*	-7041.7008	16217.037	-10.606747
328.00000	* 6.8300000-14	.0030487805	-13.165579	*	-7041.7008	16217.037	-10.606747
328.00000	* 6.6800000-14	.0030487805	-13.175224	*	-7041.7008	16217.037	-10.606747
328.00000	* 6.0700000-14	.0030487805	-13.216811	*	-7041.7008	16217.037	-10.606747
328.00000	* 6.7900000-14	.0030487805	-13.168130	*	-7041.7008	16217.037	-10.606747
341.50000	* 7.8600000-14	.0029282577	-13.103474	*	-7041.7008	16217.037	-10.606747
341.50000	* 8.5900000-14	.0029282577	-13.066007	*	-7041.7008	16217.037	-10.606747
341.50000	* 8.8300000-14	.0029282577	-13.054039	*	-7041.7008	16217.037	-10.606747
341.50000	* 7.2100000-14	.0029282577	-13.142065	*	-7041.7008	16217.037	-10.606747
341.50000	* 7.9200000-14	.0029282577	-13.101275	*	-7041.7008	16217.037	-10.606747

A

* 2.4731669-11
* 2.4731669-11
* 2.4731669-11
* 2.4731669-11
* 2.4731669-11

* 2.4731669-11
* 2.4731669-11

* 2.4731669-11
* 2.4731669-11
* 2.4731669-11

* 2.4731669-11
* 2.4731669-11
* 2.4731669-11
* 2.4731669-11
* 2.4731669-11

* 2.4731669-11
* 2.4731669-11

* 2.4731669-11
* 2.4731669-11
* 2.4731669-11
* 2.4731669-11
* 2.4731669-11

* 2.4731669-11
* 2.4731669-11

* 2.4731669-11
* 2.4731669-11
* 2.4731669-11

* 2.4731669-11
* 2.4731669-11
* 2.4731669-11
* 2.4731669-11
* 2.4731669-11

LIST OF COMMANDS, DATA AND DIAGNOSTICS

```
$       PROGRAM TO CALCULATE THE ACTIVATION ENERGY OF A REACTION FROM
$       PAIRS OF TEMPERATURE AND RATE CONSTANT VALUES
$
$       READ IN DATA TEMPERATURE INTO COL 1 RATE CONST INTO COL 2
$       METHYL NITRITE
$
        READ  1  2
```

298.	3.52E-14
298.	3.76E-14
298.	3.73E-14
298.	3.74E-14
298.	3.91E-14
298.	3.62E-14
298.	3.58E-14
298.	3.27E-14
298.	3.47E-14
298.	3.61E-14
298.	3.70E-14
298.	3.54E-14
298.	3.46E-14
285.5	2.08E-14
285.5	2.73E-14
285.5	2.77E-14
285.5	2.67E-14
285.5	2.87E-14
314.5	5.10E-14
314.5	4.89E-14
314.5	4.80E-14
314.5	5.06E-14
314.5	5.21E-14
314.5	4.73E-14
328.	6.24E-14
328.	6.82E-14
328.	6.83E-14
328.	6.66E-14
328.	6.97E-14
328.	6.79E-14
341.5	7.86E-14
341.5	8.59E-14
341.5	8.83E-14
341.5	7.21E-14
341.5	7.92E-14

```
$
$       CONVERT TEMPERATURE INTO ITS INVERSE, THE RATE CONSTANT INTO ITS LOG
$
        DIVIDE  1.0 BY TEMP IN COL 1 PUT INV T IN COL 3
        LOGTEN OF RATE CONST IN COL 2 INTO COL 4
$
$       LEAST SQUARES ANALYSIS
$
```

LIST OF COMMANDS, DATA AND DIAGNOSTICS

```
      POLYFIT LOGRATE IN COL 4 WEIGHTS 1.0 DEGREE 1 TO INVT IN COL 3 ANS IN 5
$
$     SLOPE IS IN ROW 2 OF COL 5 THE INTERCEPT IN ROW 1 CONVERT THESE
$     INTO ACTIVATION ENERGY AND ARRHENIUS FACTOR
      MULTIPLY SLOPE *2,5* BY GAS CONST *R* PUT ANS IN COL 6
      MULTIPLY COL 6 BY -2.303 PUT EA INTO COL 7
      DEFINE LOG A IN ROW 1 OF COL 5 INTO COL 8
      RAISE 10.0 TO THE POWER OF COL 6 PUT A IN COL 9
$
$     CALCULATE THE PREDICTED VALUES OF LOG RATE CONST
$
      MULTIPLY SLOPE *2,5* BY INV T IN COL 3 PUT IN COL 10
      ADD COL 10 TO INTERCEPT *1,5* PUT PREDICTED VALUES IN COL 11
$
$     TITLE GRAPH AXES
TITLEX                1/T
TITLEY          LOG K
      PLOT  COLS 4AND 11 THE LOG RATE CONST VALUES AGAINST INV T IN COL 3
$
$     HEAD COLUMNS PRIOR TO PRINTING
$
$
      HEAD1/      T  K
      HEAD 2/K CC/MOLEC.S
      HEAD3/      1/T
      HEAD 4/     LOG K
      HEAD 7/ EA  J/MOL
      HEAD 8/     LOG A
      HEAD 9/     A
      PRINT COLS  1,2,3,4,5,6,7,8,9
  STOP
```

NATIONAL BUREAU OF STANDARDS, WASHINGTON, D. C. 20234, OMNITAB II VERSION 5.00 MAY 15, 1971

REFERENCES

1. Clyne, M.A.A. and Coxon, J.A., Trans Faraday Soc. 62, 1175 (1966).
2. Bemand, P.P., Clyne, M.A.A., and Watson, R.T., J.C.S. Faraday I 69, 1356 (1973).
3. Calvert, J.G. and M^{c}Quigg, R.D., Int. J. Chem. Kinet. Symposium 1, 113 (1975).
4. Schiff, H.I., in Physics and Chemistry of Atmospheres, B.M. M^{c}Cormac Ed., D. Reidel Publ. Co. (1976).
5. Tarte, P., J. Chem. Phys. 20, 1570 (1952).
6. M^{c}Graw, G.E., Bernitt, D.L. and Hisatsune, I.C., J. Chem. Phys. 45, 1392 (1966).
7. Demerjian, K.L., Kerr, J.A. and Calvert, J.G., Advances in Environ. Sci. Technol., 4, 1 (1974).
8. Bielski, B.H. and Timmons, R.B., J. Phys. Chem. 68, 347 (1964).
9. Davidson, J.A. and Thrush, B.A., J.C.S. Faraday I 71, 2413 (1975).
10. Langmuir, I., J. Amer. Chem. Soc. 34, 1310 (1912).
11. Langmuir, I. and MacKay, G.M.J., J. Amer. Chem. Soc. 36, 1708 (1914).
12. Langmuir, I., J. Amer. Chem. Soc. 37, 417 (1915).
13. Tollefson, E.L. and Le Roy, D.J., J. Chem. Phys. 16, 1057 (1948)
14. Wood, R.W., Proc. Roy. Soc. A 102, 1 (1922).
15. Bonhoeffer, K.F., Z. Phys. Chem. 113, 199 (1924).
16. Bonhoeffer, K.F., Z. Phys. Chem. 113, 492 (1924).
17. Bonhoeffer, K.F., Z. Phys. Chem. 116, 391 (1925).

18. Melville, H. and Gowenlock, B.G., Experimental Methods in Gas Reactions, M^{c}Millan and Co., New York, (1964) p182.

19. Geib, K.H. and Harteck, P., Trans. Faraday Soc. 30, 131 (1934).

20. Harteck, P., Trans. Faraday Soc. 30, 134 (1934).

21. Steacie, E.W.R., Atomic and Free Radical Reactions, Rienhold, New York, (1954).

22. Meinel, A.B., Astrophys. J. 112, 120 (1950).

23. Gaydon, A.G. and Wolfhard, H.G., Flames:Their Structure, Radiation and Temperature, Third Ed., Chapman and Hall, London (1970) p101.

24. M^{c}Ewan, M.J. and Phillips, L.F., Chemistry of the Atmosphere, Edward Arnold Ltd., London, (1975), p7, 6, 87.

25. Westenberg, A.A., Ann. Rev. Phys. Chem. 24, 77 (1973) and references contained therein.

26. Donovan, R.J., Husain, D. and Kirsch, L.J., Annual Reports of the Chemical Society 69 1 (1972) and references contained therein.

27. Baulch, D.L. et al., High Temperature Reaction Rate Data, The University, Leeds.

28. Gavin, D. and Hampson, R.F. Chemical Kinetics Data Survey VII, NBSIR 74-430.

29. Reference 24, p275-288.

30. e.g. Int. J. Chem. Kinet. Symposium 1, (1975).

31. Fifteenth Symposium (International) on Combustion. The Combustion Institute, (1976). also previous Symposia.

32. Mulvihill, J.N., Thesis, Ph.D., University of Canterbury (1975).

33. Foner, S.N. and Hudson, R.L., J. Chem. Phys. 21, 1374 (1953).

34. Gaydon, A.G., The Spectroscopy of Flames, Chapman and Hall, London, (1957) p137-162.

35. Bulewicz, E.M., James, C.G. and Sugden, T.M., Proc. Roy. Soc. A 235, 89 (1956).

36. M^{c}Ewan, M.J. and Phillips, L.F., Combustion and Flame 9, 420 (1965).

37. Halstead, C.J. and Jenkins, D.R., Combustion and Flame 11, 363 (1967).

38. Bulewicz, E.M. and Sugden, T.M., Trans. Faraday Soc. 54, 1855 (1958).

39. Bradley, J.N., Shock Waves in Chemistry and Physics, Methuen, London (1962).

40. Gaydon, A.G., and Hurle, I.R., The Shock Tube in High Temperature Chemistry and Physics, Rienhold, New York, (1963).

41. Schott, G.L. and Getzinger, R.W., in Physical Chemistry of Fast Reactions, B.P. Levitt Ed. Plenum Pub, Co. (1973) p81.

42. Norrish, R.G.W. and Porter, G., Nature 164, 658 (1949)

43. Braun, W. and Lenzi, M., Disc. Faraday Soc. 44, 252 (1967).

44. Ridley, B.A., Davenport, J.A., Stief, L.J. and Welge, K.H., J. Chem. Phys. 57, 520 (1972).

45. Lee, J.H., Michael, T.V., Payne, W.A., Whytock, D.A. and St f, L.J., J. Chem. Phys. 65, 3280 (1975).

46. Willets, F.W., Prog. React. Kinet. 6, 51 (1972).

47. Thrush, B.A., Prog. React. Kinet. 3, 97 (1965).

48. Cvetanovic, R.J., Prog. React. Kinet. 2 39 (1964).

49. Herschbach, D.R., Adv. Chem. Phys. 10, 319 (1966).

50. M^{c}Donald, J.D., Breton, P.R., Lee, Y.T. and Herschbach, D.R., J. Chem. Phys. 56, 759 (1972).

51. Geddes, J., Krause, H.F. and Fite, W.L., J. Chem. Phys. 56, 3298 (1972).

52. Silver, J.A., Dimpfl, W.L., Brophy, J.H. and Kinsey, J., J. Chem. Phys. 65, 1811 (1976).

53. Herschbach, D.R., in Faraday Disc. Chem. Soc. 55, Molecular Beams, p233.

54. Camilleri, P. Marshall, R.M. and Purnell, J.H., J.C.S. Faraday I 70, 1434 (1974).

55. Ridley, B.A., Schultz, W.R. and Le Roy, D.J., J. Chem. Phys. 44, 3344 (1966).

56. Westenberg, A.A., Prog. React. Kinet. 7, 23 (1973).

57. Spencer, J.E. and Glass, G.P., J. Phys. Chem. 79, 2329 (1975).

58. Westenberg, A.A. and de Haas, N., J. Chem. Phys. 48, 4405 (1968).

59. Brown, J.M., Thrush, B.A. and Tuck, A.F., Proc. Roy. Soc. A 302 311 (1968).

60. M^{c}Kenzie, A., Mulcahy, M.F.R. and Steven, J.R., J.C.S. Faraday I 70, 549 (1974).

61. Michael, J.V. and Western, R.E., J. Chem. Phys., 45, 3632 (1966).

62. Choo, K.Y., Gaspar, P.P. and Wolf, A.A., J. Phys. Chem. 79, 1752 (1975).

63. Monkhouse, P.B. and Clyne, M.A.A., paper presented at the 4th International Conference on Gas Kinetics, Edinburgh (1975).

64. Phillips, L.F. and Schiff, H.I., J. Chem. Phys. 37, 1233 (9962).

65. Clyne, M.A.A. and Stedman, D.H., Trans. Faraday Soc. 62, 2164 (1966).

66. Clyne, M.A.A. and Thrush, B.A., Proc. Roy. Soc. A 275, 559 (1963).

67. Freeman, C.G., Thesis Ph.D., University of Canterbury, (1967).

68. Dunn, M.R., Thesis Ph.D., University of Canterbury, (1971).

69. Foner, S.N., Adv. in Mol. Phys. 2 385 (1966).

70. Slemr, F. and Warneck, P. Ber. Bunsenges. 79 153 (1975). (In English)

71. Jones, I.T.N. and Bayes, K.D., Fourteenth Symposium (International) on Combustion, The Combustion Institute (1973) p277.

72. Ogryzlo, E.A., Canad. J. Chem., 39 2557 (1961).

73. Berg, H.C. and Kleppner, D., Rev. Sci. Inst. 33, 248 (1962).

74. Wittke, J.P. and Dicke, R.H., Phys. Rev. 103, 620 (1956).

75. Mulcahy, M.F.R. and Pethard, M.R., Aust. J. Chem. 16, 527 (1963).

76. Mulcahy, M.F.R., Gas Kinetics, Thomas Nelson, London, (1973) p59.

77. Reference 24, Chapter I

78. Friedman, H., Physics of the Upper Atmosphere, J.A. Ratcliffe Ed., Academic Press, New York, (1960).

79. Reference 24, p7.

80. Urbach, F. and Davies, R.E. Proceedings of the 4th Conference on C.I.A.P. (1975) p66.

81. Biggs, R.H., ibid p62.

82. Mac Cracken, M.C., ibid p183.

83. Chapman, N.A., Mem. Roy. Meterol. Soc. 3 103 (1930).

84. Reference 24, p70.

85. Johnstone H.S. Ann. Rev. Phys. Chem. 26, 315 (1975).

86. Hampsen, J., Photochemical Behaviour of the Ozone Layer, Canadian Armament Res. Develop. Estab. 1627/64 (1964).

87. Bates, D.R. and Nicolet, M., J. Geophys. Res. 55, 301 (1950).

88. Nicolet, M., Canad. J. Chem. 52, 1381 (1974).

89. Hunt, B.G., J. Atmos. Sci. 23, 88 (1966).

90. Hunt, B.G., J. Geophys, Res. 71, 1385 (1966).

91. M^{c}Elroy, M.B., Wofsy, S.C., Penner, J.E. and M^{c}Connell, J.C., J. Atmos. Sci. 31 287 (1974).

92. Johnstone, H.S., Environ. Conserv. 1, 163 (1974).

93. Bates, D.R. and Hayes, P.B., Planetary Space Sci. 15, 189 (1967).

94. M^{c}Elroy, M.B. and M^{c}Connell, J.C., J. Atmos. Sci. 28, 1095 (1971).

95. Crutzen, P.J., J. Geophys. Res. 76, 7311 (1971).

96. Nicolet, M., J. Geophys. Res. 70, 679 (1965).

97. Ridley, B.A., Schiff, H.I., Shaw, A.W., Bates, L., Howlett, L.C., Le Vaux, H., Megill, L.R., and Ashenfelter, T.E., Planetary Space Sci. 22 19 (1974).

98. Ackerman, M., Fontella, J.C., Frimont, D., Girard, A., Luisnard, N., Canad. J. Chem. 52, 1532 (1974).

99. Garvin, D., Hampson, R.F., and Kurylo, M.J., Proceedings of the Fourth Conference on C.I.A.P. 391 (1975).

100. Simonaitis, R. and Heicklen, J., J. Phys. Chem. 78, 653 (1974).

101. Leighton, P.A., Photochemistry of Air Pollution, Academic Press, New York, (1961).

102. Niki, H., Darby, E.E. and Weinstock, B., Advances in Chemistry Series 113, 16.

103. Pitts, J.N. and Findlayson, B.J., Agnew. Chem. (Int. Ed,) 14, 1 (1975).

104. Pitts, J.N., Lloyd, A.C. and Sprung, J.L., Chem. in Brit. 11, 247 (1975).

105. Calvert, J.G., Demerjian, K.L. and Kerr, J.A., Environ. Lett. 4, 123 (1973).

106. Calvert, J.G., Demerjian, K.L. and Kerr, J.A., Environ. Lett. 4, 281 (1973).

107. Kerr, J.A., Calvert, J.G. and Demerjian, K.L., Chem. in Brit, 8, 252 (1972).

108. Reference 24, Chapter VII.

109. Dodge, M.C. and Hecht, T.A., Int. J. Chem. Kinet. Symposium 1, 155 (1975).

110. Lloyd, A.C., Darnall, K.R., Winer, A.M. and Pitts, J.N., J. Phys. Chem. 80, 789 (1976).

111. Demerjian, K.L., Kerr, J.A., and Calvert, J.G., Environ. Lett. 3, 137 (1972).

112. Wu, C.H., Wang, C.C., Japar, S.M., Davis, L.I., Hanabuse, H., Killinger, D., Niki, H., and Weinstock, B., Science 189, 797 (1975).

113. Wang, C.C. and Davis, L.I., Phys. Rev. Lett. 32, 349 (1974).

114. M^{c}Afee, J.M., Pitts, J.N. and Winer, A.M., J. Chem. Phys. 80, 1635 (1976).

115. Thomson, H.W., and Purkis, C.H., Trans. Faraday Soc. 32, 1466 (1936).

116. Gray, J.A. and Style, D.W.G., Trans. Faraday Soc. 48, 1137 (1952).

117. Brown, H.W. and Pimentel, G.C., J. Chem. Phys. 29, 883 (1958).

118. Hanst, P.L. and Calvert, J.G., J. Phys. Chem. 63, 2071 (1959).

119. M^{c}Grath, W.D. and M^{c}Garvey, J.J., Trans. Faraday Soc. 60, 2196 (1964).

120. Napier, I.M. and Norrish, R.G.W., Proc. Roy. Soc. A. 299, 317 (1967).

121. Wiebe, H.A. and Heicklen, J., J. Amer. Chem. Soc. 95, 1 (1973).

122. Wiebe, H.A., Villa, A., Hellman, T.M. and Heicklen, J., J. Amer. Chem. Soc. 95, 7 (1973).

123. Baker, G. and Shaw, R. J.C.S. 6965 (1965).

124. Gay, B.W., Noonan, R.C., Hanst, P.C. and Bufalini, J.J., Paper presented to the A.C.S. Conference Sept. 1974.

125. Steacie, E.W.R. and Shaw, G.W., Proc. Roy. Soc. A. 146, 388 (1934).

126. Steacie, E.W.R. and Shaw, G.W., J. Chem. Phys. 2, 345 (1934).

127. Steacie, E.W.R., and Calder, D.S., J. Chem. Phys. 4, 96 (1936).

128. Steacie, E.W.R. and Rosenberg, S. J. Chem. Phys. 4, 223 (1936).

129. Carter, A.G. and Travers, M.N., Proc. Roy, Soc. A. 158, 495 (1937).

130. Rice, F.O. and Rodowskas, E.L., J. Amer. Chem. Soc. 57, 350 (1935).

131. Levy, J.B., J. Amer. Chem. Soc. 78, 1780 (1956).

132. Adler, D.G., Pratt, M. and Gray, P., Chem. and Ind. 1517 (1955).

133. Phillips, L. J.C.S. 3082 (1961).

134. Batt, L., M^{c}Culloch, R.D. and Milne, R.T., Int. J. Chem. Kinet. Symposium 1, 441 (1975).

135. Mendenhall, G.D., Golden, D.M. and Benson, S.W., Int. J. Chem. Kinet. 7, 725 (1975).

136. Campbell, I.M. and Goodman, K., Chem. Phys. Lett. 36, 382 (1975).

137. Moortgat, G.K., Slemr, F. and Warneck, P., Paper Submitted to Int. J. Chem. Kinet. 17-3-1976.

138. Melton, C.E., Rev. Sci. Inst. 29, 250 (1958).

139. Hanley, E.T., J. Appl. Phys. 19, 583 (1948).

140. Organic Synthesis, Collected Volume 2, A.H. Blatt, Ed., Wiley, New York, 1943, p412.

141. Nightingale, R.E., Downie, A.R., Rolenberg, D.C., Crawford, B. and Ogg, R.A., J. Phys. Chem. 58, 1047 (1954)

142. Reference 18 pg. 180.

143. Verhoek, F.H. and Daniels, F., J. Amer. Chem. Soc, 53, 1250 (1931).

144. Cher, M., K. Chem. Phys. 37, 2564, (1962).

145. Westenberg, A.A. and de Haas, N., J. Chem. Phys., 40 3037 (1964)., 43, 1550 (1965).

146 Jolly, W.L., Inorganic Chemistry of Nitrogen W.A. Benjamin, New York, (1964).

147. Asquith, P.L. and Tyler, B.K., Chem. Comm. 744 (1970).

148. Nash, T., Tellus 26 175 (1974).

149. Atkins, D.H.F. and Cox, R.A. The 365nm Photolysis of Nitrous Acid Vapour in Air, A.E.R.E. Rep. R. 7615 (1973).

150. Cox, R.A., J. Photochem. 3 175 (1974).

151. Cornu, A. and Massot, R. Compilation of Mass Spectral Data, Heydon, London (1975).

152. Gray, D., Lissi, E. and Heicklen, J., J. Phys. Chem. 76, 1919 (1975).

153. Spokes, G.N. and Benson, S.W., J. Amer. Chem. Soc. 89, 6032 (1967).

154. Anderson, J.G., Margiton, J.J. and Kaufman, F,, J. Chem. Phys. 60, 3310 (1974).

155. Atkinson, R., Hansen, D.A. and Pitts, J.N., J. Chem. Phys. 62, 3284 (1975).

156. Westenberg, A.A. and de Haas, N., J. Chem. Phys. 58, 4066 (1973).

157. Venugoplan, M. and Jones, R.A., Chemistry of Dissociated Water Vapour and Related Systems, J. Wiley & Sons, New York (1968).

158. Kaufman, F. and Del Greco, F.P. J. Chem. Phys. 35, 1895 (1961).

159. Wilson, W.E., J. Chem. Phys. Ref. Data 1, 535 (1972).

160. Brown, J.F., J. Amer. Chem. Soc. 77, 6341 (1955).

161. Swinbourne, E.S., Analysis of Kinetic Data, Nelson and Sons, London (1971) p79.

162. Huie, R.E. and Herron J.T., Int. J. Chem. Kinet. Symposium 1, 165 (1975).

163. Benson, S.W., The Foundations of Chemical Kinetics, M^{c}Graw-Hill, New York (1960) p280.

164. Benson, S.W., Thermochemical Kinetics J. Wiley & Sons New York (1968).

165. Cruickshank, F.R. and Benson, S.W., Int. J. Chem. Kinet. 1, 381 (1969).

166. Slemr, F. and Warneck, P. Submitted to Int, J. Chem, Kinet. 17-3-1976.

167. Morris, E.D. and Niki, H., J. Chem. Phys. 55, 1991 (1971).

168. Kerr, J.A. and Trotman-Dickenson, A.F., Prog. React. Kinet. 1, 107 (1961).

169. Bromberger, B. and Phillips, L., J.C.S. 5302 (1961).

170. O'Neil, H.E. and Benson, S.W., Kinetic Data on Gas Phase Unimolecular Reactions NSRDS-NBS21 (1970),

171. M^{c}Knight, C., Niki, H. and Weinstock, B. J. Chem. Phys. 47, 5219 (1967).

172, Carr, R.W., Gay, I.D., Glass, G.P. and Niki, H., J. Chem. Phys. 49, 847 (1968).

173. Morris, E.D., Stedman, D.H. and Niki, H., J. Amer. Chem Soc. 93, 5370 (1971).

174. Klemm, R.B., Payne, W.A. and Stief, L.J. Int. J. Chem. Kinet. Symposium 1 61 (1975).

175. Yokota, T. Ahmed, M.G., Safarik, I., Strausz. O.P. and Gunning, H.E., J. Phys Chem. 79 175 (1975).

176. Wagner, H. Gg., Welzbacher, U. and Zellner, R., Ber. Bunsenges. 80 1023 (1976) (In English).

177. Jamieson, J.W.S. and Brown, G.R., Canad. J. Chem. 42, 1638 (1964).

178. M^{c}Nesby, J.R., Scheer, M.D. and Klein, R., J. Chem. Phys. 32, 1814 (1960).

179. Gray, P. Shaw, R. and Thynne J.C.J. Prog. React. Kinet. 4, 63 (1967).

180. Stull, D.R. and Prophet, H. NSRDS-NBS 37 (1971).

181. Cox, J.D. and Pilcher, G. Thermochemistry of Organic and Organometallic Compounds, Academic Press, London (1970).

182. Franklin, J.L. et al. NSRDS-NBS 26 (1969).

183. Leichnitz, K., Detector Tube Handbook, Drager Co (1971)

184. Reference 18, p188.

185. Cook, G.A., Kiffer, A.D., Klump, C.V., Malik, A.H. and Spence, L.A., in Ozone Chemistry and Technology, Advances in Chemistry Series 21, p44.

186. Perry, P.H. and Chilton, C.H., Chemical Engineers Handbook, 5th Ed., M^{c}Graw Hill, Japan (1974).

187. Handbook of Chemistry and Physics, R.C. Weast Ed., Chemical Rubber Co., (1971).

188. Hirschfelder, J.O., Curtis, C.F. and Bird, R.B., J. Wiley and Sons, New York, (1954).

189. Hogben, D. Peary, S. and Varner, R., NBS Tech. Note. 552 (1971).